EXPLORING METHODS FOR FUNCTIONAL STUDIES OF CBM33-TYPE LYTIC POLYSACCHARIDE MONOOXYGENASES

Stefan Leonardo Marinai

Norwegian University of Life Sciences
Department of Chemistry, Biotechnology and Food Science
Master Thesis 60 credits 2013

ACKNOWLEDGEMENTS

The present work was carried out at the Department of Chemistry, Biotechnology and Food Science at the Norwegian University of Life Sciences with Professor Vincent Eijsink and Dr. Gustav Vaaje-Kolstad as supervisors.

I would like to express my gratitude to Vincent Eijsink for giving me the opportunity to write my thesis in the Protein Engineering and Proteomics (PEP) group. I would also thank Gustav Vaaje-Kolstad for ideas, inspiration and guidance in the work of my thesis. Thanks to all the members of the PEP group.

Ås, June 14, 2013

Stefan Leonardo Marinai

ABSTRACT

Conversion of biomass to sustainable sources of soluble sugars for fermentation has been subject of intensive research in the field of biorefinery the last decade. The recalcitrant nature of many polysaccharides create a technical barrier to the cost-effective transformation of biomass to fermentable sugars, but a novel discovery have given more insight into efficient conversion of recalcitrant polysaccharides. Bacterial proteins categorized as Lytic Polysaccharide Monooxygenases (LPMO) member of family 10 auxiliary activities (AA) (former family 33 carbohydrate-binding modules) were recently shown to boost degradation of crystalline chitin using a mechanism involving an oxidative and a hydrolytic step. A better understanding of chitin degradation can be used for optimizing conditions for degradation of other polysaccharides in a crystalline context, such as cellulose.

The aim of this study was to gain more insight into the binding properties and the catalytic mechanism of chitin-binding protein 21 (CBP21), a surface-active AA10-type LPMO, produced by the well known chitinolytic soil bacterium *Serratia marcescens*. The functional role of seven conserved residues located close to the active site (Ser-58, Thr-111, Gly-112, Trp-178, Ile-180, Thr-183 and Phe-187) were probed by site-directed mutagenesis, binding assays and product analysis. All mutations lowered the affinity for CBP21 to β-chitin and their ability to degrate the substrate, but CBP21 variant I180R showed a substantially lower activity than the wild-type and the mutants.

A novel assay to measure enzyme activity based on detection of hydrogen peroxide from a futile side reaction of LPMOs was tested on CBP21, showing that the copper present in the enzyme contributes to formation of hydrogen peroxide by autooxidation. In addition, various AA10s known to interact with the human gut were tested for substrate specificity by a glycan array screen. GbpA from *Vibrio cholerae* was the only enzyme that showed binding, an enzyme which was also proven to have LMPO activity.

SAMMENDRAG

Nedbrytning av biomasse til bærekraftige sukkerarter som kan brukes til fermentering har lenge vært tilstand for intens forskning innenfor feltet bioraffinieri.
Vankelig nedbrytbare polysakkarider har lenge skapt en barriere til kostnadseffektiv omdannelse av biomasse til fermenterbare sukkerarter, men en nylig oppdagelse har gitt mer innsikt i effektiv omdannelse av vanskelig nedbrytbare polysakkarider. Bakterielle proteiner klassifisert som lytisk polysakkarid monooksygenaser (LPMO), medlem i familie 10 av auxiliar activities (AA) (tidligere kjent som familie 33 av karbohydrat-bindinde moduler), ble nylig vist å kunne øke nedbrytningen av kitin ved å bruke en mekanisme som involverer oksidasjon og hydrolyse. En bedre forståelse av nedbrytning av kitin kan bli brukt til å optimalisere betingelser for degradering av andre polysaccharider, som for eksempel cellulose.

Hovedmålet med denne oppgaven var å få mer innsikt i bindingsegenskapene og den katalytiske mekanismen til det kitin-bindindende proteinet CBP21, en overflate-aktiv AA10-type LPMO, produsert av den kjente jordbakterien *Serratia marcescens*. Den funksjonelle rollen til sju konserverte residuer lokalisert i nærheten av det aktive setet (Ser-58, Thr-111, Ala-112, Trp-178, Ile-180, Thr-183 og Phe-187) ble undersøkt ved bruk av sete-rettet mutagenese, bindingseksperimenter og produkt analyse. Alle mutasjonene førte til lavere affinitet for CBP21 til β-chitin og enzymets evne til å degradere substratet. CBP21 variant I180R viste en betydelig lavere aktivitet enn villtypen og de andre mutantene.

En ny essay for å måle enzymaktivitet basert på måling av hydrogen peroksid fra en sidereaksjon hos LPMO ble testet for CBP21. Denne essayen viste at kopperet som er bundet til enzymet bidrar til dannelse av hydrogen peroksid ved auto oksidasjon. I tillegg ble ulike AA10`s som er kjent for å reagere med mennesketarmen testet for substrat spesifisitet mot ulike polysakkarider. GbpA fra *Vibrio cholerae* var det eneste proteinet som viste tegn til binding, ett enzym som også fikk påvist LPMO aktivitet.

ABRAVIATIONS

AA	Auxiliary activities
CAZY	Carbohydrate-active enzymes
CBM	Carbohydrate binding module
CBM33	Carbohydrate binding module of family 33
CBP	Chitin-binding protein
CBP21	Chitin-binding protein 21
CDH	Cellobiose dehydrogenase
dH_2O	Sterile water (Milli-Q)
DP	Degree of polymerization
EC	Enzyme commission
g	gravity
GH	Glycosyl hydrolase
GH61	Glycoside hydrolase of family 61
GlcNAc	*N*-acetyl-β-glucosamine
HRP	Horseradish peroxidase
ITC	Isothermal titration calorimetry
kb	Kilobases
K_d	Dissociation constant
kDa	Kilo Dalton
LB	Luria Bertani
LPMO	Lytic polysaccharide monooxygenase
MALDI-TOF	Matrix-assisted laser desorption and ionization time of flight
MW	Molecular weight
MWCO	Molecular weight cut off
m/z	Mass/charge (mass-to-charge ratio)
PCR	Polymerase chain reaction
rpm	Revolutions per minute
SDS-PAGE	Sodium dodecyl sulphate polyacrylamide gel electrophoresis
UHPLC	Ultra high pressure liquid chromatography
UV	Ultraviolet
v/v	Volume/volume
w/v	Weight/volume

CONTENTS

1. INTRODUCTION

1.1 Polysaccharides

Carbohydrates have the general formula $C_y(H2O)_x$ and can be found in all living organisms, as a result they are widely available and inexpensive. Three major classes of carbohydrates exist; monosaccharides, oligosaccharides and polysaccharides. Monosaccharides are the simplest form of carbohydrate and consist of one carbohydrate molecule, often referred to as a mono sugar, which may be linked together by glycosidic bonds to form carbohydrate chains of variable length. An oligosaccharide contains from 2 to 20 sugar units, while polysaccharides usually contains a high number (>20) of monosaccharides linked together. Polysaccharides differ from each other based on type of monosaccharide unit, type of linkage, degree of branching and degree of polymerization (Fennema et al. 2007). Polysaccharides are widely available and have multiple roles in biological systems such as energy storage and being part of structural components. Glycogen and starch involved in energy storage, while cellulose, chitin and xylan often function as structural components. Several types of polysaccharides, such as cellulose and chitin, form a crystalline network of polymer chains held together by strong hydrogen bonds, thus creating insoluble and highly rigid structures.

1.1.1 Chitin

Chitin is the second most abundant natural occurring biopolymer in nature. The annual production of chitin is estimated to be 100 billion tons. Chitin occurs in nature as ordered insoluble crystalline microfibrils and is used by many organisms for protection against mechanical and chemical stress. It is a common constituent of the exoskeleton of arthropods and crustaceans and the cell walls of many fungi and yeast (Horn et al. 2006c; Vaaje-Kolstad et al. 2012). This linear biopolymer consists of repeated monomers of *N*-acetyl-β-D-glucosamine (GlcNAc), which are covalently linked by β-1,4 glycosidic linkages. The unbranched chains are of variable length and the GlcNAcs are rotated 180° relative to each other, making the functional and structural unit a disaccharide as shown in figure 1.1 (Zakariassen et al. 2009).

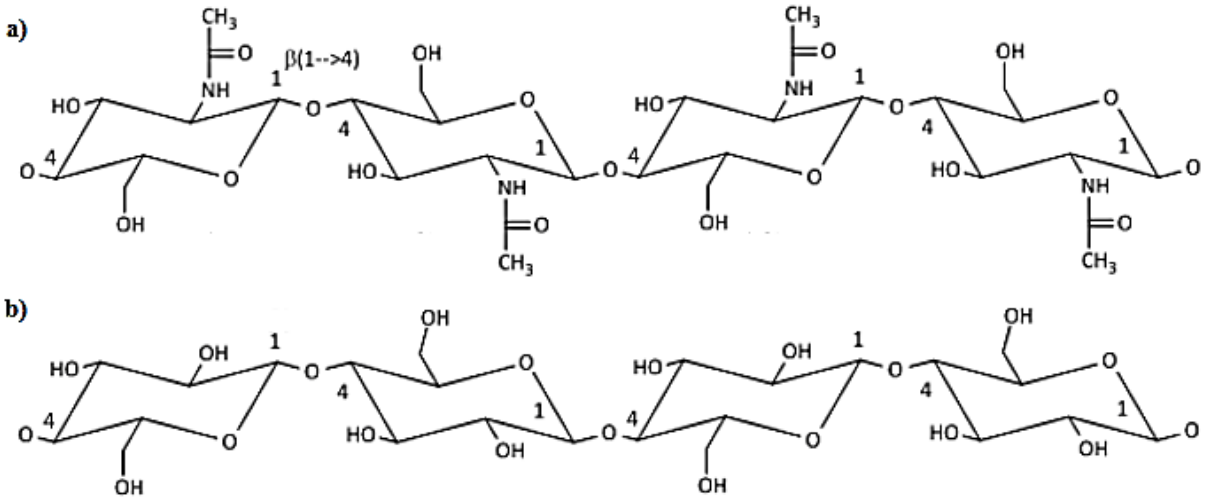

Figure 1.1. Chemical structure of chitin and cellulose. Chitin (a) is structurally similar to cellulose (b), apart from the hydroxyl group (-OH) in cellulose on C2, which is replaced by an acetamido group (-$NHCOCH_3$). The presence of the acetamido group makes the crystalline structure of chitin less compact that of cellulose (Eijsink et al. 2008). The figure is adapted from http://biowiki.ucdavis.edu/Biochemistry/Carbohydrates/Polysaccharides.

Two major allomorphs of crystalline chitin occur in nature dependent on the orientation of the chitin chains, α- and β-chitin. The most abundant form is α-chitin whose chains are arranged in an antiparallel fashion, while in β-chitin the chins are oriented in a parallel fashion. A minor form of chitin, γ-chitin, has a mixture of parallel and antiparallel chain packing. In both α-chitin and β-chitin, the chains are stabilized by intramolecular hydrogen bonds, but α -chitin exhibits additionally strong intermolecular hydrogen bonds. β-chitin has fewer intermolecular hydrogen bonds, which results in a less rigid chain structure (Jang et al. 2004). α-chitin is found in cell walls of many types of fungi, protistan and invertebrate exoskeletons, while β-chitin can be found in squid pen and in some algae. The less common form, γ-chitin, can be found in the stomach lining of squid. Chitin is not commonly found in a pure form in nature, but is usually associated with proteins or other polysaccharides, often covalent linked to chitin, such as glucans in the cell walls of fungi or different proteins in insects or other vertebrates (Gooday 1990; Spindler et al. 1990). In crustacean exoskeletons, chitin is also found associated with minerals such as calcium carbonate.

1.1.2 Degradation of chitin

Different chemical modifications can either weaken or break inter- or intramolecular bonds in the compact structure of chitin. One such modification is deacetylation of chitin, which is an effective way to make the biopolymer soluble (Synowiecki 2003). In nature, chitin may be partially deacetylated; the degree of acetylation of chitin is usually more than 90 %. If the degree of deacetylation reaches ~35 % chitin becomes soluble in dilute acids due to protonation of the amino groups present in the GlcNAc units, and is then called chitosan (Fig. 1.2) (Jayakumar et al. 2010) . In nature chitosan is the product of *N*-deacetylation of chitin by chitin deactylases (EC 3.5.1.41, belonging to family 4 of carbohydrate esterase; see section 1.2 for more details on enzyme classification) and is further degraded by chitosanases (EC 3.2.1.132, belonging to family 5, 7, 8, 46, 75 and 80 of glycoside hydrolases), which hydrolyse the β-1, 4 glycosidic bonds (Eijsink et al. 2010). Commercial chitosan is usually not made by enzymatic conversion, but by treating chitin under alkaline conditions at high temperature until the desired degree of deacetylation has been reached (Liu et al. 2006; Rinaudo 2006).

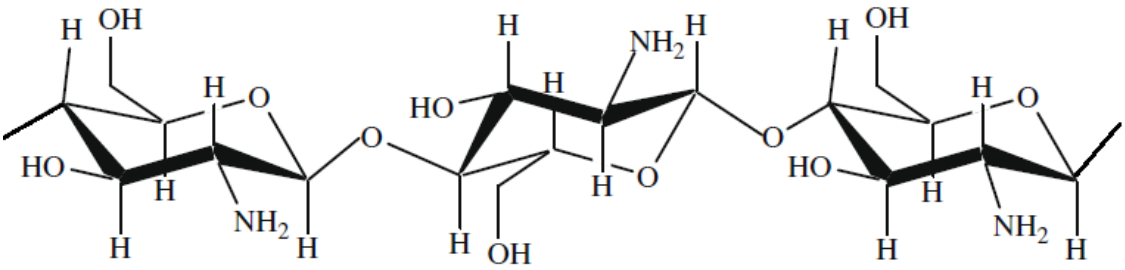

Figure 1. 2. Chemical structure of chitosan. Enzymatic or chemical removal of acetyl groups in the acetamido group converts chitin to chitosan. The figure is taken from Jayakumar et al. (2010).

Despite the high insolubility and the abundant annual production, chitin does not accumulate in nature, suggesting nature has evolved efficient systems to degrade this polysaccharide. Chitin turnover is an important process for recycling carbon and nitrogen in the biosphere. Chitin is primary utilized and degraded by microorganisms that possess chitinolytic enzyme systems, such as fungi and bacteria (Gooday 1990). Complete hydrolysis of chitin is achieved by endo- and exo-acting enzymes (called chitinases) working in synergy. Chitin-degrading bacteria produce various chitinases (EC 3.2.1.14, belonging to glycoside hydrolase family 18 and 19), which hydrolyse the β-1, 4 glycosidic linkages in chitin. The main product of chitinase action chitobiose $(GlcNAc)_2$, which is further degraded to GlcNAc monomers by

chitobiase (EC 3.2.1.29, belonging to glycoside hydrolases family 20). Chitin targeting lytic polysaccharide monooxygenases (LPMOs) cleave glycosidic bonds in crystalline regions of the chitin by an oxidative mechanism, thereby increasing substrate accessibility for chitinases and ensuring effective hydrolysis of chitin (Vaaje-Kolstad et al. 2010) (see also 1.2.4 for more details).

1.2 Enzymatic degradation of recalcitrant polysaccharides

1.2.1 Classification of carbohydrate –active enzymes

Enzymes responsible for synthesis, modification and degradation of carbohydrates are called carbohydrate-active enzymes (CAZymes) and play an important role in nature and commercial industry. All enzymes are given an Enzyme Commission (EC) number by the Nomenclature Committee of the International Union of Biochemistry and Molecular Biology (IUBMB), reflecting their main catalytic reaction and sometimes their substrate specificity. This classification does not take into account homology, protein structure or chemical mechanism (IUBMB 2013). The carbohydrate-active enzyme database (CAZy; www.cazy.com), present an alternative classification system based on similarities in amino acid sequence, enzymatic mechanism and protein folds. Because protein structure is more conserved than amino acid sequence, CAZy families are grouped into superfamilies that unite enzymes with similar overall structures (Bourne 2001). Until recently, carbohydrate-active enzymes were grouped into four classes; glycoside hydrolases (GH), polysaccharide lyases (PL), carbohydrate esterases (CE) and glycosyltransferases (GT). Very recently a fifth class, called auxiliary activities (AA), was introduced to the CAZy database; these accessory activities are redox enzymes associated with carbohydrate degradation/modification (Levasseur et al. 2013). A sixth class of protein in CAZy are the non-catalytic carbohydrate-binding modules (CBM33) (Cantarel et al. 2009). CAZy is continuously updated and contains sequence annotations from the National Center for Biotechnology Information (NCBI), reference information, family classification and known functional information. As of March 2013, 132 families of GHs, 94 families of GT, 22 families of PLs, 16 families of CE, 10 families of AA and 66 of CBMs are listed in the database (CAZy 2013). Carbohydrate-active enzymes often have multiple domains, i.e. one or more catalytic domains or more CBMs that help the enzyme to bind the substrate.

1.2.2 Carbohydrate-binding modules

Carbohydrate-binding modules were originally defined as cellulose-binding-domains (CBD) because they were thought to only bind cellulose (Gilkes 1988), but a more general name was introduced when it turned out that these modules had binding preferences toward various ligands. Proteins targeting carbohydrates usually have one or more CBMs as part of their overall structure. The CAZy database defines carbohydrate-binding modules as a contiguous amino acid sequence within a carbohydrate-active enzyme with a discrete fold having carbohydrate-binding activity (CAZy 2013). CBMs are thought to have three general roles; (i) concentrate the enzyme on the substrates surface (ii) substrate targeting (i.e. substrate specificity) and (iii) substrate disruption (the latter is rarely encountered and not well studied yet; Eijsink et al. 2008). Generally, increased enzyme concentrations on the substrate surface result in enhanced degradation. CBMs may also increase the rate of degradation by directing binding to specific regions on the substrate that are easier to attack, e.g. a less rigid part of the carbohydrate structure. CBMs with chitin-binding properties are found in CBM families 1, 2, 3, 5, 12, 14, 18, 19, 33, 37 and 50 (Frederiksen et al. 2013).

1.2.3 Glycoside hydrolases

Glycoside hydrolases are enzymes hydrolyzing the glycosidic bonds in di-, oligo-, and polysaccharides. As mentioned above, enzymes belonging to GHs are divided into 132 families in the CAZy database based on their amino acid sequence similarities. GHs in each family share a similar catalytic mechanism and 3D-structure, but substrate specificity and mode of activity (e.g. endo/exo- activity and processivity) may differ. Structural diversity between GHs is high, but active site topologies tends to be conserved and can be divided into three main groups; (i) pocket (ii) cleft and (iii) tunnel (Fig. 1.3) (Davies & Henrissat 1995). GHs cleaving glycosidic bonds at random positions in the polymeric chain are named "*endo*" and normally have their active site located in an open cleft which allows random binding. Enzymes attacking the chain from the end are called "*exo"* and usually have their active site located within a pocket (Henrissat & Davies 1997). Long and often deep tunnels are usually associated with processivity (see below). Whether the initial binding of the enzyme is "endo" or "exo" is a matter of debate and probably varies between enzymes and substrates (Horn et al. 2006c)

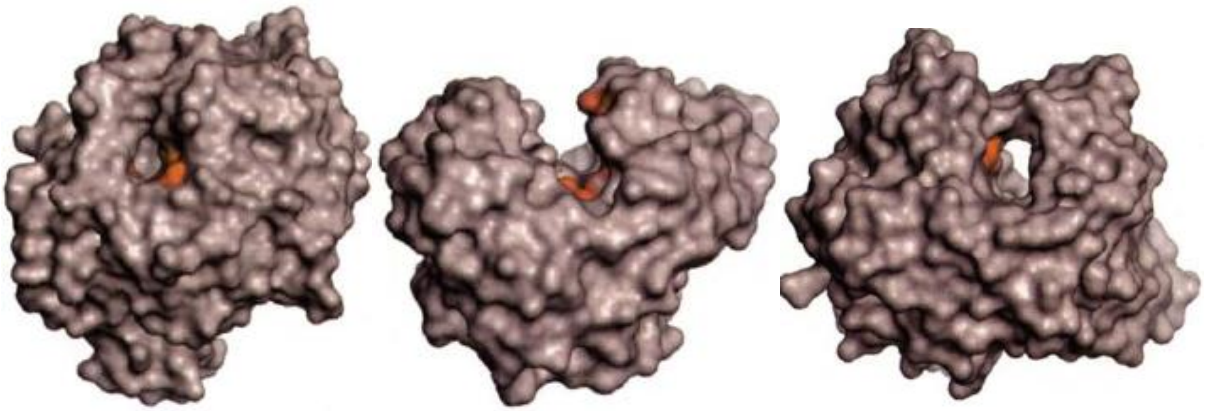

Figure 1.3. Various active-site topologies among GHs; pocket (left), cleft (middle) and tunnel (right). The active-site is marked in red. The figure is adapted from Davies & Henrisatt (1995).

GHs hydrolyses glycosidic bonds by general acid catalysis, usually using two acidic amino acid residues, one acting as a general acid and one as a nucleophile/base. Usually the acid and the nucleophile/base are an aspartate (Asp) or glutamate (Glu). For GH catalyzed hydrolysis to occur, a single chain must be extracted from the substrate surface and guided into the catalytic site of the enzyme were the catalysis take place (Beeson et al. 2012; Horn et al. 2006c). Hydrolysis can take place by two major mechanisms referred to as retaining (double displacement) or inversion (single displacement) (fig. 1.4) (Henrissat & Davies 1997; McCarter 1994; Sinnott 1990).

Retaining enzymes use one residue acting as both an acid and a base, while the other functions as a nucleophile and a leaving group. In the first step, the catalytic acid protonates the glycosyl oxygen in the scissile bond, which stimulates departure of the leaving group. The nucleophile attacks the anomeric carbon, forming a covalent intermediate. In the second step, the deprotonated catalytic acid acts as a base and activates a water molecule, which conducts a nucleophilic attack on the anomeric carbon of the glycosyl–enzyme intermediate (Vuong 2010). Chitinases in the GH18 family lack a correctly positioned second acidic residue acting as a nucleophile (Brurberg et al. 2001). Instead, the acetamide group in the substrate is acting as a nucleophile and the intermediate is not a covalent glycosyl-enzyme complex, but an oxazolinium ion formed by the substrate. This form of mechanism is called substrate-assisted hydrolysis.

In enzymes using the inverting mechanism (or single-displacement mechanism) one residue acts as a general acid and the other acts as a general base. The residue acting as an acid protonates the leaving group and the residue acting as a base activates a water molecule, to conduct a nucleophilic attack at the anomeric center (Vuong 2010).

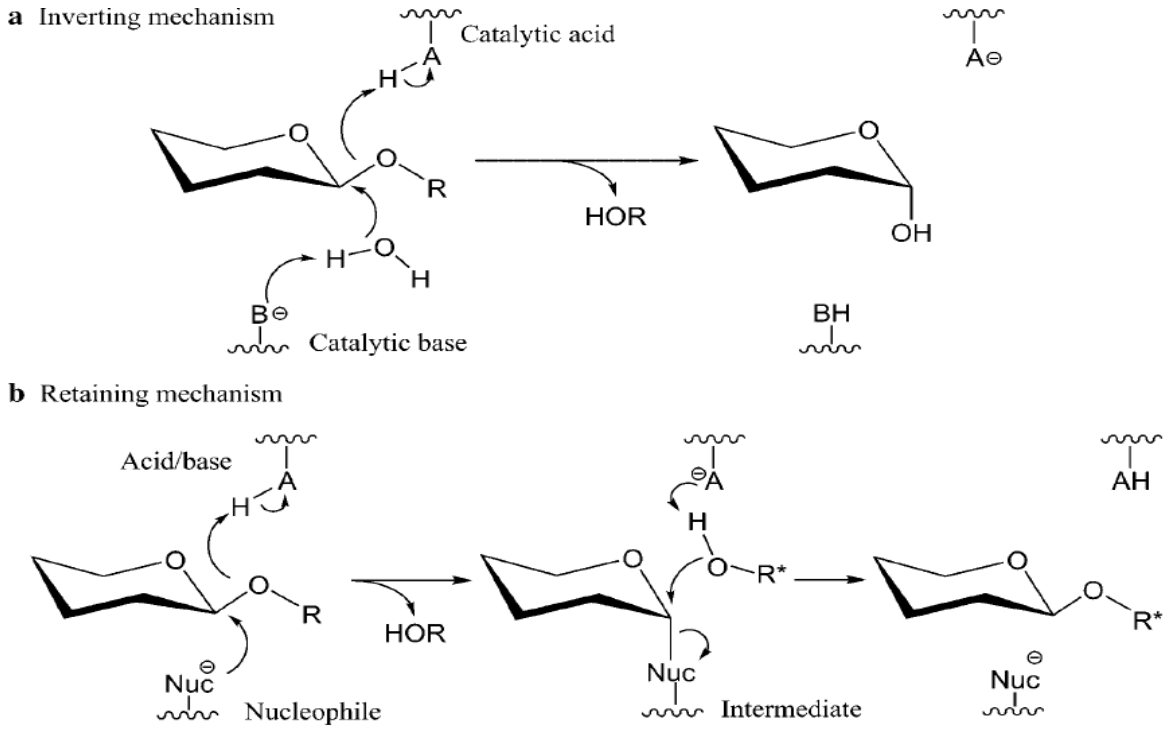

Figure 1.4. (a) Inverting and (b) retaining mechanism used by GHs to hydrolyze glycosidic bonds. The figure is taken from Vuong et al. (2010).

One important difference between inverting- and retaining GHs is the distance between the two acidic residues in the enzyme, which is greater in inverting GHs. In retaining GHs, the water molecule involved in hydrolysis attacks the anomeric center from the same side as the catalytic acid leaving the anomeric carbon hydroxyl in the original configuration, while in inverting GHs the water molecule attacks from the opposite site, leading to inversion of the configuration of the terminal hydroxyl (Sinnott 1990).

In the context of the degradation of recalcitrant polysaccharides, another feature of GHs is worth mentioning: processivity. Usually, recalcitrant polysaccharides are degraded by a mixture of processive and non-processive GHs working in synergy. Non-processive enzymes disrupt the ordered substrate surface and provide attachment sites for processive enzymes (Payne et al. 2012). Processive enzymes stay closely associated with the substrate in between hydrolytic steps, meaning that the single polymer chain in its active site is prevented from re-

associating with the insoluble material. This enables the enzyme to conduct several hydrolytic attacks on the chain while it slides along the polymer chain. In this way the enzyme reduces the number of times it has to gain access to a single chain, which is an energetically unfavourable process (Horn et al. 2006c; Zakariassen et al. 2009). GHs acting in a processive manner are typically multi-modular enzymes containing at least one CBM. Both exo- and endo- acting GHs can act in a processive manner, but since the two ends of the polymer chain are different after hydrolysis, two types of exo-acting enzymes exists. One type of exo-acting enzymes act on the reduced end of the polymer chain, whereas the other type acts on the non-reduced end (Horn et al. 2006a). Processive GHs usually exhibit characteristic active-site architectures with deep clefts or tunnels lined with aromatic residues (in particular tryptophan residues) that ensure binding and sliding of the chain through the active site. In contrast, non-processive enzymes have more open clefts with fewer aromatic residues. Hydrogen bonding and stacking with aromatic residues are the dominant interactions in carbohydrate-protein complexes (Payne et al. 2012; Sørlie et al. 2012) and mutagenesis of various conserved aromatic residues in or near the catalytic site have proven the importance of these residues for processivity in GHs (Horn et al. 2006c; Koivula et al. 1998; Zakariassen et al. 2009; Zhou et al. 2004).

Classical hydrolytic enzymes such as chitinases have to bind tightly to a single polysaccharide chain, which can be energetically demanding and often rate limiting when acting on crystalline substrates. Recently a new type of enzymes called lytic polysaccharide monooxygenases (LPMOs) was discovered, that appears to target the crystalline parts of the recalcitrant polysaccharides, complementing the endo- and exo-acting GHs.

1.2.4 Lytic Polysaccharide Monooxygenases

It is energetically demanding for GHs such as chitinases and cellulases (EC 3.2.1.4) to extract a single sugar chain from non-soluble and perhaps even crystalline substrates (Beckham & Crowley 2011). As early as 1950, Reese and co-workers suggested the presence of nonhydrolytic factors that made insoluble polysaccharides more accessible for other degrading enzymes (Reese et al. 1950). Today, it seems that Lytic Polysaccharide Monooxygenases (LPMO) are the factors that Reese et al were referring to.

Prior to the discovery of their enzymatic activity, LPMOs were classified in families CBM33 and GH61 in the CAZy enzyme classification database. Whereas GH61 are exclusively of fungal origin, CBM33 are found in different organisms, such as bacteria, viruses and fungi (Horn et al. 2012). As of April 2013, the CBM33 and GH61 families were reclassified into families 10 and 9, respectively, of the auxiliary activities (AA) (Levasseur et al. 2013). At the time of writing, the AA10 and AA9 families contained 680 and 259 sequences, respectively (CAZy 2013). In order to avoid confusion and to be in-line with the naming schemes used in the literature cited, AA10s and AA9s will be referred to as CBM33s and GH61s, respectively, throughout the rest of this thesis. CBM33 domains most often occur in proteins lacking other enzymatic domains, meaning that they tend to exists as individual entities (Vaaje-Kolstad et al. 2005a). The main topic of this thesis is CBP21, a single domain chitin-active CBM33-type lytic polysaccharide monooxygenase, produced by *Serratia marcescens*, a well-known chitin-degrading bacterium.

Enzymes acting on recalcitrant polysaccharides, such as chitin, face the problem of binding to the substrate, disrupting the crystalline surface, and directing a single polysaccharide-chain into the catalytic center (Eijsink et al. 2008). In 2005, Vaaje-Kolstad et al. discovered that a chitin-binding CBM33 from *S. marcescens*, called chitin-binding protein 21 (CBP21), increased substrate accessibility for hydrolytic enzymes acting on crystalline chitin. Five years later, a breakthrough was made when Vaaje-Kolstad and co-workers showed for first time that CBP21 is a metal-dependent enzyme that catalyses cleavage of glycosidic bonds in crystalline chitin by a mechanism that involves a hydrolytic and an oxidative step (Vaaje-Kolstad et al. 2010). By cleaving glycosidic bonds and thereby leaving a charged carboxylic acid on the substrate surface (reaction product), the enzyme both depolymerizes and disrupts the crystalline packing of the substrate and makes it more accessible for further degradation by chitinases. The same activity was also shown for *Ef*CBM33A from *Enterococcus faecalis*

V583 (Vaaje-Kolstad et al. 2012). Characterization of the CBM33 proteins E7 and E8 from *Thermobifida fusca* indicated that CBM33s did not *only* act on chitin (Moser et al. 2008). In 2011, Forsberg and co-workers showed that CelS2, a CBM33-containing protein from *Streptomyces coelicolor* A3(2) is capable of cleaving cellulose, generating oxidized chain ends (analogous to the product generated by CBP21) and increasing cellulase activity (Forsberg et al. 2011).

Harris et al. (2010) were first to show that GH61 increase degradation of cellulose, when added to cellulases. Harris and co-workers tested activity of several GH61s (GH61B and GH61E from *Thielavia terrestris* and GH61A from *Thermoascus aurantiocus*) on different cellulosic substrates. They concluded that GH61s are unlikely to be typical GHs, but seemed to have similar roles as CBP21. CBM33 and GH61 share less than 10% sequence identity, but since they are structurally similar it was proposed that GH61 acts on cellulose with a similar mechanism (Vaaje-Kolstad et al. 2010). Experimental studies of several GH61s Have confirmed this theory. Quinlan et al. (2011) showed that *Ta*GH61A, a GH61 from *Thermoascus aurantiacus*, catalyses oxidative cleavage of cellulose. The same group described the crystal structure of the enzyme and pointed out that enzyme activity was copper-dependent. In the same year, Westereng et al. (2011), showed that *Pc*GH61D from *Phanerochaete chrysosporium* was a metal-dependent oxidative enzyme that cleaves cellulose.

Both GH61 and CBM33 break glycosidic bonds in a crystalline environment and release oxidized products, although non-oxidized oligosaccharides have also been detected in some studies (Forsberg et al. 2011; Westereng et al. 2011)**.** Classical GHs, such as chitinases and cellulases, with substrate-binding grooves/pockets/tunnels bind to free polysaccharide chains and are active on soluble (oligomeric) substrates, GH61s and CBM33s are inactive on "soluble" polysaccharides, suggesting that they do not act on single chains. This can be explained by their flat active site surface architecture consisting of mostly polar residues and only few aromatic residues. The flat active site suggests that GH61 and CBM33 are optimized for binding to the surfaces of ordered and more complex polysaccharide structures and not to single chains (Vaaje-Kolstad et al. 2010; Westereng et al. 2011).

GH61 and CBM33 LPMOs have a highly conserved N-terminal histidine that together with its free amino group and a second highly conserved histidine coordinate a copper ion in a type-2 copper site geometry, which is essential for activity (fig. 1.5) (Aachmann et al. 2011; Phillips et al. 2011; Quinlan et al. 2011). Copper is one of the dominating metals involved in O_2 activation by proteins. The metal can cycle between several redox states and is capable of one-electron transfer which is necessary for O_2 activation by CBM33s and GH61s (see Fig. 1.6 for the role of copper and O_2 in the proposed reaction mechanism) (Solomon et al. 2001). The importance of a metal ion has been investigated by addition of ethylenediaminetetraacetic acid (EDTA, a metal chelator) and metal binding site mutations in both CBM33s and GH61s, which led to reduced or absent activity (Forsberg et al. 2011; Phillips et al. 2011; Vaaje-Kolstad et al. 2005a). LPMOs require an electron donor in order to function efficiently, which can either be a naturally occurring reducing agent (e.g. the polyphenol lignin in plant cell walls) or an externally provided compound (e.g. ascorbic acid), or an enzyme capable of providing electrons like cellobiose dehydrogenase. CBM33 efficiency is highly increased by addition of an external reducing agent, such as ascorbic acid or reduced gluthatione. (Forsberg et al. 2011; Vaaje-Kolstad et al. 2010). The same activity is seen for GH61 when the fungal enzyme cellobiose dehydrogenase (CDH) is available (together with CDH substrate) (Langston et al. 2011; Phillips et al. 2011).

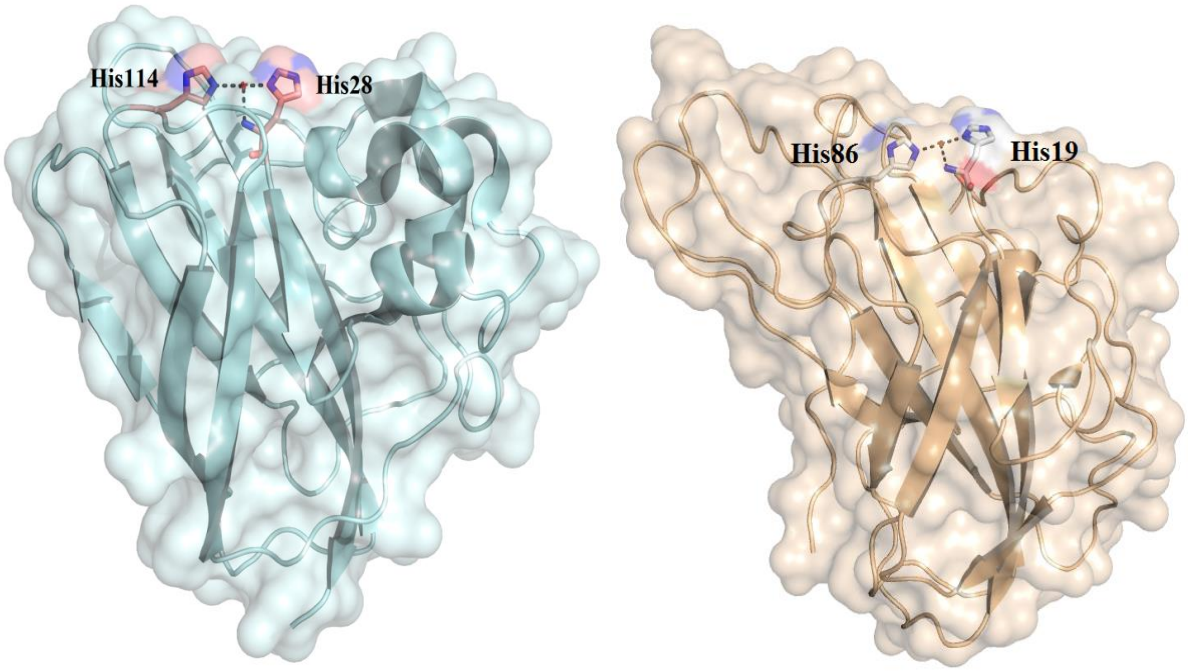

Figure 1.5. Crystal structure of CBP21 (Uniprot ID: O83009; PDB ID: 2BEM) from *Serratia marcescens* (left) and GH61E (Uniprot ID: D0VWZ9; PDB ID: 3EII) from *Thielavia terrestris* (right), a thermophilic cellulose degrading ascomycete. His28 (CBP21)/His19 (GH61E) is the N-terminal residue of the protein after the signal peptide cleaved off. The red sphere represents the metal ion. The figures were generated using PyMOL (DeLano 2002).

All experimental evidences described above indicated that enzymes belonging to the CBM33 and GH61 families were erroneously classified. This was, as mentioned, taken into account by the CAZy curators, and the families were re-classified in 2013. Details of the catalytic mechanism remain to be elucidated, but Phillips et al. (2011) proposed a reaction mechanism (Fig. 1.6) and also suggested naming of these enzymes polysaccharide monooxygenases (PMO). The name used by most workers in the field today is lytic polysaccharide monooxygenase, which is also adopted in this thesis. Phillips and co-workers divided LPMOs into three groups based on their structure and observed variation in reaction products generated from cellulose. LPMO-type I oxidizes the glucose unit at the C1 position releasing lactones (i.e. the same reaction as CBP21), which in turn are spontaneously hydrolysed to aldonic acids under alkaline conditions, while LPMO-type II oxidize glucoses at C4 and release ketoaldose (Fig. 1.7). LPMO-type III does not have a clear specificity towards C1 or C4 and generates both reducing and non-reducing end oxidized products (Beeson et al. 2012; Phillips et al. 2011). Oxidation of C1 is the most common activity of LPMOs studied so far (Beeson et al. 2012; Forsberg et al. 2011; Vaaje-Kolstad et al. 2010; Westereng et al. 2011).

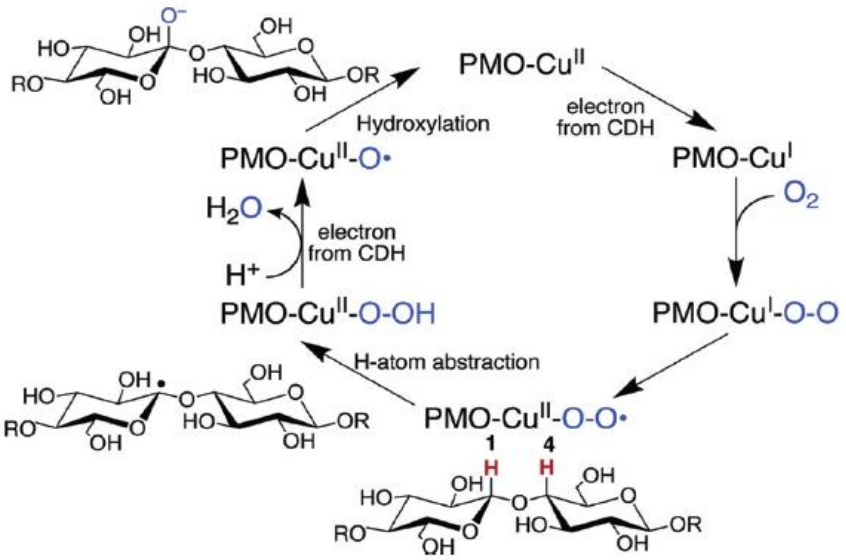

Figure 1.6. Proposed general mechanism of LPMOs. By donating an electron, CDH reduces the Cu(II) to Cu(I) by one-electron transfer. Molecular oxygen binds to Cu(I) and by one-electron transfer, a copper superoxo intermediate is formed, which then abstracts a proton from C1 or C4 on the carbohydrate. A second electron from CDH leads to cleavage of the Cu-bound hydroperoxide. The copper oxo-species (Cu–O•) then couples with the substrate radical, which introduces a hydroxyl group to the substrate. The addition of the hydroxyl group destabilizes the glycosidic bond leading to elimination of the adjacent glucose unit (Phillips et al. 2011) .The figure is taken from Phillips et al. (2011).

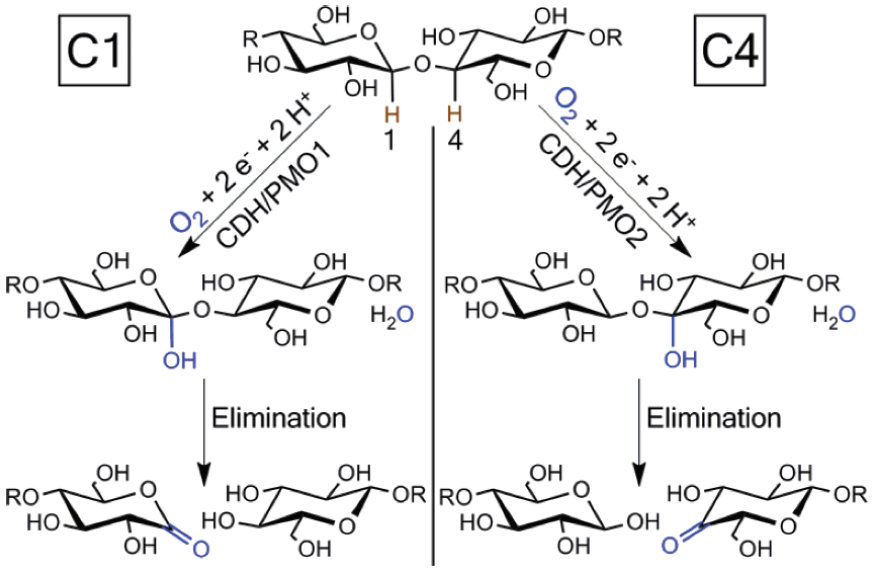

Figure 1. 7. The difference between LPMO-types I and II. (C1) LPMO-type I hydroxylates C1 leading to formation of lactones that spontaneously convert to aldonic acids (Westereng et al. 2013). **(C4)** LPMO-type II hydroxylate C4 leading to formation of ketoaldoses. Introduction of oxygen at either C1 or C4 is thought to lead to an elimination reaction and breaking of the glycosidic bond. The reaction is irreversible since the carbon on the reducing- or non-reducing end is oxidized. (Beeson et al. 2012). The figure is taken from Beeson et al. (2012).

The discovery of LPMO has changes the paradigm for enzymatic conversion of recalcitrant polysaccharides. An overview of LPMO acting in synergy with other enzymes to degrade cellulose is illustrated in Figure 1.8.

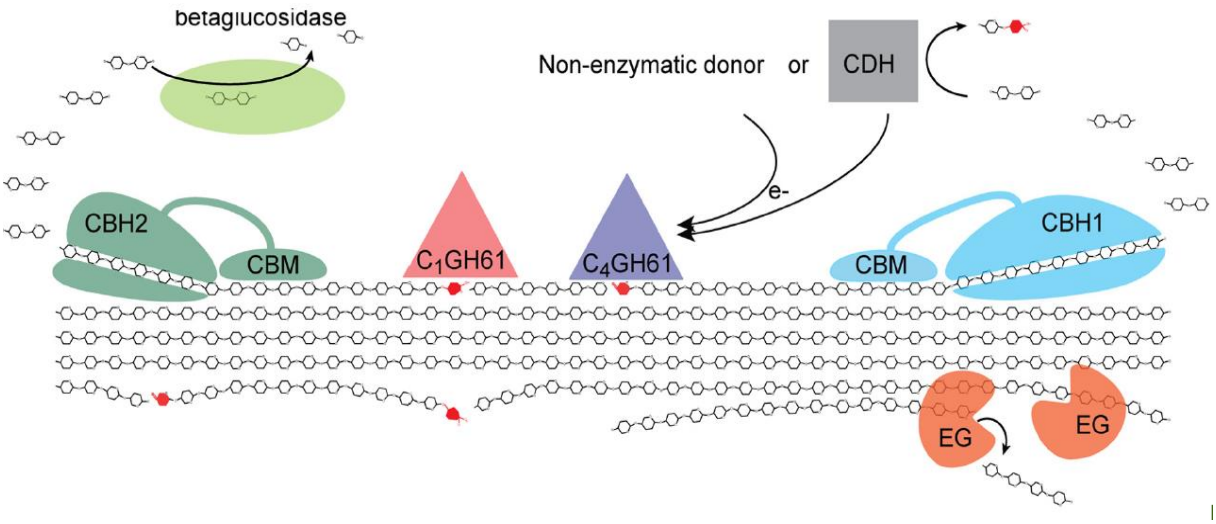

Figure 1.8. Overview of enzymatic degradation of cellulose in the presence of LPMOs acting in synergy with other cellolytic enzymes. C_1GH61 oxidizes C1, while C_4GH61 oxidizes C4. The GH61s open up the crystalline substrate generating oxidized sugars (marked red), which generates new chain ends that cellobiohydrolases (CBH1/CBH2) act upon. CBH1/CBH2 are processive enzymes, and convert the cellulose into cellobiose, which is further cleaved to glucose monomers by β-D-glucosidases (Horn et al. 2012). Electrons to the GH61s may be provided by cellulose dehydrogenase (CDH). Endoglucanases (EGs) are thought to act on the less crystalline regions of the substrate. The figure is taken from Horn et al. (2012).

1.3 The chitinolytic machinery of *Serratia marcescens*

The presence of chitinolytic organisms, such as *Serratia marcescens*, plays an important role in maintaining the ecological balance in nature. *S. marcescens*, a gram-negative soil bacterium, classified as a member of the *Enterobacteriacae* family, is one of the best known enzyme systems for the conversion of crystalline chitin (Monreal & Reese 1969; Suzuki et al. 1998; Vaaje-Kolstad et al. 2013). In the late stage of bacterial growth, this bacterium is known to synthesize a characteristic red pigment, prodigiosin (2-methyl-3-amylmethoxyprodigiosene), which makes the bacteria slightly pink (Venil & Lakshmanaperumalsamy 2009). When grown on chitin, the bacterium synthesizes three different chitinases belonging to family GH18: ChiA, ChiB and ChiC. ChiA and ChiB are exo-acting processive chitinases, while ChiC is a non-processive endo-acting chitinase (Horn et al. 2006a; Hult et al. 2005; Synstad et al. 2008). The chitinases cleave the β-1,4 glycosidic linkage between adjacent GlcNAc residues. Cleaving of the glycosidic linkage between GlcNAc residues creates soluble oligosaccharides. The main product from chitinase action is *N,N*-diacetylchitobiose $(GlcNAc)_2$, which, together with other soluble oligomeric products, is further hydrolysed from the non-reducing end to single GlcNAc units by chitobiase (EC 3.2.1.52), a family GH20 β-*N*-acetylhexosaminidases (EC 3.2.1.52) (Fig.1.9). Efficient chitin degradation by *S. marcescens* also depends on CBP21, the family CBM33 LPMO standing at the basis of the discovery of this enzyme family (Vaaje-Kolstad et al. 2013).

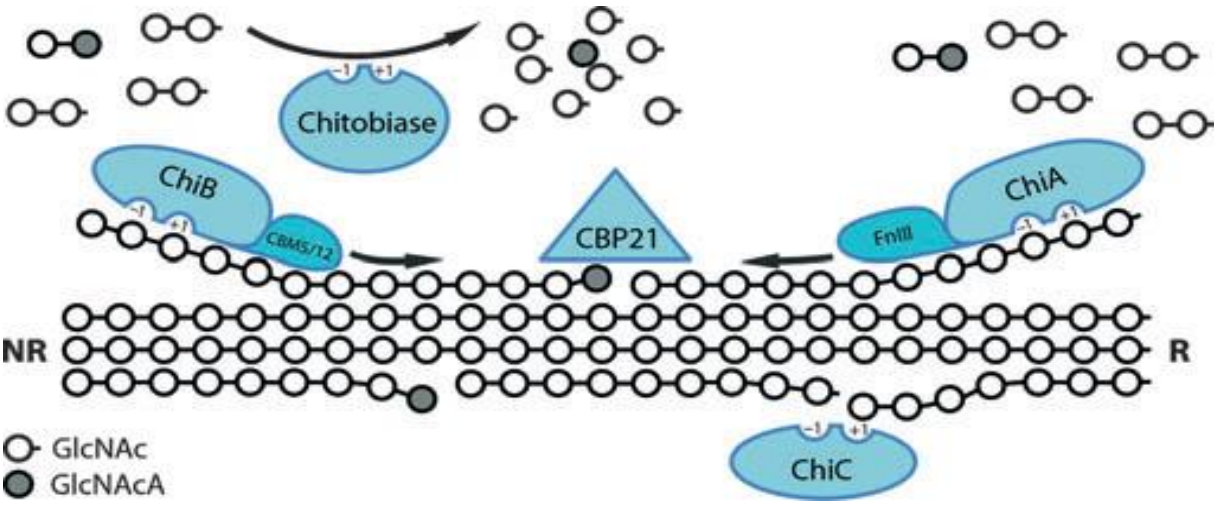

Figure 1.9. An overview of the chitinolytic machinery of *S.marcescens*. The figure shows how the enzymes are working in synergy to degrade chitin (GlcNAc units are illustrated as open circles)**.** CBP21 and ChiC open up the substrate making it more accessible for ChiA and ChiB, which in the case of CBP21 generates oxidized

chain ends (marked grey). ChiA degrades the polymer chain from the reducing (R) end while ChiB degrades from the non-reducing (NR) end (Hult et al. 2005). Note that ChiA and ChiB comprise binding module(s) located in opposite directions relative to their catalytic domains. ChiC contain a family 12 and a fibronectin type III-like CBM, which are not shown since there is no structural information on their location. Products from chitinase action are further degraded to monomers by chitobiase. The figure is taken from Vaaje-Kolstad et al. (2013).

1.4 Chitin-binding protein 21, a family CBM33 lytic polysaccharide monooxygenase

CBP21 from *Serratia marcescens* was first described by Fuchs and his co-workers in 1986 and (erroneously) claimed to be a catalytically active chitinase with a molecular mass of 21 kDa (Fuchs et al. 1986). In 1997, Watanabe et al. showed that this protein, in the culture supernantant of *S. marcescens* 2170, adsorbed to chitin but did not have chitinase activity. The fact that this protein had chitin binding activity and was produced in large amounts by this strain in the presence of colloidal chitin, suggested that CBP21 was somehow involved in the chitin degrading system of this bacterium (Watanabe 1997). Suzuki and co-workers demonstrated that all five proteins secreted by *S. marcscens* 2170 when grown in presence of chitin were regulated in parallel and produced in large amount. The same group elucidated the nucleotide sequence of the CBP21 gene and showed that it was located 1.5 kb downstream of the ChiB gene (but not in the same operon). The full length protein consists of 197 amino acid residues including an N-terminal signal peptide of 27 amino acids, which is cleaved off during secretion of the protein to the culture medium. The mature protein is 170 residues with a molecular mass of 18.8 kDa. It was further shown that CBP21 protein had strong affinity for β-chitin and somewhat lower affinity for regenerated chitin and colloidal chitin, while binding to cellulose was low and to chitosan almost negligible (Suzuki et al. 1998). The fact that the protein has strong affinity for β-chitin led to the name chitin-binding protein 21, where the number reflects the molecular weight in kDa. (Vaaje-Kolstad et al. 2013).

Proteins with chitin-binding activity similar to CBP21 are produced by various organisms. CHB1 from *Streptomyces olivaceoviridis* was the first CBM33 to be characterized and was shown to bind specifically to a-chitin (Schnellmann et al. 1994). CbhB, another CBM33 with features similar to CBP21 was identified in *Bacillus amyloliquefaciens*. CbhB has 45% amino acid sequence identity to CBP21 and binds to both α- and β-chitin (Chu et al. 2001). A

CBM33 named CbpD was also reported in the opportunistic bacterium *Pseudomonas aeruginosa*, but as for all CBM33s, the role of this protein in chitin degradation was unknown (Folders et al. 2000). In 2005, demonstrated that CBP21 boosted chitinase activity suggesting that CBP21 introduces structural changes in the substrate making it more accessible for hydrolysis by chitinases (Vaaje-Kolstad et al. 2005b) . Five years later, a breakthrough was made when Vaaje-Kolstad and co-workers showed that CBP21 in fact are an enzyme that catalyses cleavage of glycosidic bonds in crystalline chitin (Vaaje-Kolstad et al. 2010)

1.4.1 Structure of CBP21

The structure of CBP21 was solved by X-ray crystallography and revealed a three-stranded and a four-stranded β-sheet forming a β-sandwich (Fig. 1.10). Between β-strand one and two, a short α-helix, two short 3_{10} helices and loops, make up a pseudo domain of 65 residues. The fold of CBP21 is similar to fibronectin type III fold, which is often seen in various eukaryotic proteins, but only in carbohydrate-active proteins in bacteria (Vaaje-Kolstad et al. 2005a). Experiments conducted by Watanabe et al. showed that Fn-III type modules are not involved in chitin binding, but have an important role in hydrolysis in chitin (Watanabe et al. 1994). In what way the domain contributes to hydrolysis is unknown, but it has been suggested that it could function as a flexible linker between the catalytic site and the chitin-binding domain. Fn-III type modules have been proposed to be involved in cell adhesion (see section 1.5) (Frederiksen et al. 2013). Four cysteine residues create two disulphide bridges, one in the pseudo domain and one connecting β-strands 4 and 5. Interestingly, the structure of CBP21 does not reveal any cleft, tunnel, pocket or surface with exposed aromatic residues, which is a common property for enzymes that interact with carbohydrates. On the other hand, the core of CBP21 consists of several aromatic residues, in particular W94, W108, W119, Y121, W128, W178, F187 and Y188. The enzyme has a surface patch with highly conserved solvent exposed polar residues and only one conserved solvent-exposed aromatic residue, Tyr-54 (Vaaje-Kolstad et al. 2005a). Highly conserved surface-exposed residues of CBP21 have been mutated for investigation of their involvement in substrate binding and "chitinase-boosting activity". Mutation of Y54, E55, E60, H114, D182 to alanine showed modestly decreased affinity to β-chitin, suggesting they have a role in substrate binding. Y54A and E60A showed the largest increase in K_d. Since no single mutant was incapable of binding to the substrate, it was suggested that several residues have to be involved in the binding event (Vaaje-Kolstad et al. 2005a). An experiment determining the ability of CBP21 wild type and "binding mutants"

to boost chitinases showed that mutant N185A had low binding affinity, but was still able to increase chitinase activity, suggesting this residue is not involved in disrupting the substrate. On the other hand mutants Y54A, E55A, E60A, H114A and D182A were no longer able to increase chitin turnover by chitinase, suggesting that these residues are involved in disruptive interactions with the chitin substrate. (Vaaje-Kolstad et al. 2005b). Moreover recent data obtained from nuclear magnetic resonance (NMR) experiments have revealed that residue H28, Q53, Q57, S58, A111 and G112 also are involved in substrate-binding (Vaaje-Kolstad et al. 2013). All residues mentioned above are illustrated in Figure 1.10; most of these residues show high degree of conservation among CBM33s. Figure 1.10 also shows details of the active site. Chelation/removal of the copper ion by EDTA or mutation of the metal binding residue His114 knocks out the activity of CBP21 (absence of soluble oxidized oligosaccharides), which confirms the importance of the copper. The same loss of activity has been observed for GH61E when corresponding residue, His86, was mutated to alanine (see section 1.2.4, Fig.1.5 for comparison of the catalytic site of CBP21 and GH61E) (Vaaje-Kolstad et al. 2010).

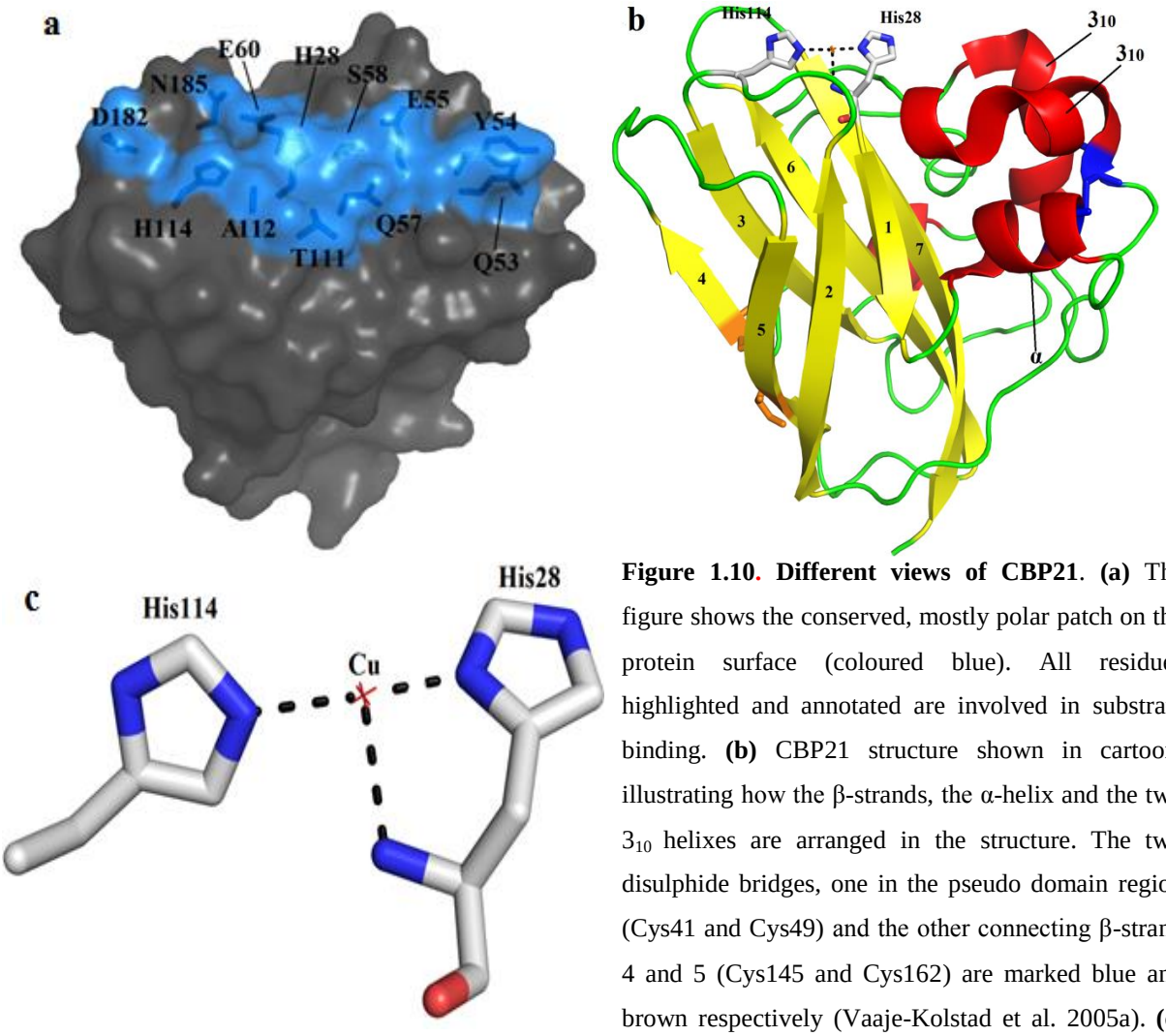

Figure 1.10. Different views of CBP21. **(a)** The figure shows the conserved, mostly polar patch on the protein surface (coloured blue). All residues highlighted and annotated are involved in substrate binding. **(b)** CBP21 structure shown in cartoon, illustrating how the β-strands, the α-helix and the two 3_{10} helixes are arranged in the structure. The two disulphide bridges, one in the pseudo domain region (Cys41 and Cys49) and the other connecting β-strand 4 and 5 (Cys145 and Cys162) are marked blue and brown respectively (Vaaje-Kolstad et al. 2005a). **(c)** A close-up picture of the metal binding site showing how the N-terminal His28 and His114 bind the metal ion. All figures are generated using PyMOL (DeLano 2002).

1.4.2 Insight into LPMO mechanism and functionality from work on CBP21

The role played by CBM33s and GH61s in carbohydrate degradation remained elusive for a long time until it was discovered that CBP21 is a an enzyme which cleaves glycosidic bonds in a oxidative manner generating two new chain ends; a normal non reducing chain end and a chain end with a C1 oxidized sugar, (2-(acetylamino)-2-deoxy-D-gluconic acid (GlcNAcA), also referred to as an aldonic acid (Vaaje-Kolstad et al. 2010).

One essential experiment conducted by Vaaje-Kolstad to reveal the mechanism of CBP21 was to perform experiments with isotope labelled reactants (both H_2O^{18} and $^{18}O_2$). These experiments showed that the oxidized reaction product, the aldonic acid, contained one

oxygen atom coming from dioxygen and the other coming from bulk water (Fig. 1.11). Furthermore, it was shown that the reaction was highly inhibited by cyanide, an O_2 mimic, indicating that one of the reactants indeed was dioxygen. Experiments also showed that external electron donor such as reduced glutathione, ascorbic acid or Fe(II)SO_4 boosted the activity of CBP21 to unexpected levels. The chain break caused by CBP21 driven glycosidic bond cleavage results in generation of negatively charged aldonic acid, which, obviously, no longer adopts the normal chair confirmation of a hexose (Fig. 1.11). It has been suggested that introduction of negative charges to the structure of chitin leads to disruption of substrate packing, making it less rigid and more accessible. Complete conversion of chitin by ChiC is achieved approximate six times faster in the presence of CBP21 and ascorbic acid. (Vaaje-Kolstad et al. 2010).

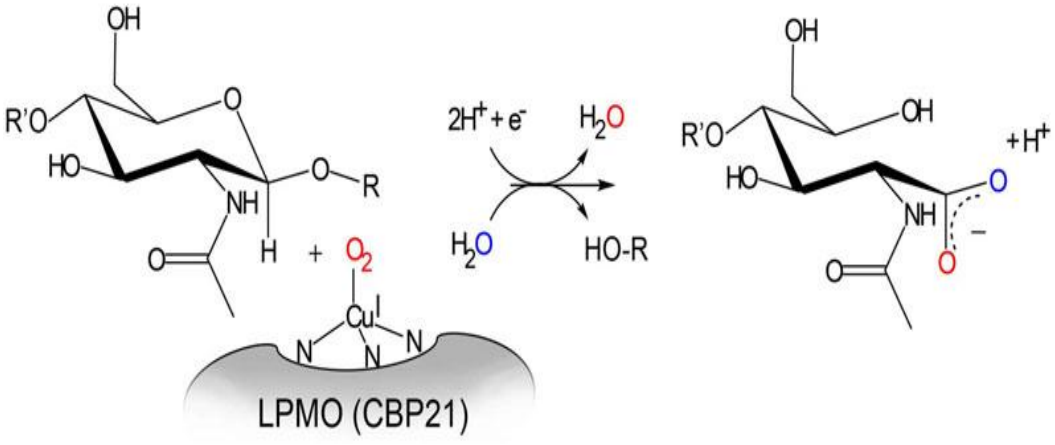

Figure 1.11. The reaction catalysed by CBP21. Copper(II) is reduced to copper(I) by either an external or natural reductant. Subsequently, the oxygen is activated by the reduced copper in a reaction that is not fully understood (see fig. 1.6 for a proposed mechanism). Two products are formed, one with a novel non-reducing end (HO-R) and one with an oxidized end in the form of a lactone, which is hydrolysed to an aldonic acid at physiological pH. Oxygen marked red comes from molecular oxygen, while the oxygen marked blue is introduced during the hydrolysis step (Vaaje-Kolstad et al. 2013). The figure is taken from Vaaje-Kolstad et al. (2013).

Most of the soluble products generated by CBP21 are even-numbered oligosaccharides (the structural unit of chitin is a disaccharide, see section 1.1.1, Fig. 1.1) with a degree of polymerization (DP) below ten. This is compatible with the idea that CBP21 acts on crystalline chitin, which can be approached from one side, the crystal surface, only. Products with a higher DP are hard to detect due to their low solubility and they most likely remain bound to the remaining insoluble chitin particles (Vaaje-Kolstad et al. 2010).

1.5 Proteins of the CBM33 family related to host-microbe interactions and/or virulence

Many bacteria live in symbiotic relationships with humans and other higher organisms. The bacteria get nutrition and a stable growth environment, while the host gets digestive and metabolic help. Interactions between human cells and bacteria are especially important in the gastrointestinal tract (Neish 2009). In recent years, several proteins belonging to the CBM33 family from microbes interacting with humans have been identified and characterized. Some of these have been reported to play a role in in host-microbe interactions and/or virulence in humans or other animals. Various pathogenic bacteria secrete CBM33s during cell surface attachment or in response to stress during colonization (e.g. Folders et al. 2000; Bhowmick et al 2008).

As mentioned in section 1.4, Folders et al. identified a CBM33 secreted by *Pseudomonas aeruginosa* named chitin-binding protein D (CbpD). The protein was shown to be expressed in response to high-density conditions, such as in biofilms and during pathogenesis (colonization). CbpD was only found in clinical isolates of *P. aeruginosa*, but not in strains living in soil where biomass is abundant. The group suggested that CbpD play a role in bacterial adhesion protecting the bacteria against elastase and also aids formation of biofilm (Folders et al. 2000). *P. aeruginosa* colonize the lungs of cystic fibrosis patients and is an important threat to the health of these patients. Manos et al reported that CbpD is highly up-regulated during lung infection in patients with cystic fibrosis (Manos et al. 2009).

Another CBP that have been associated with virulence is *Ef*CBM33A from *Enterococcus faecalis*, which is an opportunistic bacterium that normally lives peacefully in the intestinal tract of humans. Besides being able to metabolize and degrade chitin (especially β-chitin) (Vaaje-Kolstad et al. 2012), the bacterium is involved in infection and has been found to be an important hospital pathogen. The bacterium is known to cause urinary tract infection in humans and a study by Vebø et al. showed that several proteins are up-regulated in the presence of urine, including the gene encoding *Ef*CBM33A (Vebo et al. 2010). The same gene was also up regulated when the bacterium was incubated with blood (Vebo et al. 2009). *Vibrio cholerae* is also a bacterium that causes infections in humans. The infection is located in the small intestine and cause watery diarrhea and possible death if not treated properly. A multi-modular protein called *N*-acetylglucosamine binding protein (GbpA) has a N-terminal

CBM33 domain which is involved in *V. cholerae* intestinal colonization. Experiments done by Kirn et al. shoved that this protein is secreted during colonization and is important for bacterial survival. GbpA mediates attachment to human epithelial cells by binding to *N*-acetylglucosamines (GlcNAcs) on the cell surface. The same group suggested this protein as a potential vaccine target (Kirn et al. 2005). *V. cholerae* was also shown to bind to mucin, which is the first surface the bacterium meets in the gastrointestinal tract. The surface of mucin consists of many types of sugars, including monomers of chitin (GlcNAc). Initial attachment of the bacterium to mucin in mouse was shown to increase mucin production, which led to increase production of the colonization factor GbpA by the bacteria. Mutation studies of GbpA showed a decrease in intestinal adherence by the bacterium and thus to less production of mucin and a lower degree of bacteria colonization (Bhowmick et al. 2008). Wong et al showed that domain 1 (N-terminal domain) of the protein, which is a chitin-binding domain, was important for mucin binding and colonization of the intestines (Wong et al. 2012).

Lactobacillus plantarum is a probiotic bacterium found in the gastrointestinal tract of humans. The bacterium is part of the human microbiota (Izquierdo et al. 2009) and has been extensively studied. *L. plantarum* is in constant contact with mucin and secrets a CBM33 called *Lp*CBM33, which has been proven to bind to chitin and to glycoproteins on the surface of mucin (Sanchez et al. 2011). Several species of *L.plantarum* are present in the human vaginal microflora, including the WTC1 strain producing *Lp*CBM33. Liu and co-workers proved that the WTC1 strain inhibits the growth of *Staphylococcus aureus* (a bacterium that can cause toxic shock syndrome in women) when grown in modified genital tract secretion medium (mGTS). Since *Lp*CBM33 was one of few heavily secreted proteins the group suggested the CBM33 plays a role in inhibiting growth of *S. aureus* in the vaginal tract of women (Liu et al. 2011).

Yersinia enterocolitica is a bacterium causing infection when ingested as contaminated food or water. Proteins secreted via the type II secretion pathway are often associated with pathogenesis (Korotkov et al. 2012) and among the three proteins secreted by the type II pathway in *Y. enterocolitica*, is a CBM33-type chitin-binding protein called ChiY. Shutinoski et al. suggested that this protein is important for interactions with and/or degradation of polysaccharides during infection (Shutinoski et al. 2010).

Several of the bacteria mentioned above use sugar-binding mechanisms in cell adhesion, but the relevance of LPMO activity in this context is still unknown (Frederiksen et al. 2013). The evidence provided above clearly suggests that the role of CBM33s in nature is more than biomass degradation. Since the role of CBM33s in cell-adhesion and/or virulence is a relative new and unexplored field, more research has to be done to elucidate these novel roles of LPMOs.

1.6 Purpose of this study

The enzymatic activity of CBP21 was discovered in 2010, but many aspects of its catalytic mechanism remain unknown and further studies are needed. Furthermore, today, there are very limited options for precise quantitative determinations of LPMO activity.
The primary purpose of this study was to gain more insight into the binding properties and the catalytic mechanism of CBP21. To achieve this goal several conserved residues were mutated by site-directed mutagenesis followed by protein expression, purification and characterization. Seven different mutants of CBP21 were constructed, and to investigate whether the mutations had effect on substrate binding and/or the catalytic mechanism, various activity assays and binding assays were conducted followed by product analysis. This analytical part included the testing of a novel assay to measure enzyme activity based on detection of hydrogen peroxide from a futile side reaction of LPMOs, which was recently developed by Kittl et al. (2012).

Available literature suggests that members of the CBM33 family have other important roles than mere biomass degradation, in particular roles in host-microbe interaction and pathogenesis. As a side project in this thesis, five fluorescently labelled CBM33 from bacteria known to interact with the human gut, were tested for substrate specificity by a glycan array screen.

2 MATERIALS

2.1 Laboratory instruments

Instrument	Brand
Agilent 1290 Infinity UHPLC	Agilent Technologies
Äkta purifier	GE Healthcare
BioLogic LP chromatographic system	BioRad
Centrifuges	
Avanti™ J-25 centrifuge with JA-14 rotor	Beckman Coulter
Centrifuge, 5415 R	Eppendorf
Centrifuge, 5430 R	Eppendorf
DNA electrophorese power supply, Model 200/2.0	BioRad
Fraction collector, Frac 920	GE Healthcare
Multitron eco incubator	INFORS
MALDI-TOF MS, Ultra flex instrument	Bruker Daltonics
Mastercycler gradient, PCR cycler	Eppendorf
$MultiScreen_{HTS}$ Vacuum Manifold	Millipore
Multiskan FC photometer	Thermo Scientific
Open Heating Bath Circulator, ED-7A/B	Julabo
pH meter 827	Metrohm
Power Pac 300 power supply	BioRad
Qubit fluorometer	Invitrogen
Rotator mixer,Multi RS-60	BioSan
Rotary shaker, IKA ® HS 260 basic	Bie & Berntsen
Semi micro cells, 104-OS 10 mm	Hellma
Spectrophotometer, Biophotometer	Eppendorf
Spectrophotometer, U-1900	Hitachi
Thermomixer, Comfort	Eppendorf
Thermomixer, Vortemp	Thermo Scientific
Vacuum pump, High Output	Millipore
VP-ITC MicroCalorimeter	MicroCal
Water bath, SWB	VWR
Water bath	Stuart

2.2 Chemicals

Chemical	Supplier
3-Hydroxyanthranilic acid	Sigma-Aldrich
2,5-Dihydroxybenzoic acid (DHB)	Bruker Daltonics
Agar bacteriological (Agar No. 1)	Oxoid
Agarose, SeaKem®	Lonza
Acetic acid, CH_3CO_2H	VWR
Acetonitrile, CH_3CN	VWR
Ammonium sulphate, $NaSO_4$	Merck
Ampicillin	Sigma-Aldrich
Bacto™ Peptone	Becton, Dickinson and Co
Bacto™ yeast extract	Becton, Dickinson and Co
Bacto™Tryptone	Becton, Dickinson and Co
Bis-Tris methane	Sigma-Aldrich
Catechin	Sigma-Aldrich
Copper sulphate, $Cu(II)SO_4$	Sigma-Aldrich
Coomassie Brilliant Blue R250	Merck
DL-Dithiothreitol (DTT)	Sigma-Aldrich
Ethanol, 96 % (w/v)	Arcus
Ethylenediaminetetraacetic acid (EDTA)	Sigma-Aldrich
Glycerol, 85 % (w/v)	Merck
Gallic acid	Sigma-Aldrich
Hydrochloric acid, HCl	Merck
Hydroquinone	Sigma-Aldrich
-L -Ascorbic acid	Sigma-Aldrich
Magnesium chloride, $MgCl_2$	Qiagen
Methanol, 85 % (w/v)	Merck
Potassium phosphate dibasic, K_2HPO_4	Sigma-Aldrich
Potassium dihydrogen phosphate, KH_2PO_4	Sigma-Aldrich
Phenylmethanesulfonylfluoride (PMSF)	Sigma-Aldrich
Potassium chloride, KCl	Merck
Sucrose	VWR
Sodium chloride, NaCl	J.T. Baker

Sodium phosphate dibasic heptahydratem, Na_2HPO_4 x $7H_2O$	Sigma-Aldrich
Sodium hydroxide, NaOH	Sigma-Aldrich
Sulphuric acid, H_2SO_4	Sigma-Aldrich
Tartaric acid	Sigma-Aldrich
Trizma® base	Sigma-Aldrich
L-Gluthatione, reduced	Sigma-Aldrich

2.3 Bacterial strains

Table 2.1. Bacteria strains used for protein expression, transformation and plasmid isolation.

Strain	Application	Supplier
Escherichia coli OneShot® BL21 *(*DE3) Star™	Protein expression	Agilent Technologies
Escherichia coli XL1-Blue®	Plasmid replication/ storage/preparation	Stratagene
Escherichia coli DH5α™	Plasmid replication/ storage/preparation	Invitrogen

2.4 CBM33s and plasmids

Table 2.2. CBM33s and plasmids

Protein	Strain	Plasmid	Reference
CBP21	*Serratia marcescens* BJL 200	pRSET-B/*cbp21*	(Vaaje-Kolstad et al. 2005a)
*Ef*CBM33A	*Enterococcus faecalis* V583	pBAD/HisB-*Ef0362*	(Vaaje-Kolstad et al. 2012)
LpCBM33(1697)	*Lactobacillus plantarum* WCFS1	pRSET-B/*Lp_1697*	(Johansen 2012)
*Ll*CBP33A	*Lactococcus lactis* IL1403	Purified protein was provided by Gustav Vaaje-Kolstad	(Vaaje-Kolstad et al. 2009)
GbpA	*Vibrio cholerae* serotype O1	Purified protein was provided by Gustav Vaaje-Kolstad	(Wong et al. 2012)

2.5 Substrates

Table 2.3. Substrates and their specifications

Substrate	Specifications
β-chitin^{A}	Dried and milled β-chitin from squid bone. 80 mesh-sized particles, France Chitin, France.
β-chitin^{B}	β-chitin^{A} in 1.8 mM acetic acid sonicated for 8 minutes (pulse on/off 0.5/0.5 sec with amplitude of 35%) in TraceSELECT® Ultra water
β-chitin^{C}	β-chitin^{B} in 50 mM Tris, pH 8

2.6 Kits

Table 2.4. Kits and their applications

Kit	Supplier	Application
Alexa Fluor® 488 Protein Labelling	Invitrogen	Protein labelling
Amplex® Red Hydrogen Peroxide Assay	Invitrogen	Hydrogen peroxide detection
NucleoSpin® Plasmid/Plasmid (NoLid)	Machery-Nagel	Plasmid isolation
Quant-iT® dsDNA BR Assay	Invitrogen	Determination of dsDNA concentration
QuikChange® Site-Directed Mutagenesis	Agilent	Site-directed mutagenesis

2.7 Mutagenic primers

Table 2.5. Mutagenic primers utilized in site-directed mutagenesis. The primes names are composed of the original amino acid (e.g. T111Af), the residue number (e.g. T111Af), the new amino acid (e.g. T111Af) and forward or reverse primer (T111Af or T111Ar, respectively). Mutated nucleotides are underlined and printed in bold face Primer sequences are indicated from 5' to 3'.

Primer name	Primer sequence	GC-content, %	T_m, °C
S58Af	GTACGAACCGCAG**GCC**GTCGAGGGCCTG (28)	71.4	>75
S58Ar	CAGGCCCTCGA**CGG**CCTGCGGTTCGTAC (28)	71.4	>75
T111Af	TACCTGGAAGCTG**G**CCGCGCGTCACAG (27)	66.7	72.6
T111Ar	CTGTGACGCGCGG**C**CAGCTTCCAGGTA (27)	66.7	72.6
A112Gf	GGAAGCTGACCG**G**GCGTCACAGCAC (25)	68	71.2
A112Gr	GTGCTGTGACGC**C**CGGTCAGCTTCC (25)	68	71.2
W178Ff	GTGATCCTTGCCGTGT**TC**GACATAGCCGACACCG (34	59	69
W178Fr	CGGTGTCGGCTATGTC**GA**ACACGGCAAGGATCAC (34)	59	69
I180Rf	CCTTGCCGT**G**TGGGACAGAGCCGACAC (27)	66.7	72.6
I180Rr	GTGTCGGCTCTGTCCCA**C**ACGGCAAGG (27)	66.7	72.6
T183Af	GGGACATAGCCGAC**GCC**GCTAACGCCTTC (29)	65.5	73.7
T183Ar	GAAGGCGTTAG**CGG**CGTCGGCTATGTCCC (29)	65.5	73.7
F187Yf	CACCGCTAACGCCT**A**CTATCAGGCGATCG (29)	58.6	70.9
F187Yr	CGATCGCCTGATAG**T**AGGCGTTAGCGGTG (29)	58.6	70.9

3 METHODS

3.1 Cultivation and storage of bacteria

3.1.1 Growth media for bacteria

Luria-Bertani (LB) liquid medium (1 L)

- 10 g Bacto® Trypton
- 10 g NaCl
- 5 g Bacto Yeast extract

The dry components were mixed in 400 ml dH_2O and stirred for 5 minutes to fully dissolve before addition of dH_2O to a final volume of 1 L. The medium was then autoclaved at 121°C for 15 minutes before use.

LB agar plates (1 L)

- 15 g Agar bacteriological
- 100 mg/ml sterile filtrated ampicillin
- 1 L LB medium
- Petri dishes

LB agar was prepared by adding 1.5 % (w/v) agar to 1 L LB medium before autoclaving. After the solution was cooled down to ~50°C, 1 ml ampicillin was added to yield a final concentration of 100 µg/ml. Subsequently, the medium was transferred to petri dishes under sterile conditions and left to solidify. Agar plates were wrapped in plastic and stored at 4°C for no more than 3 weeks.

Terrific Broth (TB), 1 L

- 12 g Bacto Trypton
- 24 g Bacto Yeast extract
- 4 ml Glycerol
- 100 ml sterile filtrated 10 x TB salts

The components were dissolved in 900 ml dH_2O and autoclaved at 121°C for 15 minutes.

Subsequently, 100 ml sterile filtrated 10 x TB salts (see below for recipe) was added to the solution.

10 x TB salt

- 23.12 g KH_2PO_4
- 125.41 g K_2HPO_4

dH_2O was added to a final volume of 1 L.

3.1.2 Cultivation of *Escherichia coli*

Both pRSET-B and pBAD/HisB (table 2.2) express the β-lactamase gene which confers ampicillin resistance to cells harbouring the plasmid. Thus, *E. coli* cells containing the plasmids mentioned above were grown in appropriate liquid media supplemented with 100 µg/ml ampicillin. CBP21and *Ef*CBM33A were expressed using LB medium, while TB was used as growth medium to express *Lp*CBM33(1697). A small piece of glycerol stock (see below) was added to an appropriate volume of medium, followed by incubation overnight in an incubator shaker (INFORS) at 37^{o}C and 200 rpm.

3.1.3 Long-term storage of bacteria

Bacterial cultures were stored as glycerol stocks at -80 in cryo-tubes. To prepare a glycerol stock, one colony from a LB agar plate was transferred to an appropriate volume of LB medium containing 100 µg/ml ampicillin and incubated overnight at 37°C and 200 rpm. Subsequently, 300 µl 85% (w/v) sterile glycerol was carefully mixed with 1 ml of overnight culture in a cryo-tube under sterile conditions to avoid any contaminations. The addition of glycerol stabilizes the bacteria, preventing damage to the cell membranes and keeping the cells alive at extreme low temperatures.

3.1.4 Short-term storage

Agar plates containing bacterial colonies were wrapped in plastic and stored at 4°C for up to three days.

3.2 Site-directed mutagenesis

Site-directed mutagenesis is a widely used *in vitro* technique for creating specific changes in a known DNA sequence, usually carried out by using PCR-based methods. Commonly termed protein engineering, this process modifies the gene encoding the protein and is a powerful tool to analyze structure, stability, specificity and function of the mature protein. In this study, the QuickChange site-directed mutagenesis method (table 2.4) was used to introduce specific mutations in the gene of interest. The method is performed using a high-fidelity DNA polymerase, a vector with the gene of interest, two oligonucleotide primers containing the desired mutation and a thermo-cycler. The oligonucleotide primers, each complementary to opposite strands of the vector, are extended during temperature cycling by DNA polymerase. This generates a mutated plasmid, which can be transformed into an appropriate host cell. To remove non-mutated template plasmid, a restriction enzyme that can distinguish between template DNA and newly synthesized DNA is added. In order to conduct site-directed mutagenesis, mutagenic primers have to be designed and produced.

3.2.1 Mutagenic primer design

When designing mutants to investigate the functionality of the protein it is important to choose residues that are unlikely to affect the structure dramatically. For example if the importance of an amino acid in an enzyme mechanism is to be assessed, the replacement should be of similar size and polarity, but differ in an important chemical characteristic. Oligonucleotide primers can be designed to create desired mutations at specific sites in the DNA. Primers used in this study were designed using the QuikChange® Primer Design program (Agilent Technologies; https://www.genomics.agilent.com) and synthesized by Eurofins MWG Synthesis. Mutagenic primers utilized in this procedure are listed in table 2.5. The design was based on the following general considerations:

- Both the forward and the reverse primer must contain the desired mutation. The primers must be complementary to each other and anneal to the same sequence in the opposite DNA strands.
- No complementarity within the primers (e.g. secondary structures or primer-dimer formation, which can happen if complementarity within the primer exists)
- The primers should have randomly dispersed nucleotides; there should be no long stretches of polypyrimidines or polypurines.

- The desired mutation (substitution, deletion or insertion) should be in the middle of the primer with approximate 15 nucleotides on each side.
- Primers should have a GC content of more than 40 % for optimal function and a length between 25 and 45 bases. A longer primer will increase the probability of secondary structure formation.
- The melting temperature (T_m) should be similar for the forward and the reverse primer.
- Most amino acids are encoded by more than one codon. The optimal codon should be used when designing the primers.

3.2.2 Plasmid isolation from *E.coli*

Plasmid pRSETB/*cbp21* was isolated from *E.coli* DH5α™ cells using the NucleoSpin® Plasmid/Plasmid (NoLid) kit (table 2.4). If not stated otherwise, centrifugation was conducted at 11,000 x g using a microcentrifuge (5415 R, Eppendorf) at room temperature.

Materials

• NucleoSpin Plasmid/Plasmid (NoLid) kit:
  - Resuspension buffer A1
  - Lysis buffer A2
  - Neutralization buffer A3
  - AW buffer
  - Wash buffer A4
  - NucleoSpin Plasmid/Plasmid (NoLid) column
  - Collection tubes, 2 ml
• Microcentrifuge tubes, 1. 5 ml
• dH_2O

Procedure

Bacterial cells from a 2 ml overnight culture were harvested by centrifugation for 30 seconds in an Eppendorf tube. The supernantant was removed and the pellet was resuspended in 250 µl resuspension buffer A1. To lyse the bacteria cells, 250 µl of lysis buffer A2 was added to the sample and the Eppendorf tube containing the sample was inverted 8 times. After approximately 3 minutes, when the lysate appeared clear, the lysis reaction was stopped by

adding 300 µl of neutralization buffer A3 and the tube was inverted 8 times. The lysate was centrifuged for 5 minutes. 750 µl clear supernantant was loaded onto a NucleoSpin Plasmid / Plasmid (NoLid) column, which was placed in a 2 ml collection tube and centrifuged for 1 minute (this step was done twice). The flow-through was discarded and 500 µl pre-heated AW buffer (60^{o}C) was added to the column before it was centrifuged for 1 minute. The column was further washed with 600 µl wash buffer A4 and centrifuged for 1 minute. To remove remaining liquid, the column was centrifuged for 2 additional minutes. The NucleoSpin® Plasmid / Plasmid (NoLid) Column was then placed in a new 1.5 ml microcentrifuge tube and 50 µl pre-heated dH_2O (70 ^{o}C) was added. After 3 minutes of incubation the column was centrifuged for 1 minute to elute the DNA. The dsDNA concentration was measured according to section 3.2.8, before the plasmid preparation was stored at -20°C until further use.

3.2.3 Plasmid verification

To verify whether the isolated plasmid indeed was pRSETB/*cbp21*, a restriction enzyme digestion was carried out. When setting up the reaction, account was given to the fact that the restriction enzyme storage buffer contains glycerol to allow the enzyme survive at -20°C. Since glycerol inhibits digestion, the final volume of restriction enzyme should not exceed more than 10 % of the total reaction volume. For optimized reaction conditions, NEBuffer 2 was used in all reactions.

Materials

- Plasmid (from section 3.2.2)
- NEBuffer 2 (New England Biolabs, NEB)
- EcoRI (New England Biolabs, NEB)
- XbaI (New England Biolabs, NEB)
- dH2O
- Water bath (Stuart)

Procedure

Reactions were set up in 1.5 ml Eppendorf tubes according to table 3.1. Subsequently, the samples were placed in a water bath adjusted to 37°C and incubated for 4 hours before the samples were analysed by DNA agarose gel electrophoresis according to section 3.2.4.

Table 3.1. Reaction mixtures for enzyme digestion. All volumes are in µl.

Reagent	Single digest	Double digest
Plasmid	20	20
NEBuffer 4	4	4
EcoRI	2	2
XbaI	-	2
dH2O	14	12
Total volume	40	40

3.2.4 DNA agarose gel electrophoresis

DNA agarose gel electrophoresis is a technique to separate DNA fragments of varying sizes. The phosphate backbone of the DNA molecule is negatively charged and when placed in an electric field, DNA fragments will migrate towards the positively charged anode at different rates, based on their size and the pore size of the gel. Ethidium bromide in the gel binds between the bases in the DNA fragments and can be visualized under a UV-lamp. A standard composed of DNA fragments with known sizes is used to determine the size of the fragments in the samples.

Materials

• SeaKem® LE agarose

• 50 x Tris-acetate-EDTA (TAE) stock buffer pH, 8.5:

- 242 g Tris-base
- 750 ml dH2O
- 57.1 ml acidic acid (glacial)
- 100 ml 0.5 M EDTA, pH 8

dH2O was added to a final volume of 1 L

• Ethidium bromide (EtBr), 10 mg/ml

• 10 x DNA loading buffer (Takara)

• GeneRuler™ 1 kb DNA ladder (Thermo Scientific)

• Supercoiled DNA ladder (New England Biolab, NEB)

• Mini-Sub Cell GT cell (BioRad)

• SDS-PAGE power supply, Power Pac 300 (BioRad)

Procedure

An appropriate volume TAE stock solution was diluted 50 x to make 1L of 1 x TAE buffer. To make 1 % (w/v) agarose gel, 1 g agarose was mixed with 100 ml 1 x TAE buffer and heated in a microwave-oven until dissolved. The gel solution was cooled down to approximately 60°C and 2 µl EtBr solution was added before the agarose was poured into a gel-chamber. A gel comb was inserted and the gel solution was left to solidify for 1 hour. After removing the gel comb, the gel was transferred to a Mini-Sub Cell GT cell and submerged in 1x TAE buffer. Subsequently, 15 µl sample mixed with 5 µl DNA loading buffer was applied the gel. To be able to estimate protein size, an appropriate DNA ladder containing DNA fragments of known sizes was applied in another well. The gel was run at 90 volt for 45 minutes using a power supply and analyzed using UV light.

3.2.5 Polymerase-chain reaction

The Polymerase Chain Reaction (PCR) is an *in vitro* method that amplifies DNA segments exponentially by enzymatic replication. PCR has three phases; strand separation, primer annealing and chain extension, which take place at different temperatures. The reaction involves a thermostable DNA polymerase, dNTPs and oligonucleotide primers. In this study, mutagenic primers were used to introduce specific mutations in the *cbp21* gene. The procedure was performed according to the instructions given in the QuikChange® II Site-Directed Mutagenesis Kit (table 2.4).

Materials

- QuikChange II Site-Directed Mutagenesis Kit
    - 10 x reaction buffer
    - dNTP mix
    - *PfuTurbo*® DNA polymerase
    - Dpn I restriction enzyme
- DNA template (pRSET-B/*cbp21*)
- Mutagenic primers (table 2.5)
- PCR tubes, 0.2 ml (Axygen)
- dH_2O
- Master cycler gradient (VWR)

Procedure

The sample reactions (50 µl) were prepared on ice in 0.2 ml PCR tubes according to table 3.2 and placed in a thermal cycler. Parameters for the PCR program are listed in table 3.3. DNA amplification was checked by DNA agarose gel electrophoresis according to section 3.2.4.

Table 3.2. Reaction mixture for PCR. Final concentrations are shown in brackets.

Reagent	**Volume**
dNTP mixture, 10 mM	1 µl (2 mM)
10 x reaction buffer	5 µl (1 x)
DNA Template	2 µl (~50 ng)
Forward primer	1 µl (100 ng)
Reverse primer	1 µl (100 ng)
dH2O	39.5 µl
Pfu Turbo DNA Polymerase (added last)	0.5 µl (1 U)

Table 3.3. Parameters for the PCR program**.** The PCR program was set to 16 cycles, which is the standard protocol for single amino acid changes when using the Quick Change® Site directed Mutagenesis Kit.

Segment	**Cycles**	**Temperature**	**Time**	**Step**
1	1	95 ^{o}C	30 seconds	Initial denaturation
2	16	95 ^{o}C	30 seconds	Denaturation
		55 ^{o}C	1 minute	Annealing
		68 ^{o}C	4 minutes*****	Extension

*****_PfuTurbo_® DNA polymerase has an extension rate of 1kb/min. pRSET-B/*cbp21* is ~3.5 kb, thus 4 minutes was chosen as extension time.

3.2.6 Dpn I digestion of the amplification products

The template DNA was eliminated by adding 1 µl Dpn I to the PCR mixtures before the samples were incubated at 37°C for 30 minutes. Dpn I is an endonuclease that cuts specific methylated and hemimethylated DNA from dam+ *E. coli* strains (e.g. DH5α™). The newly synthesized DNA with the incorporated mutation is not methylated, thus the endonuclease selectively digests the template DNA over the newly synthesized DNA.

3.2.7 Transformation of *Escherichia coli*

XL1-Blue® competent cells are good host strains for plasmids after cloning. The competent cells are endonuclease deficient, which improves the quality of the DNA extracted and purified from the cells. PCR mix containing the putative mutated pRSET-B/*cbp21* plasmids were transformed into XL1-Blue® competent cells in order to make plasmid preparations. It should also be noted that this procedure was also used when plasmids containing the mutated CBP21 encoding gene were transformed into expression cells, OneShot® BL21 Star™ (DE3) chemically competent *E. coli* cells.

Materials

- XL1-Blue® supercompetent *E. coli* cells (Stratagene)
- OneShot® BL21 Star™ (DE3) chemically competent *E. coli* cells (Invitrogen)
- PCR samples (after Dpn I digest) (only used for transformation into XL1-Blue® supercompetent *E. coli* cells)
- Plasmid preparation of pRSETB/*cbp21* with mutated CBP21 encoding gene (only used for transformation into OneShot® BL21 Star™ (DE3) chemically competent *E. coli* cells)
- Super optimal broth (SOC) medium (concentration in brackets):
    - 0.5 g Bacto yeast extract (0.5 % w/v)
    - 2 g Bacto tryprone (2 % w/v)
    - 0.05 g NaCl (10 mM)
    - 0.0186 g KCl (2 mM)
    - 0.24 g $MgSO_4$ (20 mM)
    - 10 % (v/v) sterile glucose

    All reagents were dissolved in 96 ml dH_2O. The solution was pH adjusted to 7.5 with NaOH and autoclaved at 121°C and for 15 minutes. After cooling the solution down to ~50°C, 4 ml sterile filtered 10 % (v/v) glucose was added.

- Falcon tube, 15 ml
- Petri dishes with LB agar containing 100 µg/mL ampicillin
- LB medium containing 100 µg/m ampicillin
- Open heating bath circulator (Julabo)

Procedure

XL1-Blue® supercompotent/ OneShot® BL21 Star™ (DE3) chemically competent cells were thawed on ice before 50 µl of the cell suspension were transferred to a pre-chilled 15 ml Falcon tube. After adding 1 µl Dpn I-treated PCR mix (or plasmid preparation of pRSETB/*cbp21* with mutated CBP21 encoding gene), the suspension was carefully mixed and placed on ice. After 30 minutes incubation on ice, the cells were exposed to heat shock for 45 seconds in an open heating bath circulator adjusted to 42^{o}C. The cell suspension was then placed on ice for 2 minutes to cool down before 500 µl preheated SOC medium (37^{o}C) was added. The mixture was first incubated in a heating cabinet at 37^{o}C without shaking for 15 min and subsequently incubated at 37^{o}C and 200 rpm for 45 min. While the transformation mixture was incubating, petri plates with LB agar were incubated at 37^{o}C to hold the same temperature as the cell suspension. After one hour of incubation, 250 µl of the cell suspension was carefully transferred to a petri plate and plated out under sterile conditions. After incubating overnight (~16 hours) at 37^{o}C, 2 colonies (potential parallels) were inoculated in separate reagent tubes with 5 ml LB medium containing 100 µg/ml ampicillin. After ~16 hours incubation at 37^{o}C and 200 rpm, plasmids were isolated from each culture according to section 3.2.2 and glycerol stocks were made according to section 3.1.3.

3.2.8 Quantification of dsDNA

Quantitation of DNA in plasmid preparations was achieved using Quant-iT™ dsDNA Broad-Range Assay Kit (table 2.4) (Invitrogen). This DNA quantification procedure is based on specific molecules that become fluorescent upon binding to DNA. Since the fluorescence intensity is directly proportional to the amount of DNA in solution, the fluorescence signal can be converted into DNA concentration using DNA standards of known concentration.

Materials

- Quant-iT™ dsDNA Broad-Range Assay Kit
  - Quant-iT dsDNA BR reagent
  - Quant-iT dsDNA BR buffer
  - λ DNA standards (standard #1: 10 ng/ml, standard #2: 100 ng/ml)
- Qubit™ assay tubes, 500 µl (Invitrogen)
- Plasmid preparations of potential mutants
- Qubit™ fluorometer

Procedure

All the components of the Quant-iT™ dsDNA Broad-Range Assay Kit were equilibrated to room temperature before use. A Quant-iT™ dsDNA BR working solution enough for 25 assays was made by diluting an appropriate amount of Quant-iT™ dsDNA BR reagent 200 times in Quant-iT™ buffer. All samples and standards were set up in 500 µl assay tubes. Standard #1 and #2 were prepared by diluting 10 µl of each standard in 190 µl Quant-iT™ dsDNA BR working solution and these standards were then used to calibrate the Quibit® fluorometer dsDNA. The samples were prepared by mixing 190 µl Quant-iT™ dsDNA BR working solution and 10 µl of plasmid preparation. All tubes were vortexed and incubated for 2 minutes at room temperature before the dsDNA concentration was measured using Qubit™ fluorometer.

3.2.9 DNA Sequencing of potential mutants

Because all DNA polymerases are prone to introduce occasional errors when replicating DNA, potential mutants were sequenced to ensure that only the desired mutation had been incorporated into the newly synthesized DNA. Two plasmid preparations from each potential mutant (see section 3.2.7) were sequenced using pRSETB sequencing primers (forward and reverse), meaning that the whole insert (i.e. the whole gene) was sequenced, for each mutant. The sequencing services were provided by GATC Biotech AG, Germany.

3.2.10 Verification of DNA sequences

The sequences of potential mutants received from GATC Biotech AG were analyzed to verify the presence of the correct mutation and absence of non-desirable additional mutations by using BioEdit, a free sequence alignment editor tool available at http://www.mbio.ncsu.edu/bioedit/bioedit.html. The CBP21 sequences were supplemented with chromatograms. The chromatograms were analyzed and data containing a high degree of "noise" were deleted before the sequences were aligned with the wild type (WT) sequence to verify correct mutations.

3.2.11 Transformation of OneShot® BL21 Star™ competent cells for protein expression

XL1-Blue® supercompetent cells were used as host strains after cloning, but they are not suitable for efficient protein expression. After verification of the sequences of the mutated CBP21-encoding genes, the plasmids were transformed into OneShot® BL21 Star™ (DE3) chemically competent *E. coli* cells for expression, using the transformation protocol described in section 3.2.7. A colony for each mutant was picked and used to inoculate 10 ml LB medium containing 100 µg/ml ampicillin and the culture was incubated overnight at 37°C and 200 rpm. To verify production of CBP21, SDS-PAGE was conducted according to section 3.4. Glycerol stocks were made for all mutants, according to section 3.1.3.

3.3 Protein production and purification

CBP21 variants, *Ef*CBM33A and *Lp*CBM33(1697) were purified from periplasmatic extracts of OneShot® BL21 Star™ (DE3) chemically competent cells harbouring the appropriate plasmids. Purified *Ll*CBM33A and GbpA-N were provided by Gustav Vaaje-Kolstad. Three different purification methods were used in this thesis. Both CBP21 and *Ef*CBM33A have strong affinity to β-chitin and were purified by chitin affinity chromatography, with chitin beads as chromatographic medium, while *Lp*CBM33(1697) was purified in a two-step procedure. The first step consisted of ion-exchange chromatography using Q Sepharose Fast Flow to separate *Lp*CBM33(1697) from the majority of proteins in the periplasmic extract. Subsequently, the protein was purified further using size exclusion chromatography.

3.3.1 Protein expression and periplasmic extracts

The gene encoding CBP21 also includes a signal peptide that directs the mature protein into the periplasmic space during expression in *E. coli.* In order to harvest the protein, the periplasmic content of the bacterial cells was extracted using a cold osmotic shock protocol. Osmotic shock is based on exposing bacterial cells to a sudden change in the surrounding solute concentration and is a widely used technique to harvest the periplasmic content of gram negative bacteria.

Materials

- 150 ml LB/TB medium
- 100 mg/ml ampicillin
- Spheroplastbuffer:
    - 51.3 g Sucrose
    - 30 ml 1 M Tris-HCl, pH 8.0
    - 600 µl 50 mM PMSF in isopropanol
    - 300 µl 0.5 M EDTA, pH 8.0

  The components were dissolved in 300 ml dH_2O
- 20 mM MgCl
- 0.22 µm sterile filter (Sarstedt)
- Syringe, 10 ml
- 20 mM PMSF in 50 mM isopropanol
- Centrifuge cups, 250 ml
- Falcon tube, 50 ml
- Centrifuge rotor, JA-14 (Beckman Coulter)
- Centrifuge, Avanti J25 (Beckman Coulter)

Procedure

A small piece of the glycerol stock was inoculated in 150 ml appropriate growth medium under sterile conditions, followed by incubation overnight at 37°C and 200 rpm. The overnight culture was transferred to a 250 ml centrifuge tube and centrifuged at 8000 rpm for 10 minutes at 4^oC. The supernatant was decanted and the pellet was resuspended in 15 ml freshly made ice-cold spheroplastbuffer. The cell suspension was then placed on ice for 5 minutes and the cells were centrifuged for 10 minutes at 8000 rpm and 4^oC. The supernatant

was decanted and the pellet was resuspended in 12.5 ml ice-cold dH_2O and placed on ice for 45 seconds. 625 µl of 20 mM $MgCl_2$ was added before centrifugation at 8000 rpm for 12 minutes at 4oC. The supernatant, which is the periplasmic extract, was filtered through a 0.22 µm sterile filter using a 10 ml syringe and collected in a sterile 50 ml Falcon tube. After adding 2 µl 50 mM PMSF per 1 µl periplasmic extract, the extract was stored at 4^oC until protein purification.

3.3.2 Chitin-affinity chromatography

To avoid cross-contamination from non-eluted protein, an individual batch of chitin beads was used for each mutant and protein. Purification was carried out using the BioLogic® LP chromatographic system and the purification process was monitored using LP Data View 1.03. If not stated otherwise, the flow rate was 1.5 ml/min during the whole procedure.

Materials

- Econo-Column® (1.5 x 15 cm)
- Econo-Column® flow adaptor
- Chitin beads (New England Biolabs, NEB)
- 0.3 M NaOH
- 20% (v/v) ethanol
- 1 M ammonium sulphate in 20 mM Tris-HCl pH 8.0 (binding buffer):
  - 132.14 g ammoniumsulphate
  - 2.4 g Tris-Base

  dH_2O was added to a final volume of 1 L and the pH was adjusted with HCl
- 20 mM acetic acid pH 3.6 (elution buffer)
- 20 ml periplasmic extract
- Falcon tube, 50 ml

Procedure

Prior to purification, the tubing in the BioLogic LP chromatographic system and the Econo-Column flow adaptor was purged (flow rate 6.5 ml/min) with 0.3 M NaOH for 5 minutes to remove any contaminations. The Econo-Column was washed with two column volumes of 0.3 M NaOH before 10 mL chitin beads were applied to the column. After settling, resulting in a total column volume of approximate 10 ml, the chitin beads were equilibrated with binding

buffer until the baseline was stable, and for at least two column volumes. The baseline was reset to zero when it was stable. For optimal binding to the chromatographic medium, the periplasmic extract (20 ml) was adjusted to 1 M ammonium sulphate and 20 mM Tris-HCl, pH 8.0 - like the binding buffer, before loading onto the column. After all periplasmic extract was loaded onto the column, binding buffer was applied until all proteins not binding to the column has passed through and the base line was stable at zero. A pH shift was used to elute bound protein from the chitin beads. This was accomplished by applying elution buffer (20 mM acetic acid, pH 3.6). The eluted protein was collected in a 50 ml Falcon tube and after adjusting the solution to approximate pH 8 with 1 M Tris-HCl, pH 8.0, it was stored at 4^{o}C until further use. After purification the system was purged (flow rate 6.5 ml/min) with 20% (v/v) ethanol for approximate 10 minutes to wash the system free from buffer and any remaining proteins. The chitin beads were then collected in a 50 ml Falcon tube and stored in 20 % (v/v) ethanol at 4°C until reuse.

3.3.3 Ion Exchange Chromatography

Ion exchange chromatography (IEC) is a popular technique to separate proteins and other charged molecules in a mixture. The method is based on the reversible interaction between charged molecules with an oppositely charged chromatographic medium. Proteins with opposite charges will interact at different strength with the chromatographic medium, based on their net surface charge, whereas uncharged proteins or those having the same charge as the medium will not interact. A gradient of increasing salt concentration is used to elute and separate the proteins binding to the column; proteins having a weak interaction with the column will elute when the salt concentration is low, while proteins with stronger interactions will elute later as the salt concentration increases.

Materials

- 20 ml periplasmic extract containing *Lp*CBM33(1697) (calculated pI = 7.02)
- 50 mM Tris-NaOH pH 10.0 (binding buffer)
- 50 mM Tris-NaOH pH 10.0 in 1 M NaCl (elution buffer):
    - 58.4 g NaCl
    - 6.0 g Tris-Base

  dH_2O was added to a final volume of 1 L and the pH was adjusted with 5 M NaOH
- 20 mM Tris-HCl, pH 8.0

- Amicon Ultra-15 Centrifugal Filter Units with 10 kDa cut-off (Millipore)
- Column: 5 ml HiTrap™ Q Sepharose Fast Flow (GE Healthcare)
- Äkta purifier chromatography system (GE Healtcare)
- Fraction collector, Frac-920 (GE Healthcare)

Procedure

The HiTrap, column which is a strong anion exchanger for small-scale protein purifications, was connected to an Äkta purifier chromatography system and washed with elution buffer to remove contaminations. The sample (periplasmic extract) was adjusted to pH 10.0 by adding an appropriate volume of binding buffer. The system was equilibrated with binding buffer before the sample was loaded onto the column. Unbound protein was eluted by running two column volumes of binding buffer, while the protein of interest was eluted using a gradient of 0-50 % elution buffer over a time period of 50 minutes with a flow rate of 2 ml/min. Fractions of 2 ml were collected using a Frac-920 fraction collector. Elution of protein was monitored by measuring absorption at 280 nm and chromatograms were recorded using UNICORN™ manager 5.31. Fractions containing protein were analyzed by SDS-PAGE (section 3.4). Fractions containing the protein of interest were pooled and concentrated to 1 ml using an Amicon Ultra-15 Centrifugal Filter Unit with 10 kDa cut-off. At the same time the buffer was changed to 20 mM Tris-HCl pH 8.0 (section 3.3.6). The sample was stored at 4^{o}C until further purification by size exclusion chromatography (section 3.3.4).

3.3.4 Size Exclusion Chromatography

Size exclusion chromatography (SEC) is a technique to separate proteins in solution based on their size. The column is packed with a porous matrix and proteins of various sizes will have different retention times. The matrix allows small proteins to enter the pores and these will thus use longer time to elute than bigger proteins. SEC is a good step for final purification, but the technique's separation is not usually sufficient to separate highly complex protein mixtures. Therefore, this technique is often used as a final "polishing step".

Materials

- 50 mM Tris, 200 mM NaCl, pH 7.5 (running buffer):
  - 11.6 g NaCl
  - 50 ml 1 M Tris
  - 900 ml dH20

  The solution was pH adjusted to 7.5 with HCl before addition of dH_2O to a final volume of 1L. The buffer was filtered through a 0.22 µm sterile filter to eliminate any particles.
- 1 ml concentrated protein from the IEC experiment (section 3.3.3)
- Column: HiLoad™ 16/60 Superdex™ 120 ml prep grade (GE Healthcare)
- Äkta purifier chromatography system (GE Healtcare)
- Fraction collector, Frac-920 (GE Healthcare)

Procedure

The column was connected to an Äkta purifier (GE Healtcare) and equilibrated with running buffer (50 mM Tris in 200 mM NaCl, pH 7.5) before the sample (1 ml) was applied the column through a 2 ml loading loop and the flow rate was set to 0.3 ml/min. One column volume of 50 mM Tris in 200 mM NaCl pH 7.5 (running buffer) was applied to elute the proteins and fractions of 2 ml were collected. Based on the recorded chromatogram, fractions containing protein were collected and analyzed by SDS-PAGE (see section 3.4) for purity and identification. Fractions containing sufficiently pure protein of interest were pooled and concentrated to 1 ml with buffer change to 20 mM Tris-HCl, pH 8.0, according to section 3.3.6. To verify presence of *Lp*CBM33(1697), MALDI-TOF MS was conducted (see section 3.7). The protein was stored at 4°C.

3.3.5 Dialysis

Materials

- Slide-A-Lyzer® dialysis cassettes, 1-3 ml capacity with 10 kDa MWCO (Thermo Scientific)
- Syringe, 1 ml
- Needle
- 1-3 ml concentrated enzyme solution
- Floating buoy
- Buffer
- Glass beaker, 1 L

Procedure

Dialysis was conducted using Slide-A-Lyzer cassettes with regenerated cellulose membrane. The Slide-A-Lyzer was hydrated in the dialysis buffer for three minutes before use. The sample was carefully injected via one of the corner ports in the gasket into the cassette chamber by a syringe. Excess air was withdrawn and the syringe was carefully removed. The Slide-A-Lyzer was then attached to a floating buoy and placed in the buffer (500 x sample volume) with continuous low-speed stirring at 4°C. After two days dialyzing with four buffer-changes, the sample was retrieved from the Slide-A-Lyzer by inserting an empty syringe needle at a second corner port. Air was injected to expand the chamber before the sample was withdrawn. Because of increased volume, the sample was subsequently concentrated as described section 3.3.6. Final protein concentration was measured according to section 3.51 or 3.5.2 before the protein was stored at 4°C

3.3.6 Protein concentration

In this study, concentration of various protein solutions, sometimes combined with buffer exchange, was done using ultrafiltration with Amicon® Ultra centrifugal filter devices. While concentrating the protein, the buffer can also be changed by performing multiple cycles of buffer addition and re-concentration.

Materials

- Amicon® Ultra-0.5 or -15 Centrifugal Filter Device with 10 kDa MWCO (Millipore)
- Centrifuge, 5430 R (Eppendorf)
- Protein solution

Procedure

The protein solution was added to the centrifugal filter device (0.5 ml or 15 ml) and concentrated by centrifugation using a fixed angle rotor at 14000 x g or 4500 x g, respectively. The centrifugation time depended on the initial concentration of the protein, the desired end concentration and the sample volume. The concentrated sample solution was collected with a pipette.

3.4 Sodium dodecyl sulphate polyacrylamide gel electrophoresis

Sodium dodecyl sulphate polyacrylamide gel electrophoresis (SDS-PAGE) is a widely used technique to separate proteins based on their size. Native proteins are denatured with an ionic detergent, such as sodium dodecyl sulphate (SDS) and a reducing agent (for reducing disulphide bridges). The proteins are simultaneously provided with a global negative charge due to binding of SDS. An electric field is applied along an acrylamide gel and proteins with various sizes will move through the gel towards the positively charged anode at rates that depend on comparing protein size. The proteins can be visualized by various staining techniques, one such being Coomassie blue staining. The protein size can be estimated with a molecular marker containing proteins with known masses. SDS-PAGE is a good method to verify purity of protein samples following purification procedures.

Materials

- 4 x NuPAGE® LDS sample buffer (Invitrogen)
- 10 x NuPAGE® reducing agent (Invitrogen)
- 20 x NuPAGE® MOPS SDS running buffer (Invitrogen)
- 10 % NuPAGE® Novex® Bis-Tris Mini precast polyacrylamide gel (Invitrogen)
- 1 x MOPS-SDS running buffer
- Bench Mark™ Protein Ladder (Invitrogen)
- Coomassie Brilliant Blue staining solution:
    - 0.1 % (w/v) Coomassie Brilliant Blue G-250

- 10 % (v/v) acetic acid (glacial)
- 50 % (v/v) methanol
- 40 % (v/v) dH_2O

• Destaining solution:

- 10 % (v/v) acetic acid (glacial)
- 40 % (v/v) methanol
- 50 % (v/v) dH_2O

• XCell SureLock™ Mini-Cell Electrophoresis System

• Power Pac 300 power supply

• Rotary shaker, IKA® HS 260 basic

Procedure

1 x MOPS-SDS running buffer was prepared by diluting 50 ml 20 x MOPS-SDS running buffer in 950 ml dH_2O. The precast polyacrylamide gel was placed in an XCell SureLock™ Mini-Cell Electrophoresis System and the inner chamber was completely filled with 1 x MOPS-SDS running buffer, while the outer chamber was filled half full. The samples were prepared by mixing 10 µl protein sample, 5 µl NuPAGE® LDS sample buffer (4 x), 2 µl NuPAGE® Reducing agent (10 x) and 3 µl H_2O. After boiling the samples for 10 minutes, the samples (20 µl) were loaded into separate wells in the gel together with a protein standard containing proteins of known sizes. The gel was run for 45 minutes at 200V using a Power Pac 300 power supply. To visualize the proteins, the protective plastic container was removed and the gel was treated with staining solution placed in a tray on a rotary shaker giving gentle mixing. After three hours staining, the gel was washed with destaining solution until the gel was transparent, after which a picture of the gel.

3.5 Protein quantification

3.5.1 Protein quantification by measuring absorbance at 280 nm

Proteins have the ability to absorb UV-light in solution and the absorbance maximum at 280 nm is mainly caused by the amino acids tryptophan and tyrosine. The molar absorption coefficient of the whole protein depends on the occurrence of these amino acids in the protein. After calculating the theoretical molar extinction coefficient of a protein, its concentration can be determined by using the Beer-Lambert's law (equation 1). Theoretical extinction

coefficients and molecular weights were calculated using ProtParam, available at http://web.expasy.org/cgi-bin/protparam/protparam. Since the molecular extinction coefficient of CBP21 had previously been determined experimentally, it was possible to estimate the relative precision of the theoretical calculation (see section 4.1, table 4.1).

$$A = \varepsilon lc$$

Equation 1. Beer-Lambert's law. A, the measured absorption at A_{280}; ε, the molar extinction coefficient of the protein; l, path length; c, protein concentration

Materials

• Disposable UVette® 220-1600 nm, 50-2000 µl (Eppendorf)
• Sample buffer
• Purified protein of unknown concentration

Procedure

Samples to be measured were centrifuged at 13.000 x g for 1 minute to sediment any particles in the solution that could interfere with the A_{280} readings. The samples were prepared in triplicates with different concentrations by diluting them in sample buffer. After the spectrophotometer (Bio Photometer) was reset to zero using sample buffer, the samples were analyzed. After correcting for the dilution factor, the mean value of the triplicates was used to calculate the concentration using the Beer-Lambert's equation.

3.5.2 Bradford assay

The Quick Start™ Bradford Protein Assay (BioRad) provides a colorimetric method originally developed by M.M Bradford (Bradford 1976). The assay involves binding of Coomassie Brilliant Blue G-250 dye to the protein. When dye binds to the protein under acidic conditions the absorption maximum is altered from 465 nm to 595 nm. The shift in absorption maximum can be measured using a spectrophotometer.

Materials

- 5 x Dye Reagent (BioRad)
- Bovine serum albumine (BSA), 2 mg/ml
- Polystyrene cuvettes, 1 ml (Brand)
- 1 x PBS
- Purified protein of unknown concentration
- Spectrophotometer, Biophotometer (Eppendorf)

Procedure

A series of standards were prepared by diluting BSA to a final concentration of 0, 0.2, 0.4, 0.6, 0.8 and 1 mg/ml in 1 x PBS. The standards were incubated in 5 x Dye reagent for 10 minutes at room temperature and each sample concentration were measured in triplicates using a spectrophotometer. Values obtained from the standards were used to construct a standard curve, which was used to determine protein concentrations in samples of unknown concentration. The point (0,0) was obtained by measuring absorbance of a reference sample prepared by diluting 800 µl 1 x PBS in 200 µl 5 x Dye reagent and adjusting the spectrophotometer read to zero.

Samples of unknown concentration were prepared in triplicates by adding 797 µl sample buffer to 3 µl concentrated protein. After adding 200 µl 5 x Dye reagent and incubation at room temperature for 10 minutes, the A_{595} was measured using a spectrophotometer. After correcting for dilution, the mean value of three replicates was used to calculate the concentration using the standard curve.

3.6 Production of CBP21 apo-enzyme

Many enzymes require a non-protein component for activity; this is termed a co-factor. One group of cofactors comprises metal ions, e.g. CBP21 requires copper for activity. Removal of copper with a metal chelator leads to inactivation of the enzyme, but the activity can be restored by addition of copper. Co-factor dependent enzymes that lack their co-factor are called apo-enzymes.

Materials

- 1 M EDTA, pH 8.0 in TraceSELECT® Ultra water (ion free water)
- 1M Tris-HCl, pH 8.0 in TraceSELECT® Ultra water
- TraceSELECT® Ultra water
- 1 ml concentrated enzyme (concentration range; 5-20 mg/ml)
- 100 µM $Cu(II)SO_4$

It is important to hold the working solutions of $Cu(II)SO_4$ at an acidic pH (~3.5) by addition of dilute sulphuric acid. If not the Cu(II) ions may form copper oxide precipitates

Procedure

A volume of EDTA stock solution was added to 1 ml concentrated enzyme to yield a final EDTA concentration that was 10 times the enzyme concentration. While the protein was being incubated with EDTA for 1 hour, 1 mM Tris-HCl pH 8.0 buffer was made by diluting the stock solution in TraceSELECT® Ultra water. The protein was dialyzed against the buffer according to section 3.3.5 and concentrated with an Amicon Ultra centrifugal filter unit with 10 kDa cut-off (Millipore). Verification of enzyme inactivity was done using the MALDI-TOF MS-based method described in section 3.7.

As mentioned above, the activity can be restored by adding copper to the protein. To get an accurate degree of copper saturation, the protein concentration was measured according to section 3.5.1, before an appropriate volume of $Cu(II)SO_4$ was added to the protein solution until desired copper saturation was achieved.

3.7 Enzyme activity measurements - Matrix-assisted laser desorption/ionization-time of flight mass spectrometry

Matrix-assisted laser desorption /ionization-time of flight mass spectrometry (MALDI-TOF MS) analysis is a widely used method in proteomics to explore protein expression levels, protein identification, protein interactions, post-translational modifications of proteins, protein activity towards different substrates etc. The method is also a powerful tool for analysis of oligosaccharides, such as carbohydrate moieties from glycosylated proteins or products generated by LPMOs or other carbohydrate active enzymes. The method, which is normally used for collection of qualitative data only, involves a matrix which co-crystalizes with the analytes. When irradiated with a UV-laser beam, the matrix protonates the analytes, making

them charged. Furthermore, the energy-transfer from the laser beam converts the matrix-analyte complex to gas the phase and the charged molecules are then accelerated through a magnetic field in vacuum. The products arrive at a detector at different times based on their mass over charge ratio (*m/z*) and can thus be separated from each other. In this study MALDI-TOF MS was used to investigate protein activity for five CBM33s using β-chitin^{A} as substrate: CBP21 variants, *Ef*CBM33A, *Lp*CBM33(1697), GbpA-N, and *Il*CBM33A (purified *Il*CBM33A and GbpA-N were provided by Gustav Vaaje-Kolstad). All enzymes mentioned above (except for GbpA-N) had previously been shown to act on β-chitin and to generate oxidized products of different length, meaning that their activity (or the absence thereof) toward this substrate can be detected with MALDI-TOF MS.

Materials

- 1 M Bis-Tris, pH 6.8
- 100 mM ascorbic acid
- 10 mg/ml β-chitin^{A} (table 2.3)
- 50 µM Enzyme
- Matrix:
    - 4.5 mg 2.5-dihydroxybenzoic acid (DHB)
    - 150 µl acetonitrile
    - 350 µl dH_2O

  The solution was vortexed until the DHB was dissolved
- Source of warm air (hair dryer)
- MTP 384 target plate ground steel TF (Bruker Daltonics)
- MALDI-TOF MS Ultraflex system (Bruker Daltonics)

Procedure

Enzymatic reactions were set up in 1.5 ml Eppendorf tubes as shown in table 3.4 and incubated for ~16 hours in a thermomixer running at 37^{o}C and 900 rpm. A reaction mixture containing CBP21$_{WT}$ was included as positive control, while a reaction without CBP21$_{WT}$ was used as negative control.

Table 3.4. MALDI-TOF MS reaction setup.

Reagents	Final concentration
Enzyme	1 µM
β-chitin[A]	2 mg/ml
Bis-Tris pH 6.8	50 mM
Ascorbic acid*	1 mM
dH_2O	To a total volume of 200 µl

* The negative control was prepared without $CBP21_{WT}$

After the incubation, the reaction mixtures were centrifuged for 3 minutes to sediment the substrate, 1 µl of the supernantant was mixed with 2 µl of matrix (DHB) on a MTP 384 target plate. The droplets were dried under a steam of warm air before the target plate was installed in the MALDI-TOF MS Ultraflex compartment. The spots containing crystalized matrix and the sample were shot approximate 250 times using a nitrogen 377 laser beam with 25-30 % intensity controlled by FlexControl 3.3**.** The results were analyzed using FlexAnalysis version 3.3.

3.8 Protein labeling with Alexa Fluor® 488 dye

Proteins to be labeled with Alexa Fluor® 488 reactive dye must be in a buffer free of primary amines. The dye reacts with primary amines of the protein and forms a stable dye-protein complex. Even trace amounts of primary amine–containing components in the buffer lower the degree of labeling. All CBM33s were stored in Tris-buffer prior to the procedure, which contains primary amines, thus a dialysis step had to be carried out.

Materials

- Alexa Fluor 488 Protein Labelling Kit (table 2.4) (Invitrogen)
  - Vials of Alexa Fluor 488 reactive dye
  - 84 mg sodium bicarbonate
- 10 x Phosphate-buffered saline (PBS), pH 7.4 (concentration in brackets):
  - 80 g NaCl (137 mM)
  - 2 g KCl (2.7 mM)
  - 14.4 g Na_2HPO_4 (10 mM)
  - 2.4 g KH_2PO_4 (1.8 mM)

  The reagents were fully dissolved in 900 ml dH_2O and the solution was pH adjusted with HCl before addition of dH2O to a final volume of 1 L. The buffer was sterile

filtrated by vacuum filtration using a Stericup-GP PES Filter Unit (Millipore) with 0.22 µm pore size.

- Slide-A-Lyzer® dialysis cassettes, 1-3 ml capacity with 10K MWCO (Thermo Scientific)
- Floating buoy
- Syringe, 1 ml
- Needle
- Solutions with purified CBP21, EfCBM33A, LpCBM33(1697) and GbpA-N in 20 mM Tris-HCl, pH 8.0.
- Absorption cuvette; semi micro cells, 104-OS 10 mm (Hellma)
- Spectrophotometer, U-1900 (Hitachi)

Procedure

Tris-buffer was replaced with 1 x PBS buffer by dialysis according to section 3.3.5. Approximate 1 ml of each protein was injected into separate hydrated Slide-A-Lyzers using a syringe and dialyzed versus 1 x PBS (500 x sample volume) with continuous stirring. After dialyzing overnight with one buffer-change, the concentration of the protein solutions were measured according to section 3.5.2 Proteins at concentrations less than 2 mg/ml will not label as efficiently and were concentrated Amicon Ultra centrifugal filter unit with 10 kDa cut-off (Millipore) as described in section 3.3.6, before the concentration re-measured.

To prepare 1 M sodium bicarbonate, 1 ml dH_2O was added to 84 mg sodium bicarbonate. The solution was vortexed until all material had dissolved and 50 µl was then added to 0.5 ml of each of the protein solutions. 0.5 ml of the protein solutions (yielding a concentration in the range of 2-4 mg/ml) were then transferred to separate vials of reactive dye containing a magnet stir bar and inverted a few times to fully dissolve the dye. The protein-dye solutions were stirred for 1 hour at room temperature before unbound dye was removed by extensive dialysis versus 1 x PBS buffer (1000 x sample volume) with continuous stirring at 4°C according to 3.3.5. The protein solutions were dialyzed for two days with four buffer-changes. In order to calculate protein concentrations and the degree of labeling, the absorbance of the conjugate solutions were measured in duplicates at two different wavelengths, 280 nm and 494 nm using a spectrophotometer. The protein concentration and the degree of labeling were determined by using equations 2 and 3, respectively (provided by the Alexa Fluor® 488 Protein Labeling Kit protocol). Labeled proteins were stored at 4°C, protected from light.

Equation 2.

$$Protein\ concentration\ (M) = \frac{[\mathrm{A280} - (\mathrm{A494} \times 0.11]}{\text{Extinction coefficient of the protein}}$$

Equation 3.

$$Moles\ dye\ per\ mole\ protein = \frac{\mathrm{A494}}{71000 \times \text{protein concentration (M)}}$$

3.9 Binding studies

Binding studies were conducted using β-chitin^{A} as substrate. Binding of protein to substrate was measured by the decline of the protein in the supernantant, measured by $A2_{80}$.

Materials

- 100 µM solutions of $CBP21_{WT}$ and mutants
- 20 mg/ml β-chitin^{A} in dH_2O
- 100 mM sodium phosphate buffer, pH 7.0
- dH_2O
- UVette® 220-1600 nm, 50-2000 µl (Eppendorf)
- Rotator mixer
- spectrophotometer, Biophotometer (Eppendorf)

Procedure

Reactions were set up in triplicates with 10 mg/ml β-chitin and 100 µg/ml protein in 50 mM sodium phosphate buffer, pH 7.0. Distilled water was added to obtain a sample volume of 300 µl. In order to obtain consistent amount of substrate when pipetting, the substrate suspension was continuously stirred. The reaction mixtures was rotated vertically at 60 rpm and at certain time points (5, 15, 45, 90, 180 and 240 min) the samples were centrifuged in a microcentrifuge for 3 min at 13.000 x g. The protein concentration in the supernatant was determined by measuring absorption at 280 nm with a spectrophotometer; 50 mM sodium phosphate buffer was used to determine zero absorbance. A sample without protein and a sample without β-chitin were used as controls.

3.10 Analysis of oxidized products by ultra high-performance liquid chromatography

Ultra high performance liquid chromatography (UHPLC) is a separation technique to identify, quantify or purify compounds from a mixture. The method involves a sample injector, mobile phase and a stationary phase (column content). High pressure applied to the system allows the column to be packed with very small particles, which gives a greater surface area for the sample to interact with. The compounds in the applied sample move through the column at different rates due to variations in the strength of their interaction with the solvent and the stationary phase. The time taken for a compound to elute is called the retention time. The compounds can be eluted either by isocratic elution, meaning that the composition of the mobile phase remains constant throughout the procedure, or by gradient elution, meaning the mobile phase composition is changed during the separation process. The latter elution technique was used in this study.

UHPLC was used to identify and quantify oxidized products generated by $CBP21_{WT}$ and mutants, when incubated with β-$chitin^{B}$ (table 2.3). Oxidized products with different degrees of polymerization (DP) were separated and identified using standards. The reaction conditions and the sequence conditions were optimized by Ph.D. student Jennifer Loose.

Materials

- 15 mM Tris-HCl, pH 8.0 (vacuum filtrated using a Stericup-GP PES Filter Unit (Millipore) with 0.22 µm pore size)
- 99.8 % (w/v) acetonitrile (HPLC grade)
- Standard: oxidized GlcNAcs with different DP
- 10 mg/mL β-$chitin^{B}$
- 1 M Tris-HCl, pH 8.0
- 100 mM ascorbic acid
- 100 µM solution of $CBP21_{WT}$ and mutants (90 % saturated with copper)
- TraceSELECT® Ultra water (ion free water)
- Eppendorf tubes with flat bottom, 2 ml (VWR)
- HPLC tubes (VWR)
- Snap ring cap for HPLC tubes, 11 mm (VWR)
- 96-well $MultiScreen_{HTS}$ filter plate with a 96-well collection plate (Millipore)

- High Output vacuum pump connected to a MultiScreen$_{HTS}$ Vacuum Manifold
- Thermomixer, Vortemp (Thermo Scientific)
- Water bath (Stuart)
- Column: HELIC, Acquity UPLC® BEH Amide 2.1x150mm with an Amide BEH VanGuard pre column, 2.1 x 5 mm (Waters). Both columns were packed with silica particles with a size of 1.7µm.
- Agilent 1290 Infinity LC system (GE Healthcare)

Procedure

Enzymatic reactions were set up in triplicate in 2 ml Eppendorf tubes with 7.5 mg/ml β-chitin^{B}, 50 mM Tris pH 8.0, 15 mM ascorbic acid and 1 µM or 5 µM enzyme. The reaction volume was adjusted to 750 µl with TraceSELECT® water. All samples were incubated in a thermo mixer in fixed positions at 20°C holding 1200 rpm. At time points (20, 40, 60, 80 and 100 minutes), 60 µl samples were withdrawn, transferred to a new Eppendorf tubes and boiled for 10 minutes in a water bath to stop the reaction. The samples were centrifuged for 1 minute to sediment sample droplets on the walls of the Eppendorf tube. After filtering the samples through a 96-well filter plate (Millipore) with a 96-well collection plate using a vacuum pump, 26 µl of each sample was transferred to HPLC-tubes and mixed with 74 µl acetonitrile.

Separation of oxidized products was done using an Agilent 1290 Infinity LC system equipped with an Acquity UPLC® BEH Amide column and an Amide BEH VanGuard pre column. The flow rate was set to 0.4 ml/min and the column temperature to 30°C. The sample volume applied to the column was 3 µl. The sequence was started by running a gradient with 74 % acetonitrile (A) and 26 % 15 mM Tris-HCl pH 8.0 (B) for 5 minutes followed by 5 minutes with 38 % A and 62 % B. A gradient holding 26% A and 74 % B was run for 2 minutes to recondition the column back to initial conditions. Eluted products were detected by measuring absorption at 205 nm. Chromeleon 7.1.2 software (Dionex) was used to monitor and supervise the procedure and to analyze the results.

3.11 Amplex® Red hydrogen peroxide assay

The activity of glucose oxidases can be measured by detection of hydrogen peroxide (H_2O_2), which is a co-product of the reaction they catalyze (Sanchez Ferrer et al. 1990). Recently, Kittl et al. developed a fast enzymatic assay to measure LPMO activity based on detection of H_2O_2. The assay was based on the idea that reduction of O_2 to H_2O_2 could occur when LPMOs was incubated in the presence of a suitable reducing agent, but in the absence of substrate (Fig. 3.1). Kittl and co-workers tested this assay in their work on the expression and purification of LPMOs from *Neurospora crassa*. Using ascorbic acid and CDH as reducing agents, the group showed that the formation of H_2O_2 was directly proportional to the LPMO concentration (Kittl et al. 2012).

Hydrogen peroxide can be measured with different methods, including several sensitive methods based on horseradish peroxidase (HRP) and substrates such as Amplex® Red (Rhee et al. 2010). Amplex® Red is a colorless substrate without natural fluorescent activity, but when it reacts with HRP and H_2O_2 it produces a pink fluorescent product called resorufin (Zhou et al. 1997). Figure 3.1 shows the suggested reaction proposed by Kittl and coworkers, when H_2O_2 is generated by LPMOs in a solution with Amplex® Red/HRP and a reducing agent. The reducing agent reduces the copper in the LPMO, which activates molecular oxygen in solution by a one-electron reduction. The putative superoxide is converted to H_2O_2 by a reaction known as disproportionation, meaning that a molecular species is reduced and oxidized to create two different types of products at the same time: $2\ O_2^- + 2\ H^+ \rightarrow H_2O_2 + O_2$. HRP uses the generated H_2O_2 to convert Amplex® Red, in combination with HRP, reacts with H_2O_2 and produces resorufin which is highly fluorescent. Since the reaction stoichiometry of Amplex® Red and H_2O_2 is 1:1, production of resorufin reflects the H_2O_2 concentration generated by the enzyme (Kittl et al. 2012). Analyses conducted by Zhou et al. (1997) indicate that Amplex® Red is converted into resorufin through oxidation.

In the present study, this assay was evaluated, with the intention of suing it to measure activity of $CBP21_{WT}$ and mutants. Detection of H_2O_2 was achieved by using the Amplex® Red Hydrogen Peroxide Assay Kit (table 2.4). Generation of H_2O_2 by autooxidation of various reducing agents was also measured.

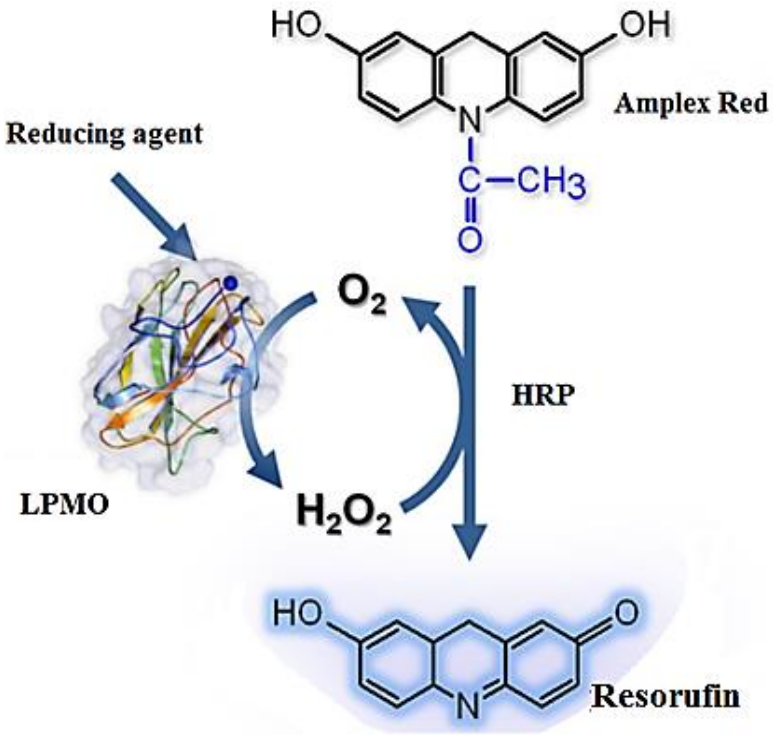

Figure 3.1. Schematic overview of the proposed reaction for detection of LPMO activity. The scheme shows what may happen when LPMOs are incubated (in the absence of their natural substrate) with Amplex Red®/HRP and a reducing agent. The figure is modified from Kittl et al. (2012).

Materials

- Amplex® Red Hydrogen Peroxide Assay Kit (table 2.4)
    - Amplex® Red reagent
    - Dimethylsulfoxide (DMSO), 0.88 M
    - 5 x reaction buffer (0.25 M sodium phosphate, pH 7.4)
    - Hydrogen peroxide, 20 mM
    - Horseradish peroxidase, 10 U
- Reducing agents (100 mM)
    - 3-hydroxyanthranilic acid
    - Ascorbic acid
    - Catechin
    - DL-dithiothreitol
    - Gallic acid
    - Hydroquinone
    - Reduced gluthatione
    - Tartaric acid

- 50 µM solution of purified CBP21 variants (90 % saturated with copper)
- TraceSELECT® Ultra water (ion free water)
- Falcon tubes, 15 ml
- Multichannel pipette
- 96-well microtiter plate
- Multiskan FC photometer

Procedure

All components of the kit were allowed to warm to room temperature before the experiment was conducted. Stock solution of all reagents was prepared as follows: to prepare 10 mM Amplex® Red reagent, 60 µl DMSO was added per one vial of Amplex® Red. The reaction buffer was made by adding 4 µl 5 x reaction buffer to 16 ml TraceSELECT® Ultra water, while one vial of HRP was dissolved in 1 ml 1 x reaction buffer to make a 10 U/ml HRP solution. Appropriate amounts of H_2O_2 were added to 1 x reaction buffer to yield 1 ml of a 20 mM H_2O_2 stock solution. To prepare a working solution of 100 µM Amplex Red reagent and 0.2 U/ml HRP, the following reagents were mixed in a 15 ml Falcon tube: 50 µl of the Amplex Red reagent stock solution, 100 µl of 10 U/ml HRP stock solution and 4.85 ml of 1 x reaction buffer.

To generate a H_2O_2 standard curve, appropriate volumes of the H_2O_2 stock solution was diluted in 1 ml 1 x reaction buffer to generate H_2O_2 concentration of 4, 8, 12, 16 and 20 µM. A control with only 1 x reaction buffer was included (0 µM H_2O_2). 50 µl of the standards and the control were applied to different wells in a 96-well microtiter plate after which 50 µl Amplex Red/HRP working solution was added to each well. The photometer was set to measure absorbance at 540 nm every 30 seconds for two hours. Resorufin exhibits excitation and emission maxima of approximately 571 nm and 585 nm, respectively in a reaction buffer at pH 7.4. The filter used in the photometer where 540 nm for excitation (540 nm was the photometer filter closest the excitation maxima). All samples and controls were measured in triplicates.

H_2O_2 generation by CBP21 variants was measured by setting up reactions (200 µl) containing 2 µM enzyme and 2 mM ascorbic acid in 1 x reaction buffer. Since ascorbic acid (and all the reductants listed above) is prone to autoxidation, the reducing agent was added last. A negative control containing 1 x reaction buffer and a background control containing 2 mM

ascorbic acid in 1 x reaction buffer were included. 50 µl of all samples and controls were added to separate wells of a microtiter plate using a multichannel pipette. Subsequently, 50 µl Amplex Red/HRP working solution was added to each which the formation of resorufin was monitored for two hours as described above.

To investigate whether H_2O_2 formation is proportional to the enzyme concentration, dose response curves were determined by varying the concentration of $CBP21_{WT}$ using 2 mM ascorbic acid as reductant. Various reductants were also tested for H_2O_2 formation by setting up reactions containing 2 mM reductant in 1 x reaction buffer. All experiments were repeated at least 5 times.

3.12 Isothermal titration calorimetry

Isothermal titration calorimetry (ITC) measure the heat generated or absorbed when two or more molecules interact and is a powerful tool to determine the thermodynamic parameters in a reaction. Applications of ITC involve study of protein-protein interactions and protein-ligand interaction. Heat released (exothermic reaction) or adsorbed (endothermic reaction) during a reaction is equal to the reaction that has occurred and is called enthalpy. Entropy is the measure of disorder in a system, while the disassociation constant is the affinity of a ligand towards a substrate (Lewis & Murphy 2005). The stoichiometry of the reaction is the average number of binding sites per mole of protein, while Gibbs energy is the total energy from the reaction that can do work. The ITC instrument consists of two cells, a reference cell and a sample cell, both surrounded by a jacket (Fig. 3.2). A syringe is used to inject enzyme into the sample cell containing the substrate (Fig. 3.3). The heat required to hold the sample cell at the same temperature as the reference cell is measured by a calorimeter. For each injection a peak appears in the thermogram (recorded continuously as the reaction occurs), representing the heat generated (or absorbed) by the system when protein bind to the substrate. When the substrate is saturated, subsequent injections produce small peaks similar to the peaks generated by heat of dilution, which

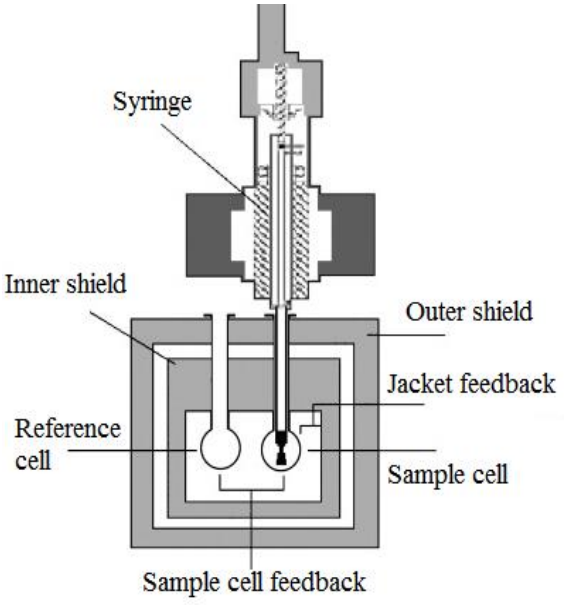

Figure 3.2. Overview of an ITC device. The figure is modified from (Sobhany & Negishi 2006)

should be subtracted from all injections before the experiment is analyzed (Leavitt & Freire 2001). The area of the peaks in the thermogram gives information about the dissociation constant (K_d), the stoichiometry of the reaction (n), and the enthalpy of binding (ΔH; the change in ΔH is positive for an endothermic reaction, while negative for an exothermic reaction.). From these parameters entropy (ΔS) can be calculated using equation 4.

Equation 4. $\Delta G = -RTlnK = RTlnK_d = \Delta H - T\Delta S$ (R = 1.987 cal/K mol and T = 298 K)

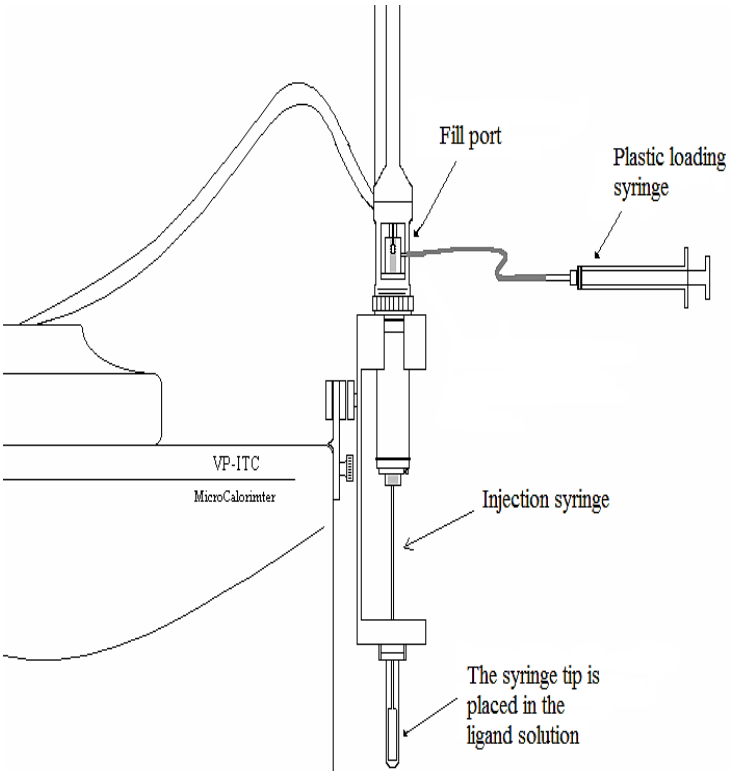

Figure 3.3. Illustration of the injection syringe connected to the ITC instrument. The figure is adopted from the VP-ITC MicroCalorimeter user manual.

Materials

- 600 µl of 50 µM $CBP21_{WT}$ solution (99 % saturated with copper) in 50 mM Tris, pH 8.0 and 1.8 mM acetic acid
- 3 mg/ml β-chitin^C (table 2.3)
- Degas instrument
- VP-ITC system (MicroCal)

Procedure

The substrate sample and the protein sample were placed in a degassing chamber and degassed for 20 minutes to avoid signals from air bubbles or the release of dissolved gasses during titration. The sample cell was washed several times with dH_2O to avoid interference of contaminants from previous runs and further washed with sample buffer using a Hamilton syringe. Once the sample cell was cleaned and equilibrated with sample buffer, 1.8 ml of the substrate sample was carefully injected into the cell without making any bubbles. Any bubbles were removed by moving the syringe up and down. A plastic syringe with tubing was connected to the fill port and the injection syringe was washed with dH_2O several times followed by two washes with the sample buffer. Air was removed from the injection syringe before the injection needle was placed into the protein sample. Approximate 500 µl of sample was drawn into the syringe until it was completely full. To ensure the injection needle was free of air, a little excess volume was drawn into the port with the attached plastic tube before the fill port was closed. Injection needle was carefully wiped clean from droplets. Subsequently, the injection syringe was placed in the sample cell and all parameters for the experiment were set up using the VPViewer software. Injection volume was set to 2 µl, measurement temperature to 30°C, stirring speed to 310, time between injections to 360 seconds, while the number of injections was set to maximum value (500). It is important that the injection time is adequate to give the heat signal enough time to return to baseline before the next injection. The sample cell was allowed to reach the same temperature as the reference cell (filled with degassed dH_2O) before the experiment was in initiated.

4 RESULTS

4.1 Mutant design

In this study seven conserved residues on the substrate binding surface close to the catalytic center of CBP21 were mutated, generating variants $CBP21_{S58A}$, $CBP21_{T111A}$, $CBP21_{A112G}$, $CBP21_{W178F}$, $CBP21_{I180R}$, $CBP21_{T183A}$ and $CBP21_{F187Y}$. A recent NMR study of CBP21 have indicate that residue S58, T111 and A112 are involved in substrate binding (Aachmann et al. 2011), but this feature has never been demonstrated by site-directed mutagenesis, nor has it been investigated if these residues are important for catalysis. Based on the proposed reaction mechanism (Fig. 1.6), the copper present in the active site is reduced by one electron transfer by a reducing agent. It is unknown how the electron transfer from the reducing agent to the copper occurs. In order to investigate whether a possible long-range electron transfer through the protein, two residues located in the interior of the protein was mutated, W178 and F187. To explore the importance of a putative binding-pocket on the substrate binding surface, residue I180 and T183 was mutated. All mutants constructed are listed in table 4.1 with a description of the location of the residue. The table also indicates whether the mutants were active, while a graphic representation of mutated residues is shown in figure 4.2. Fig. 4.3 provides a multiple sequence alignment of CBP21 and seven other bacterial CBM33s, showing to what extent the mutated (and others) residues are conserved.

Table 4.1. CBP21 mutants. The table describes the location of the mutated residue and indicate whether the mutant was active or not. Theoretical molecular weights (MW) and theoretical extinction coefficients are also given. The theoretical extinction coefficient of secreted $CBP21_{WT}$ is 35200 (the value has previously been calculated experimentally to 29823 by Gustav Vaaje-Kolstad), while the theoretical MW is 18793.9 Dalton. The column "conserved" refers to the sequence alignment of Fig. 4.3 with seven sequences; e.g. "6/8" means that the residue is conserved in 6 out of 8 sequences shown.

Mutation	**Location on CBP21**	**Conserved**	**Ext. coef.**	**MW**	**Status**
S58A	Positioned at the end of the surface-exposed pseudo domain	6/8	35200	18777.9	Active
T111A	Positioned on a surface-exposed loop connecting β-strand 2 and 3, close to the copper binding site	6/8	35200	18763.8	Active
A112G	Positioned on a surface-exposed loop connecting β-strand 2 and 3, close to the copper binding site	8/8	35200	18779.8	Active
W178F	Positioned on β-strand 6 inside the protein	8/8	29700	18754.8	Active
I180R	Positioned on β-strand 6 in the bottom of a surface "pocket"	3/8	35200	18836.9	Active
T183A	Positioned on a surface-exposed loop at the side wall of the surface "pocket" connecting β-strand 6 and 7	6/8	35200	18763.8	Active
F187Y	Positioned on β-strand 7 inside the protein	7/8	36690	18809.8	Active

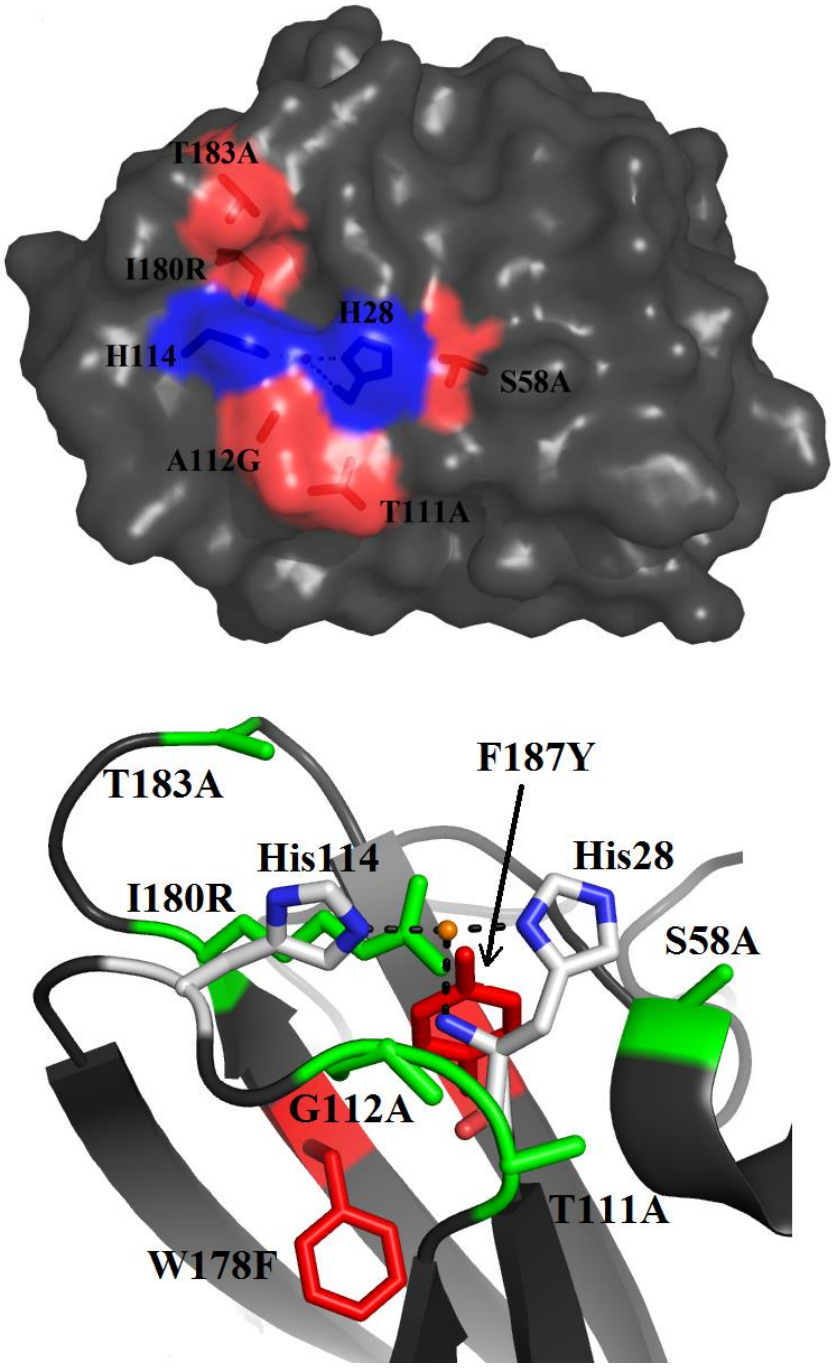

Figure 4.2. Overview of mutated residues in CBP21. In the upper image the view is onto the active site (His28 & His114) and the substrate-binding surface. Mutated residues are shown in sticks and highlighted (red), while His114 and His28 (blue) are only shown to indicate the relative distances between mutated residues and the active site. Note that residue I180 and T183 are located in or near a small surface "pocket" close to the copper binding site (see text for details). The lower image; shows all seven mutations. Residues in the interior of the protein are marked red, while surface exposed residues are marked green. His28 and His114 (white/blue) with a bound copper ion (represented as a gold sphere) are included to show the relative distances between the active site and the mutated residues. Mutated residues are shown in sticks. Both figures are generated using PyMOL (DeLano 2002)

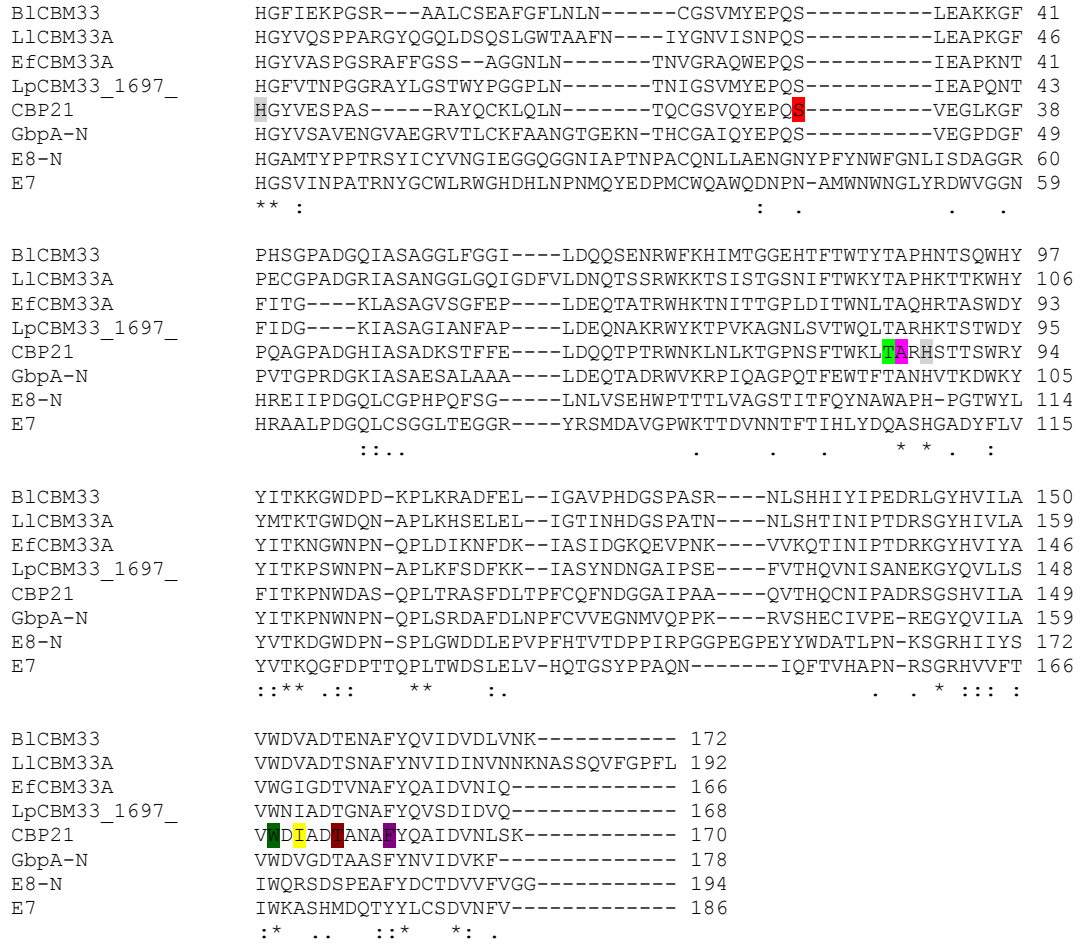

Figure 4.3. Multiple sequence alignment of bacterial CBM33s. His28 and His114 which coordinate the copper ion present in CBP21 are shaded grey, while residues mutated in this study are labelled with colour: S58 (red), T111 (green), A112 (magenta), W178 (dark green), I180 (yellow), T183 (dark red) and F187 (purple). Note that GbpA and E8 have multiple domains and that only their N-terminal CBM33 domain is included in the alignment. Information about binding preference and activity for each protein in the alignment is listed in table 4.2. The multiple alignment was generated using ClustalW.

Table 4.2. Bacterial CBM33s. The table lists information for eight bacterial CBM33s. These CBM33s were used to generate the multiple sequence alignment in figure. 4.3.

Protein	Organism and strain	Domain	Binding activity and other features	Oxidative polysaccharide cleavage	Uniprot ID	Reference
CBP21	*Serratia marcescens* BJL200	CBM33	Binds to β-chitin, regenerated chitin and colloidal chitin	Yes, chitin	O83009	(Suzuki et al. 1998; Vaaje-Kolstad et al. 2010)
GbpA-N	*Vibrio cholerae* O1 Biovar El Tor N16961	CBM33	Protein adheres to cell surfaces containing mucin; promotes bacterial adhesion	Unknown	Q9KLD5	(Wong et al. 2012)
*Ef*CBM33A	*Enterococcus faecalis* V583	CBM33	Binds both α- and β-chitin. Up regulation when bacterium grows in virulence inducing conditions, particularly in the presence of urine and blood serum	Yes, chitin	Q838S1	(Vaaje-Kolstad et al. 2012)
*Lp*CBM33(1697)	*Lactobacillus plantarum* WCFS1	CBM33	Binds to α- and β chitin. Interacts with intestinal mucin and is up-regulated in the vaginal tract during alkaline conditions	Unknown	F9UP60	(Liu et al. 2011; Sanchez et al. 2011)
*Ll*CBP33A	*Lactococcus lactis ssp. lactis* IL1403	CBM33	Binds to α- and β-chitin, and has also affinity for avicel and colloidal chitin	Yes, chitin	Q9CE94	(Vaaje-Kolstad et al. 2009)
*Bl*CBM33	*Bacillus licheniformis* ATCC 14580	CBM33	Binds to α- and β-chitin		Q65N87	(Johansen 2012)
E7 (*Tf*CBM33A)	*Thermobifida fusca* YX	CBM33	Binds to α- and β-chitin followed by bacterial microcrystalline cellulose	Unknown	Q47QG3	(Moser et al. 2008)
E8 (*Tf*CBM33B)	*Thermobifida fusca* YX	CBM33-CBM2	Binds to β-chitin and has also affinity for α-chitin and microcrystalline cellulose	Unknown	Q47PB9	(Moser et al. 2008)

4.2 Construction of CBP21 mutants

The pRSET-B/*cbp21* vector was isolated according to section 3.2.2 and further incubated with EcoRI and XbaI as described in section 3.2.3, before DNA agarose gel electrophorese (section 3.2.4) was conducted to verify the correct size of the vector. Figure 4.4a, lane 2, shows only one band at approximately ~3500 bp after treating the vector with EcoRI, which is in agreement to the vector size (see appendix A, Fig. A1 for vector map). When the vector was treated with both EcoRI and XbaI, two bands appeared respectively at 800 bp and 2800 bp (lane 3), which is consistent with the estimated outcome (incubation with both EcoRI and XbaI will in theory give two bands, one at 810 bp and another band at 2748 bp). Untreated supercoiled vector was included as a control (Fig. 4.4b). The band at ~3500 bp is consistent with the total size of the vector, while the band at approximate ~7000 bp was unexpected. Starting with the isolated plasmid, all seven CBP21 mutants were constructed by site-directed mutagenesis using mutagenic primers listed in table 2.5 and the protocol described in section 3.2.5. Mutated CBP21-encoding genes in plasmids to be used further for production of mutant protein were sequenced completely to verify the identity of the mutation and the absence of undesirable additional mutations according to section 3.2.9. First attempt to construct the mutants failed, since an additional mutation was present in all constructs. Since the same undesirable mutation was present in all constructs, the template DNA was probably a mutant and not the WT. Next attempt, using the correct template, all mutants were successfully constructed.

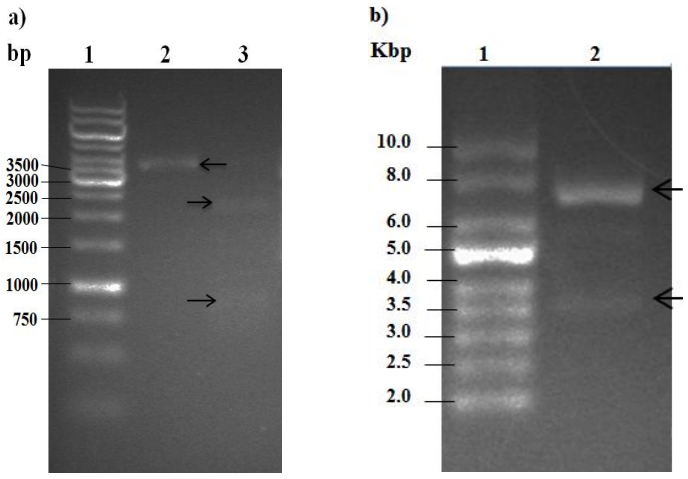

Figure 4.4. Agarose gel analysis of pRSET-B/cbp21 restriction digests. Visible bands are marked with an arrow. **a)** Lane 1, 1 kb DNA ladder (Thermo Scientific); 2, pRSET-B/*cbp21* cut with EcoRI; 3, pRSET-B/*cbp21* cut with EcoRI and XbaI. **b)** Lane 1, supercoiled DNA ladder (New England Biolabs, NEB); 2, untreated supercoiled pRSET-B/*cbp21*.

4.3 Protein purification

4.3.1 Purification of CBP21 variants and *Ef*CBM33A

Purification of CBP21 variants and *Ef*CBM33A WT was achieved by chitin-affinity chromatography according to section 3.3.2. This was found to be a very effective purification method that essentially removes all contaminating proteins (Fig. B1a and B1b in appendix B show typical chromatograms recorded during purification of CBP21 and *Ef*CBM33A, respectively). The whole purification process, from the bacterial culture to collection of purified protein, was supervised by SDS-PAGE for all proteins (Fig. 4.5; for simplicity only the purification process of $CBP21_{WT}$ is shown). Purification followed by dialysis and up-concentration yielded concentrations in the range of 5 - 20 mg/ml and a total protein yield of ~10 mg/L culture. Production levels, purification results and total yields were similar for all CBP21 variants. All obtained CBP21 variants and *Ef*CBM33A WT were purified to ~99% purity, as estimated from SDS-PAGE gels (Fig. 4.5 and Fig. 4.6).

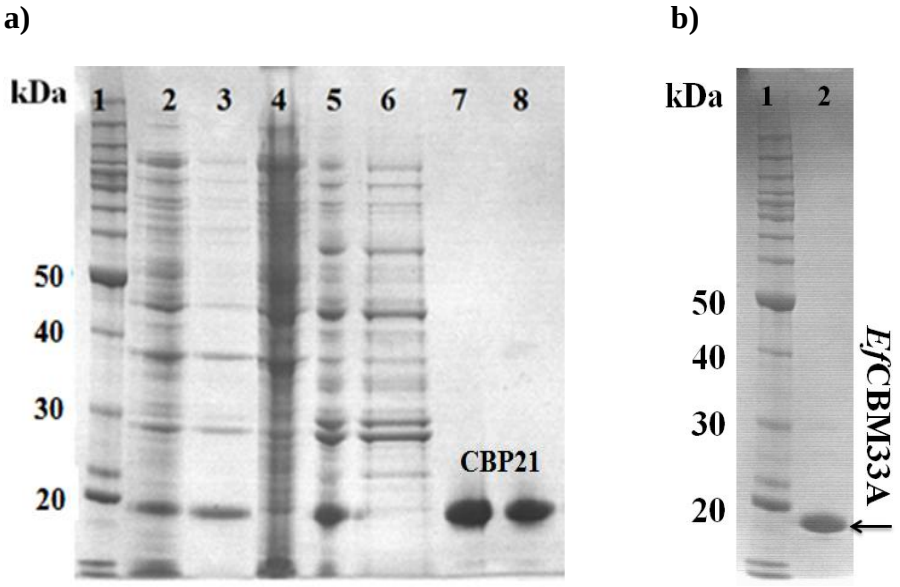

Figure 4.5. Purification of $CBP21_{WT}$ and *Ef*CBM33A. a) Lane 1, Bench Mark™ Protein Ladder (Invitrogen); 2, cell lysate; 3, spheroplast buffer (the supernatant after re-suspending the bacteria cells in sucrose followed by centrifugation); 4, bacteria pellet (after cold osmotic shock); 5, perimasmic extract; 6, flow through during chitin affinity chromatography; 7, purified protein; 8, concentrated protein (diluted 10 times in dH_2O). **b)** Lane 1, ladder; 2, purified *Ef*CBM33A. The sample size was 20 µl.

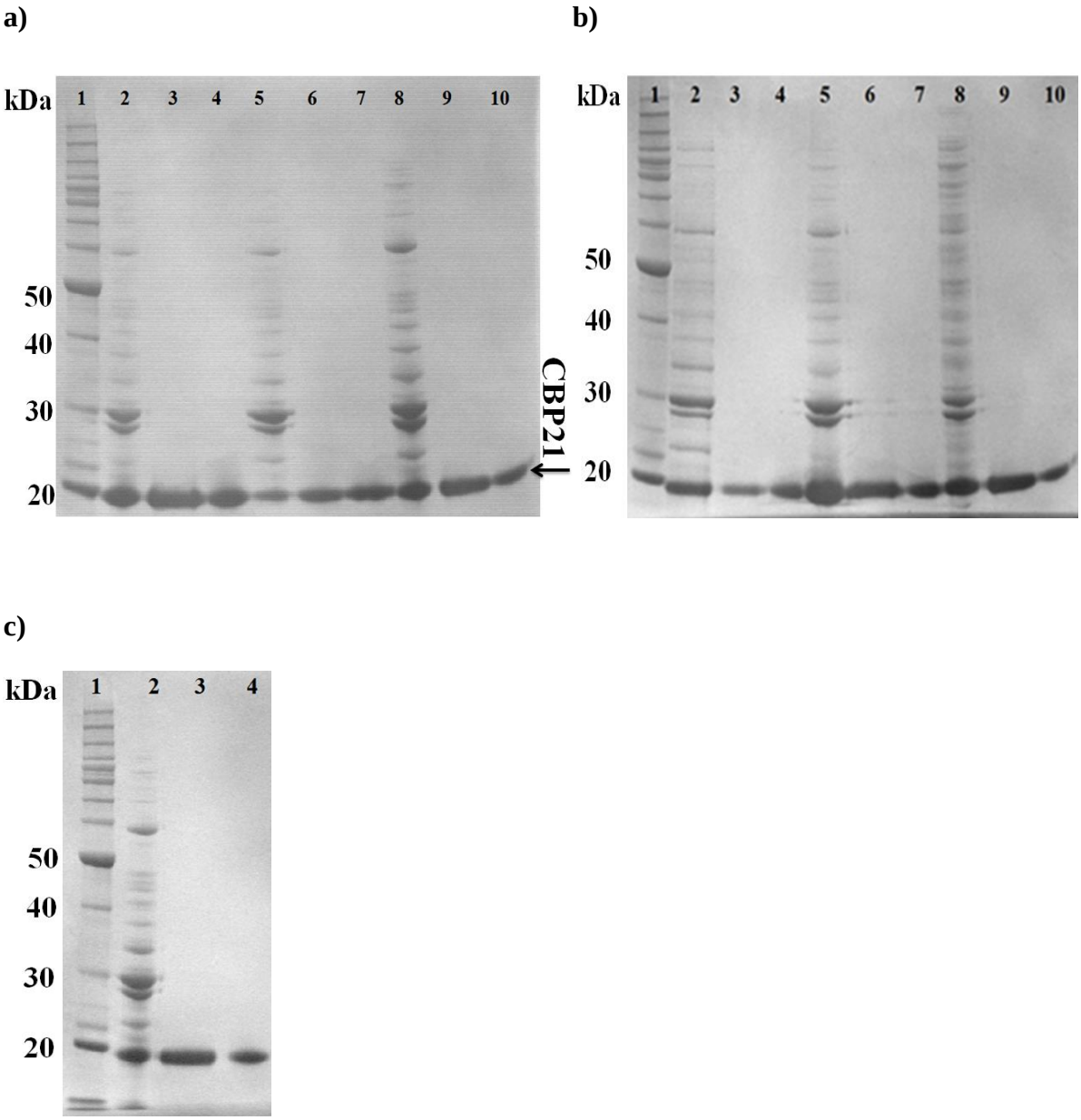

Figure 4.6. Purity of CBP21 mutants before and after purification. a) Lane 1, Bench Mark™ Protein Ladder (Invitrogen); 2, $CBP21_{S58A}$ periplasmic extract; 3, $CBP21_{S58A}$ purified; 4, $CBP21_{S58A}$ concentrated; 5, $CBP21_{T111A}$ periplasmic extract; 6, $CBP21_{T111A}$ purified; 7, $CBP21_{T111A}$ concentrated; 8, $CBP21_{A112G}$ periplasmic extract; 9, $CBP21_{A112G}$ purified; 10, $CBP21_{A112G}$ concentrated. **b)** Lane 1, ladder; 2, $CBP21_{W178F}$ periplasmic extract; 3, $CBP21_{W178F}$ purified; 4, $CBP21_{W178F}$ concentrated; 5, $CBP21_{I180R}$ periplasmic extract; 6, $CBP21_{I180R}$ purified; 7, $CBP21_{I180R}$ concentrated; 8, $CBP21_{T183A}$ periplasmic extract; 9, $CBP21_{T183A}$ purified; 10, $CBP21_{T183A}$ concentrated. **c)** Lane 1, ladder; 2, $CBP21_{F187Y}$ periplasmic extract; 3, $CBP21_{F187Y}$ purified; 4,$CBP21_{F187Y}$ concentrated. Sample size was 20 µl. All samples called "concentrated" were diluted 10 times in dH2O.

4.3.2 Purification of *Lp*CBM33(1697)

*Lp*CBM33(1697) was purified from a periplasmic extract of the producer strain in a two-step purification procedure involving IEC and SEC as described in section 3.3.3 and 3.3.4, respectively. The first purification step was IEC, which separated *Lp*CBM33(1697) from the majority of other protein molecules based on its charge. A gradient of increasing salt concentration was used to elute and separate bound protein and fractions of 2 ml were collected. Based on the recorded chromatogram (Fig.4.7), selected fractions putatively containing *Lp*CBM33(1697) were analysed by SDS-PAGE (fig.4.8). Fractions from peak 1 in the chromatogram showed protein bands of correct size (*Lp*CBM33(1697) has a MW of 18.6 kDa), but the presence of protein bands of incorrect sizes indicates that several contaminating proteins still are present. Fraction 12 – 17 were pooled and the buffer was changed to 20 mM Tris-HCl, pH 8.0 according to section 3.3.6 before MALDI-TOF MS analysis was conducted to confirm presence of *Lp*CBM33(1697) (see appendix C, fig. C1). Since the fractions contained several proteins bands of various sizes, further purification by SEC was necessary.

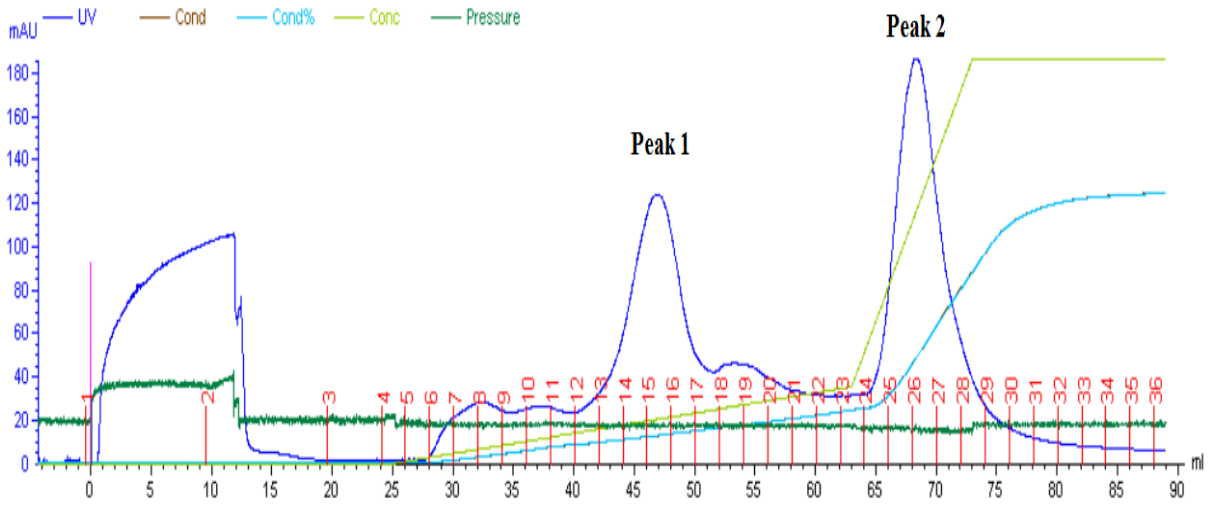

Figure 4.7. Chromatogram recorded during IEC purification of *Lp*CBM33(1697). Approximately 20 ml of periplasmic extract was applied to the column with a flow rate of 2 ml/min followed by washing with 2 column volumes (approximate 240 ml) of 50 mM Tris-NaOH pH 10.0 (binding buffer). A gradient running from 0 – 50% 50 mM Tris-NaOH pH 10.0, 1 M NaCl over 50 minutes was used to elute the proteins. The light green line represents the salt gradient, while the blue line represents protein absorption at 280 nm. Eluted proteins of interest were collected in 2 ml fractions (fractions are indicated by red vertical lines and red fraction numbers; the numbered red line appears at the end/start of the fractions).

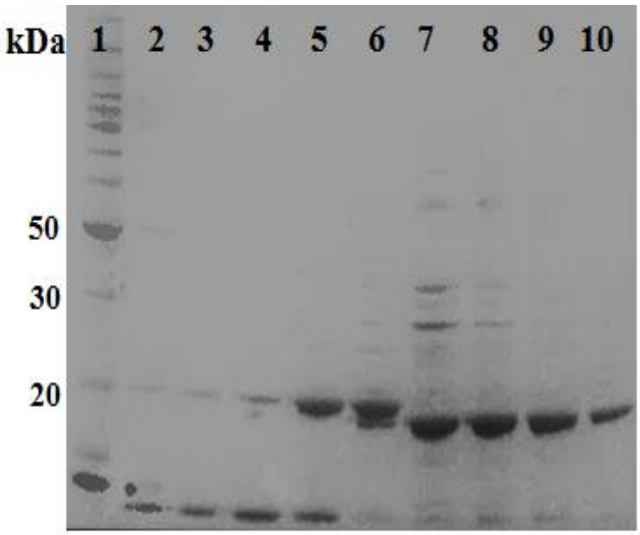

Figure 4.8. SDS-PAGE analysis of selected fractions collected during IEC purification of *Lp*CBM33(1697). Selected fractions from peak 1 and 2 (see Fig. 4.7) was analysed for *Lp*CBM33(1697). Lane 1, Bench Mark™ Protein Ladder (Invitrogen); 2, fraction 12; 3, fraction 13; 4, fraction 14; 5, fraction 16; 6, fraction 17; 7, fraction 25; 8, fraction 26; 9, fraction 27; 10, fraction 28. Fractions 1, 8, 9, 10, and 11 were also analysed by SDS-PAGE, but no protein bands of correct sizes were found (result not shown)

The chromatogram recorded during SEC showed two major peaks putatively containing *Lp*CBM33(1697) (Fig.4.9) Selected fractions from peak 1 and 2 (fraction 52, 62, 63-70) were analysed by SDS-PAGE (Fig. 4.10). Fractions containing purified *Lp*CBM33(1697) were pooled and concentrated to 1 ml before the buffer was changed to 1 x PBS by extensive dialysis according to section 3.3.5.

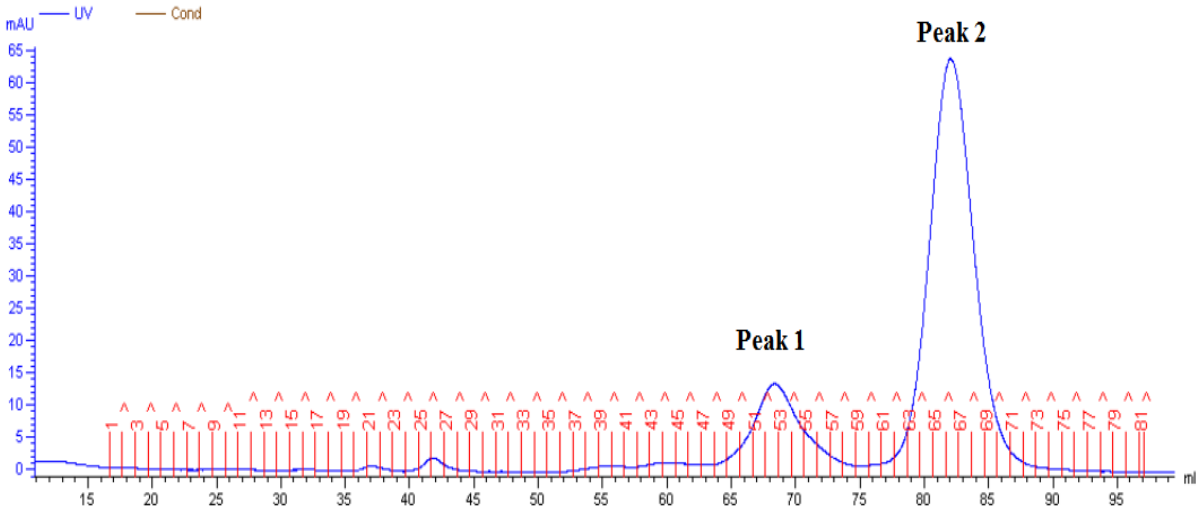

Figure 4.9. Chromatogram recorded during SEC purification of *Lp*CBM33(1697). Concentrated sample (1 ml) from the first purification step (IEC) was applied to the column with a flow rate of 0.3 ml/min, followed by one column volume of 50 mM Tris in 200 mM NaCl, pH 7.5 (running buffer) to elute the proteins. Eluted

proteins were collected in fractions of 2 ml. The blue line represents protein absorption at 280 nm, while fractions are indicated by red vertical lines and red fraction numbers; the numbered red line appears at the end/start of the fractions).

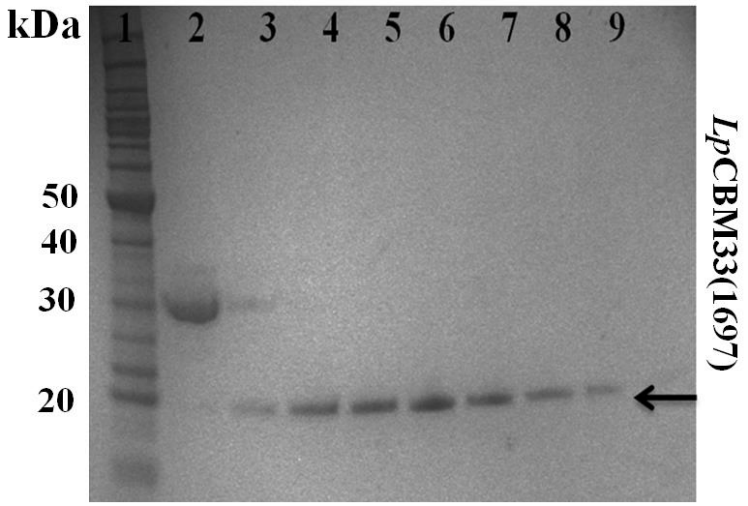

Figure 4.10. SDS-PAGE analysis of selected fractions collected during SEC purification of *Lp*CBM33(1697). The figure shows selected fractions from peak 1 and 2 in the SEC chromatogram (see fig.4.8). Lane 1, Bench Mark™ Protein Ladder (Invitrogen); 2, fraction 52; 3, fraction 62; 4, fraction 63; 5, fraction 64; 6, fraction 66; 7, fraction 68; 8, fraction 69; 9, fraction 70. Protein bands with correct size (18.6) are marked with an arrow.

4.4 Activity assays

4.4.1 Activity analysis using MALDI-TOF MS for product detection

All purified CBM33s were investigated for LPMO activity using MALDI-TOF MS according to section 3.7 for product detection. As noted in section 1.2.4, the copper ion is crucial for LPMO activity. In order to inactivate the enzymes, all CBP21 variants were treated with EDTA to remove the copper ion before degradation reactions were set up followed by MALDI-TOF MS analysis of products (appendix C, Fig. C2). The results showed no formation of oxidized chitooligosaccharides. After removing the copper, accurate copper saturation of CBP21 could be was achieved by adding appropriate amounts $Cu(II)SO_4$ to the apo enzyme preparation.

All CBP21 variants showed similar product profiles, with dominance of even numbered products (Fig. 4.11, see appendix C, Fig. C3 for MALDI-TOF MS analysis of mutants). All soluble oxidized chitooligosaccharides were observed in clusters that represent sodium and potassium adducts and the sodium adducts of the sodium salt of the aldonic acid In some instances the lactone form of the aldonic acid could be observed (Fig. 4.12; in solution aldonic acids are in equilibrium with δ1,5-lactone where the aldonic acid form is predominant at high pH). The MALDI-TOF MS analyses also showed that no partially deacetylated products was present (partially acetylated products differ from acetylated products by 42 Da per deacetylation). All reactions were set up in an identical manner, with identical enzyme and substrate concentration and identical incubation times; although quantitative interpretation of MALDI-TOF MS spectra is not straightforward, it seems safe to conclude from Fig. C3 that the mutants had varying activities. In particular, $CBP21_{I180R}$ seems to have little activity.

The MALDI-TOF MS spectra obtained from incubating β-chitin^{A} with *Lp*CBM33(1697), *Ef*CBM33A and *Il*CBM33A and GbpA, respectively, show LPMO activity for all CBM33s, displaying the same striking dominance of even numbered products observed for $CBP21_{WT}$; $DP4_{ox}$ (m/z 869), $DP6_{ox}$ (m/z 1275) and $DP8_{ox}$ (m/z 1681) (Fig.4.13). Only fully acetylated products were observed and the composition of products is similar to that of $CBP21_{WT}$.

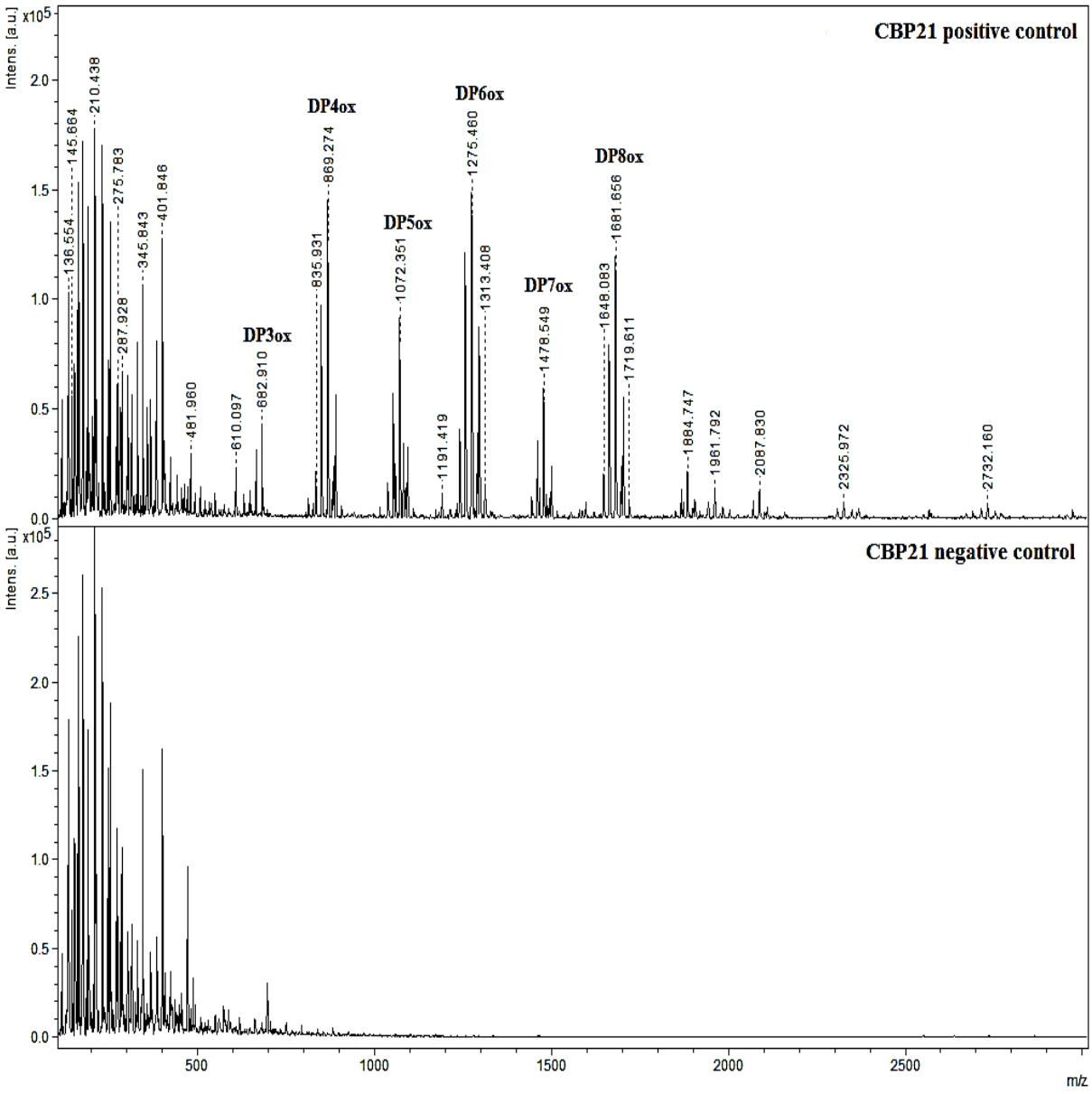

Figure 4.11. MALDI-TOF MS spectrum showing oxidized soluble chitooligosaccharides generated by $CBP21_{WT}$ when acting on β-chitin[A]. The upper spectrum shows oxidized chitooligosaccharides produced when 2 mg/ml β-chitin[A] was incubated with 1 µM $CBP21_{WT}$ and 1 mM ascorbic acid in 50 mM Bis-Tris pH 8.0 for 16 hours at 37°C and 900 rpm. The lower spectrum shows that no oxidized soluble chitooligosaccharides was detected under the same conditions, but without $CBP21_{WT}$. The peaks are labelled with their respective atomic masses and annotated according to their DP (degree of polymerization), i.e. the number of sugar moieties. Some examples: m/z 682.9 $[DP3_{ox}$ aldonic acid + $K]^+$; m/z 869.2 $[DP4_{ox}$ aldonic acid + $K]^+$; m/z 1072.3 $[DP5_{ox}$ aldonic acid + $Na]^+$; m/z 1275.4 $[DP6_{ox}$ aldonic acid + $Na]^+$; m/z 1478.5 $[DP7_{ox}$ aldonic acid + $Na]^+$; m/z 1681.6 $[DP8_{ox}$ aldonic acid – H+$Na]^+$.

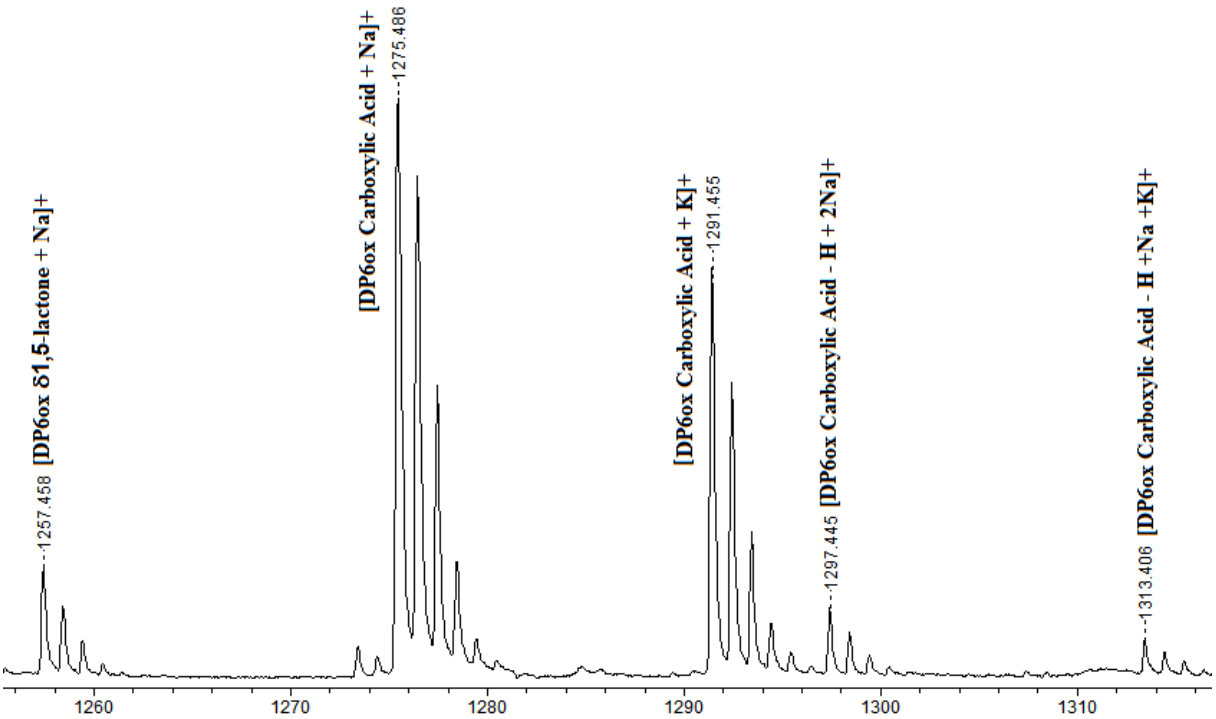

Figure 4.12. Close-up of the adduct cluster representing the hexameric oxidized chitooligosaccharide ($DP6_{ox}$). The figure shows oxidized hexameric products generated when β-chitin^{A} was incubated with $CBP21_{WT}$ in the presence of ascorbic acid as reducing agent. Adducts of hexameric products are labelled with their atomic mass and annotated with their predicted composition ("carboxylic acid"= aldonic acid)

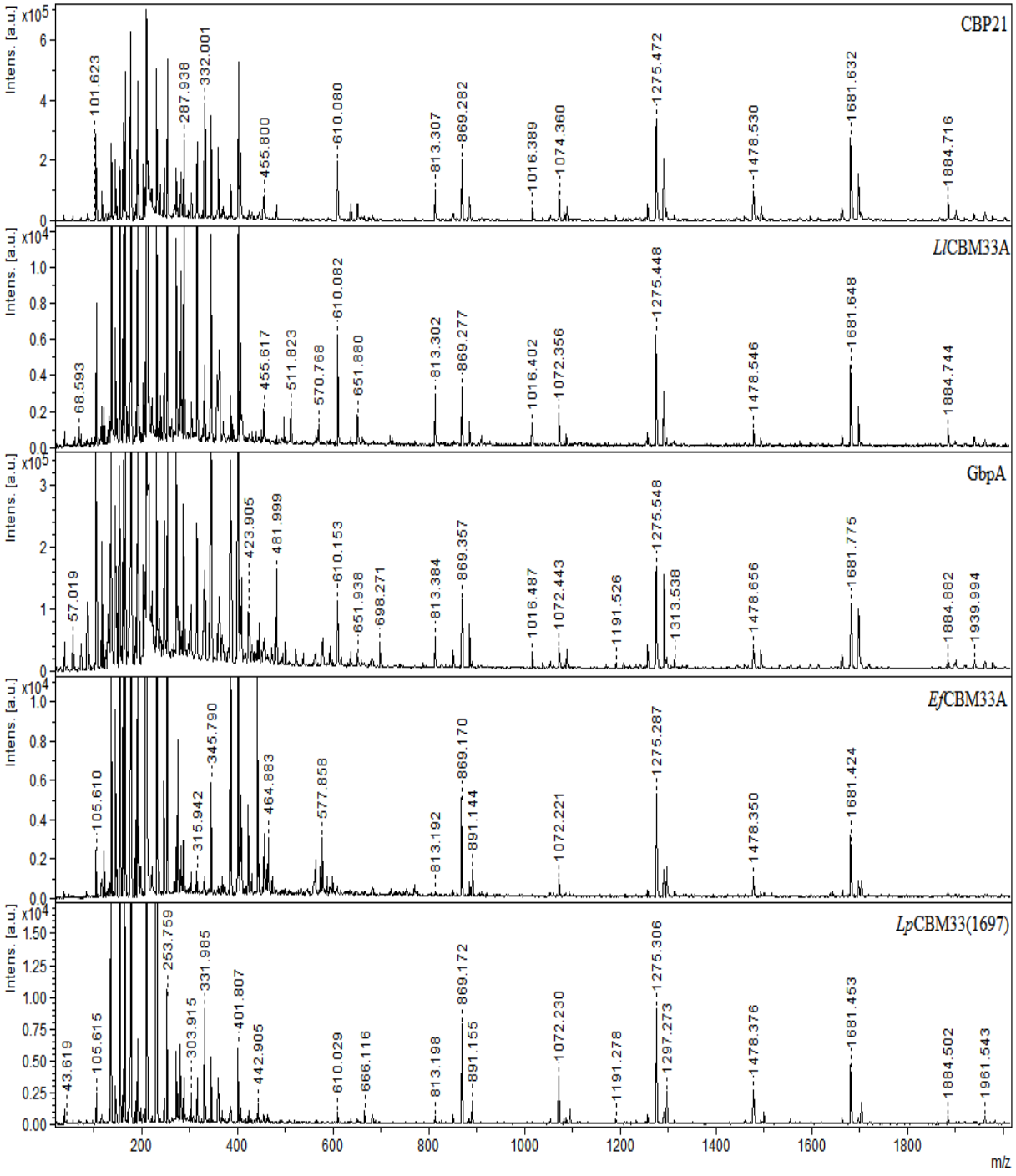

Figure 4.13. MALDI-TOF MS spectra showing oxidized soluble chitooligosaccharides generated by *Ef*CBM33A, *Ll*CBM33A, *Lp*CBM33(1697) and GbpA when acting on β-chitin[A]. The spectra show oxidized chitooligosaccharides produced when 2 mg/ml β-chitin[A] was incubated with 1 µM enzyme and 1 mM ascorbic acid in 50 mM Bis-Tris pH 8.0 for 16 hours at 37°C and 900 rpm.

4.4.2 Initial rate of CBP21 activity

The initial rate of CBP21 activity for both WT and mutants was estimated by quantifying product formation over time using a HILIC based UHPLC according to section 3.10. Oxidized products detected after degradation of β-chitin^{B} ranged from $DP4_{ox}$-$DP8_{ox}$ and accumulation of each product was quantified for all CBP21 variants are shown in Figures 4.14 – 4.18 ($DP4_{ox}$; Fig. 4.14, $DP5_{ox}$; Fig. 4.15, $DP6_{ox}$; Fig. 4.16, $DP7_{ox}$; Fig. 4.17 and $DP8_{ox}$; Fig. 4.18). Initial experiments showed that $CBP21_{I180R}$ did not produce any oxidized products when 1 µM of enzyme was used in the reaction mixture (results not shown), thus the enzyme concentration of this mutant was increased to 5 µM (it should be noted that the amount of oxidized products is not corrected for fivefold enzyme concentration in figures 4.16 and 4.18). The amount (calculated peak area represented as milli absorbance unit*minutes, mAU*min) of oxidized products formed over time showed close to linear production of oxidized products between 20-80 minutes. However, for some mutants ($CBP21_{S58A}$, $CBP21_{T111A}$, $CBP21_{A112G}$ and $CBP21_{W178F}$) product formation in the first 20 minutes of the reaction was faster than in the linear late phase of the reaction. In accordance with the results of the MALDI-TOF MS-based activity assays (see section 4.4.1, Fig. 4.11), UHPLC analyses of CBP21 products also showed a dominance of even numbered products (Fig.4.19). This is visible in Fig. 4.19 which provides a summary of the results depicted in Figures 4.14 – 4.18.

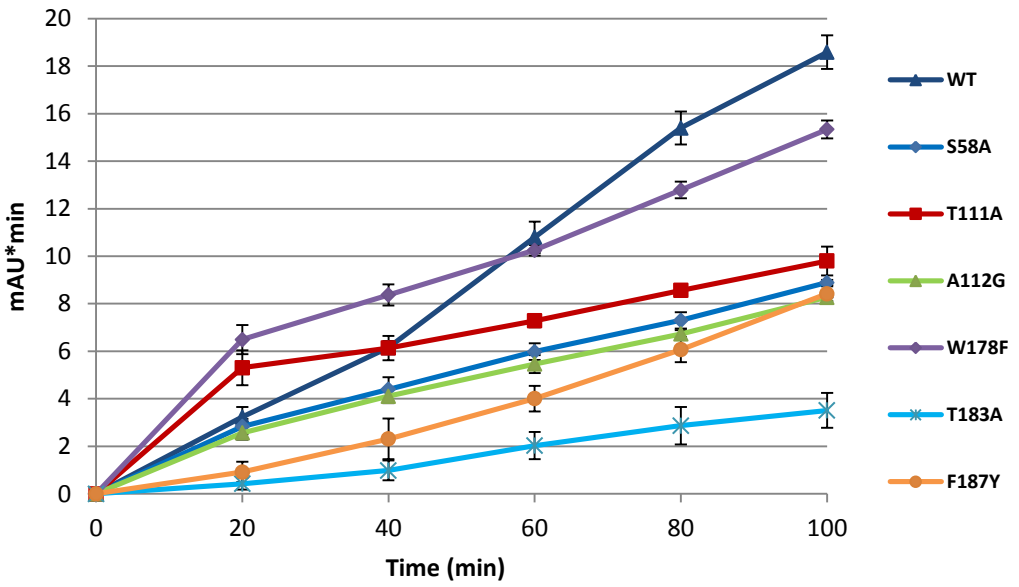

Figure 4.14. Generation of $DP4_{ox}$ upon degradation of β-chitin^{B} by CBP21 variants. Data show the formation of $DP4_{ox}$ over time when 7.5 mg/ml β-chitin^{B} was incubated with 1 µM enzyme and 15 mM ascorbic acid in 50 mM Tris-HCl pH 8.0 at 20°C and 1200 rpm. Each data point represents the mean value of three replicates (i.e. three samples were identical treated and measured in the same assay) and error bars indicate standard deviation (not visible for every point). No oxidized products could be detected for CBP21I180R, not even at five times higher (5 µM) enzyme concentration.

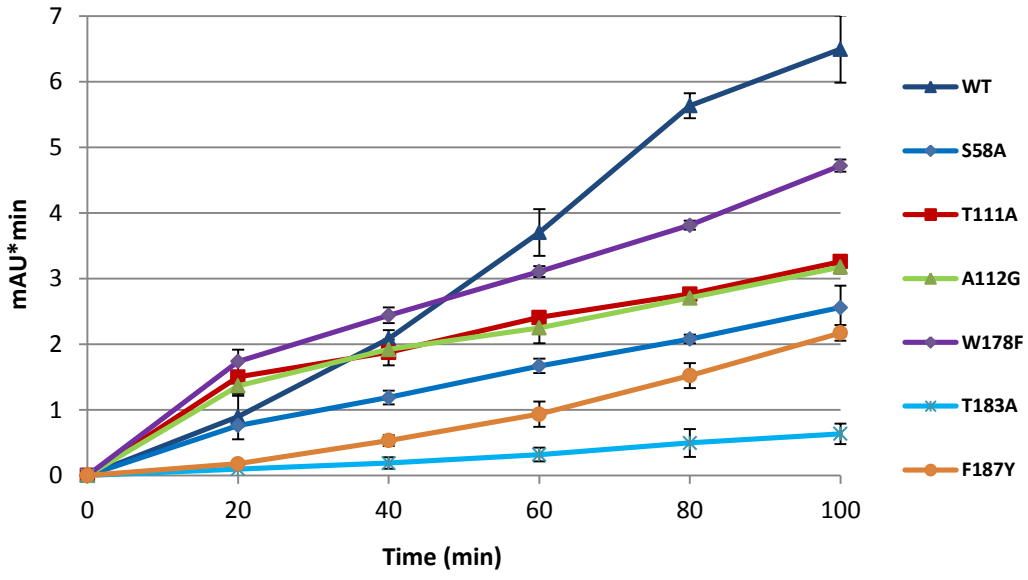

Figure 4.15. Generation of $DP5_{ox}$ upon degradation of β-chitin^{B} by CBP21 variants. Data show the formation of $DP5_{ox}$ in the same experiment as that described in the legend to Fig. 4.14. Each data point represents the mean value of three replicates (i.e. three samples were identical treated and measured in the same assay) and error bars indicate standard deviation (not visible for every point).). No oxidized products could be detected for CBP21I180R, not even at five times higher (5 µM) enzyme concentration.

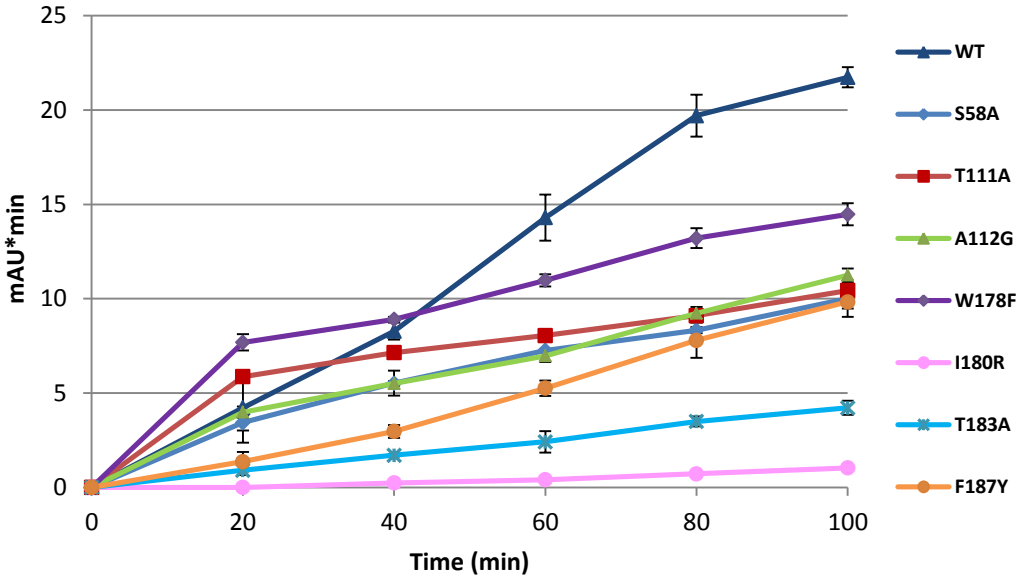

Figure 4.16. Generation of $DP6_{ox}$ upon degradation of β-chitin^{B} by CBP21 variants. Data show the formation of $DP6_{ox}$ in the same experiment as that described in the legend to Fig. 4.14. Each data point represents the mean value of three replicates (i.e. three samples were identical treated and measured in the same assay) and error bars indicate standard deviation (not visible for every point).

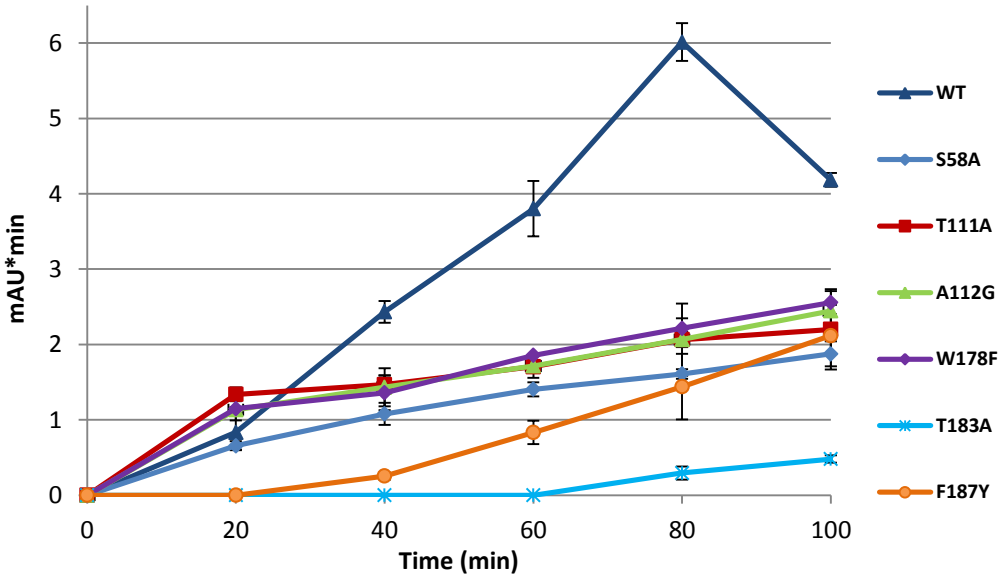

Figure 4.17. Generation of $DP7_{ox}$ upon degradation of β-chitin^{B} by CBP21 variants. Data show the formation of $DP7_{ox}$ over time when 7.5 mg/ml β-chitin^{B} was incubated under same conditions as noted in figure 4.14. Each data point represents the mean value of three replicates (i.e. three samples were identical treated and measured in the same assay) and error bars indicate standard deviation (not visible for every point). Note the drop in $DP7_{ox}$ from ~6 mAU*min to ~4 mAU*min by $CBP21_{WT}$ after 80 minutes of incubation.

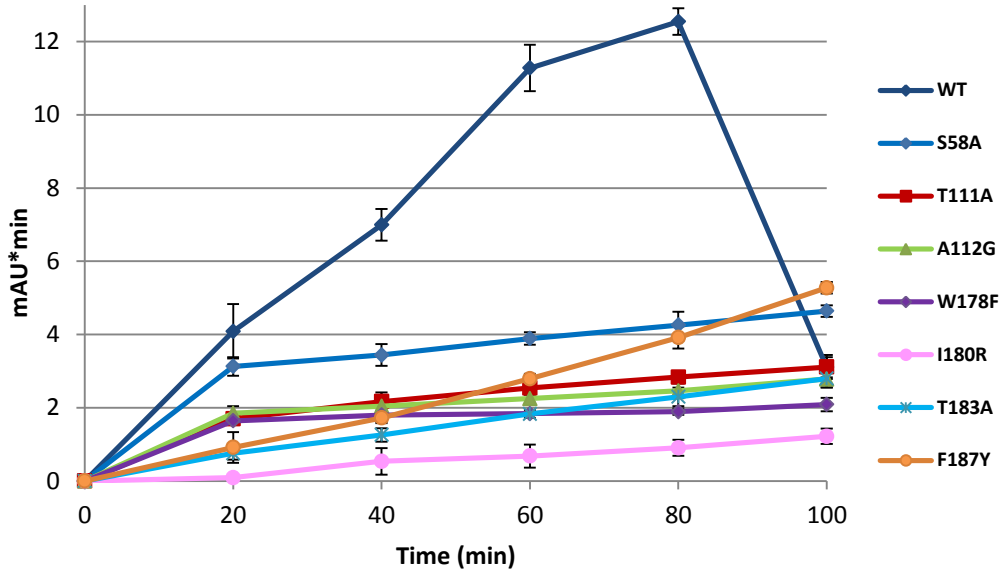

Figure 4.18. Generation of $DP8_{ox}$ upon degradation of β-chitin^{B} by CBP21 variants. Data show the formation of $DP8_{ox}$ in the same experiment as that described in the legend to Fig. 4.14. Each data point represents the mean value of three replicates (i.e. three samples were identical treated and measured in the same assay) and error bars indicate standard deviation (not visible for every point). Note the striking drop in $DP8_{ox}$ from ~12 mAU*min to ~4 mAU*min by $CBP21_{WT}$ after 80 min of incubation.

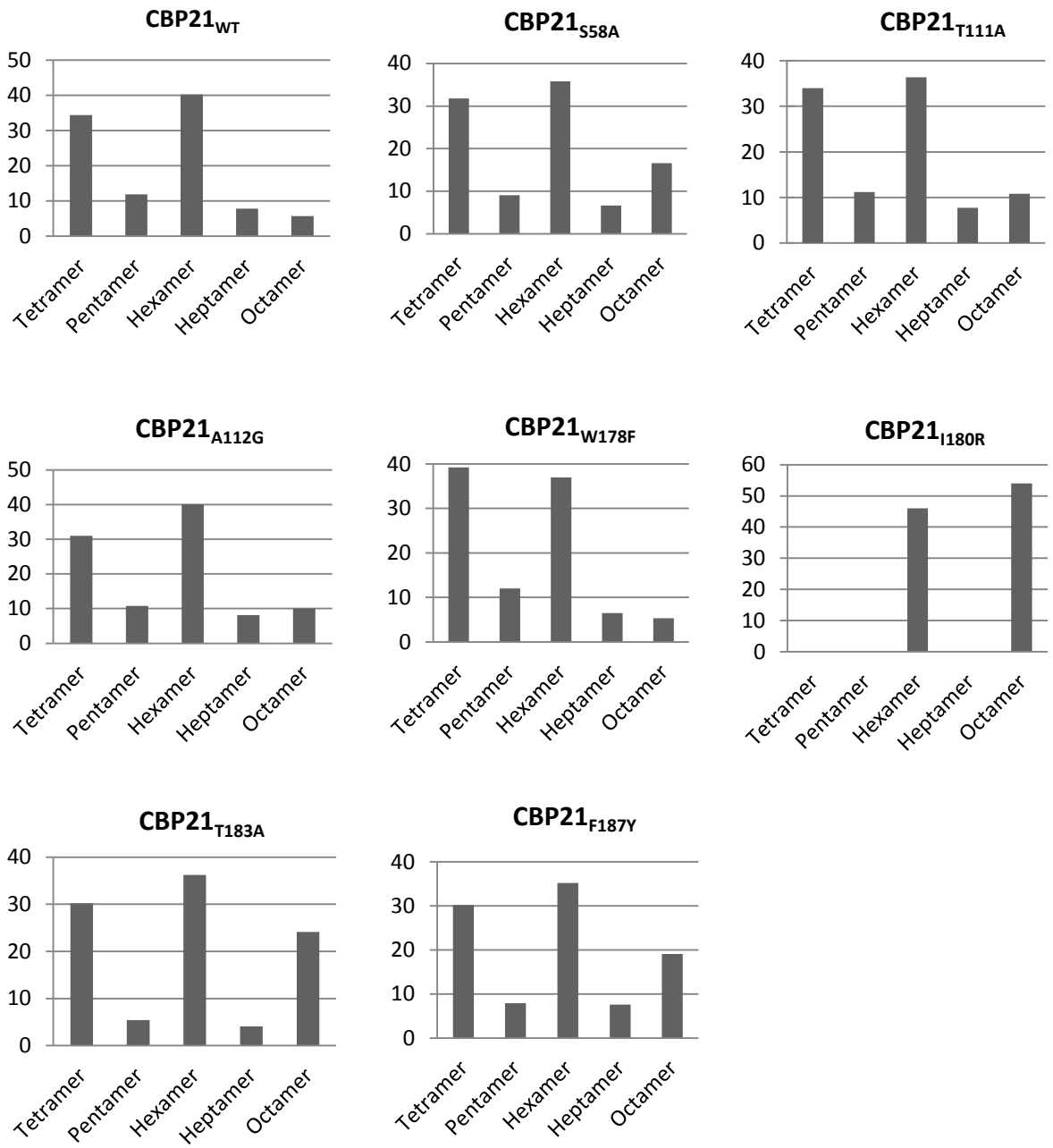

Figure 4.19. Product profile for WT and mutant CBP21. The figure shows the relative amounts of accumulated products (Y-axis, %) after 100 minutes of incubation. product. In order to convert the amount of each individual product to percentage, the amount (mAU*min) of each individual product was divided by the total amount of product. Tetramer = $DP4_{ox}$, pentamer = $DP5_{ox}$, hexamer = $DP6_{ox}$, heptamer = $DP7_{ox}$ and octamer = $DP8_{ox}$. While $CBP21_{WT}$ and most mutants generate products in the range of $(GlcNAc)_4$-$(GlcNAc)_8$, $CBP21_{I80R}$ only generates $(GlcNAc)_6$ and $(GlcNAc)_8$.

To quantify enzyme activities, the data for all soluble products generated by $CBP21_{WT}$ and mutants, as depicted in Figures 4.14 – 4.18, were combined and the result is shown in 4.20. The Figure shows that $CBP21_{I180R}$ is clearly the least active (not that the enzyme concentration used was 5 µM in this case, as opposed to 1 µM in all other cases). $CBP21_{T183A}$ also showed low activity, while $CBP21_{W178F}$ is the most active mutant with almost almost 15 % more end product than $CBP21_{T111A}$. The data show that several mutants produced higher or equal amount of oxidized products compared to $CBP21_{WT}$ within the first 20 minutes of the experiment, but after 100 minutes $CBP21_{WT}$ had generated a considerably higher amount of oxidized products than all mutants. A drop in the total amount of oxidized products produced by $CBP21_{WT}$ can be observed after 80 minutes of incubation, which is the result of a decrease in $DP7_{ox}$ and $DP8_{ox}$ (a chromatogram illustrating this remarkable observation is presented in appendix D, Fig. D1). By comparing the slopes of the reaction product curves in the linear area (from 20-80 minutes) a crude estimate for the relative velocities of various CBP21 variants was made (Table 4.1 and Fig. 4.21). Note that mutants in or nearby the surface "pocket" show the lowest activity of all mutants (see section 4.2, Fig. 4.2 for a graphic illustration of the mutations). Usually it is not possible to choose data to include when calculating the enzyme velocity. If the data are not linear, it is important to find conditions that make them linear. Because of time limitations, only a crude estimate of the velocity between 20 and 80 minutes was calculated.

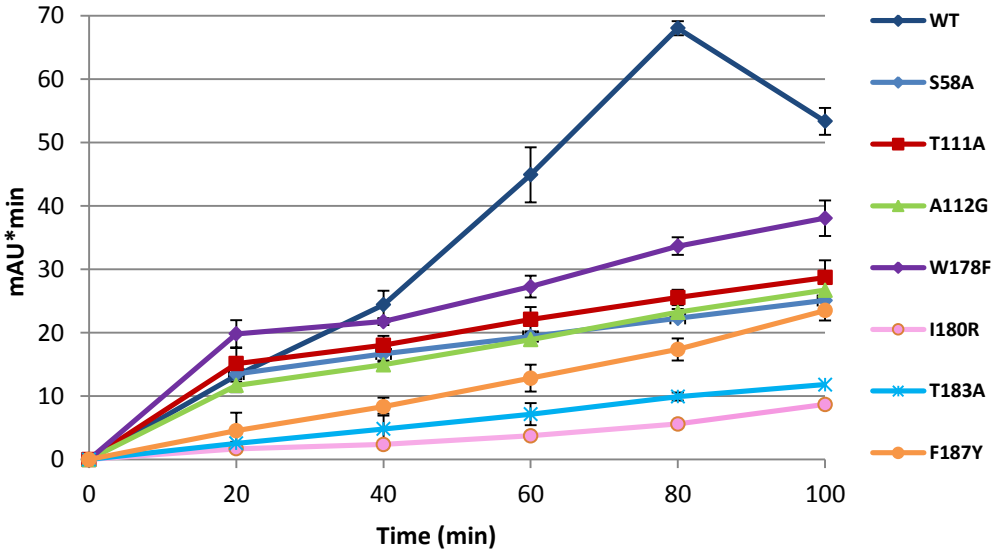

Figure 4.20. Generation of $DP4_{ox}$ -$DP8_{ox}$ upon degradation of β-chitin^{B} by CBP21 variants. Data show the formation of $DP4_{ox}$ -$DP8_{ox}$ in the same experiment as that described in the legend to Fig. 4.14. Each data point

represents the mean value of three replicates (i.e. three samples were identical treated and measured in the same assay) and error bars indicate standard deviation (not visible for every point). Note the striking drop in total amount of oxidized products by CBP21WT after 80 minutes of incubation.

Table 4.1. Relative activity of $CBP21_{WT}$ and CBP21 mutants. The rate of chitin degradation was calculated based on the total amount of oxidized products ($DP4_{ox}$ – $DP8_{ox}$) generated between 20 and 80 minutes. The lines and their respective equations used to calculate chitin turnover are shown in appendix D, figure D2 and D3. Chitin turnover by $CBP21_{I180R}$ has been adjusted for the fivefold higher enzyme concentration used in the assay.

CBP21	**mAU*min/sec**
WT	$1.3027*10^{-2}$
W178F	$7.7775*10^{-3}$
T111A	$6.1025*10^{-3}$
S58A	$5.3913*10^{-3}$
A112G	$5.3105*10^{-3}$
F187Y	$3.5888*10^{-3}$
T183A	$2.0417*10^{-3}$
I180R	$2.2293*10^{-4}$

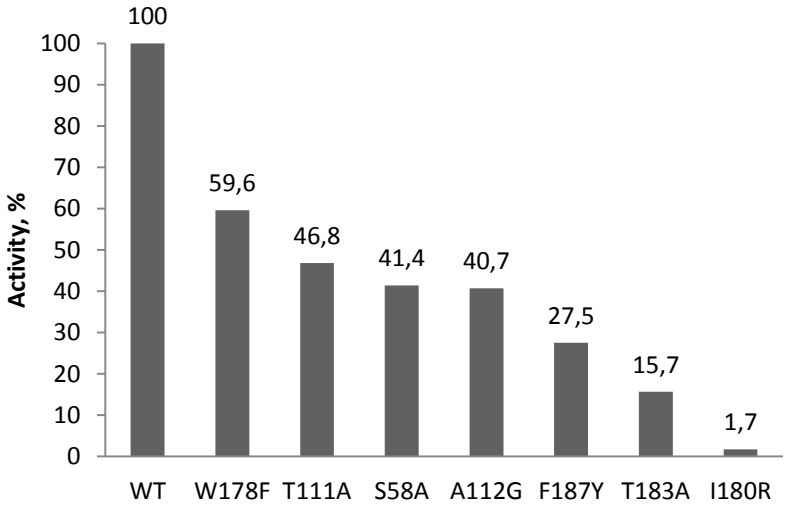

Figure 4.21. Relative activity of $CBP21_{WT}$ and mutants. Relative activity of all CBP21 variants is calculated based on data from Table 4. Note that mutants in or nearby the surface "pocket" show the lowest activity of all mutants (see section 4.2, Fig. 4.2 for a graphic illustration of the mutations). $CBP21_{WT}$ represents the 100 % value and the activity of $CBP21_{I180R}$ has been corrected for fivefold enzyme concentration.

4.4.3 Generation of H_2O_2 by autooxidation of various reductants

Generation of H2O2 by autooxidation of various reductants was measured according to section 3.11. To ensure the validity of the assay, the stability of resorufin fluorescence was tested by measuring the absorbance (A_{540}) over a time course of 240 minutes by. In order to convert the fluorimetric readout into H_2O_2 concentration, a standard curve with various concentration of H_2O_2 was made (appendix E, Fig. E1).

Formation of H_2O_2 by autooxidation of eight individual reductants (ascorbic acid, reduced glutathione, tartaric acid, 3-hydroxyanthranilic acid, catechin, hydroquinone, dithiothreitol and gallic acid) was investigated using Amplex Red®/HRP according to section 3.11. It should be noted that the reproducibility of these experiments was poor for most of the reductants (see Discussion section). The data presented in figure 4.22 and 4.23 illustrate a trend over seven experiments. Gallic acid and dithiothreitol generated most H_2O_2 over time, with end concentrations of 40 µM and 5 µM H_2O_2, respectively), whereas substantially lower amounts (0.2 – 2 µM) were generated by the other reductants. It should be noted that generation of H_2O_2 by autoxidation was only linear over the time span of the assay in the case of 3-hydroxyanthranilic acid, catechin and hydroquinone. For the other reductants, the progress curves were non-linear and rather sigmoidal in shape.

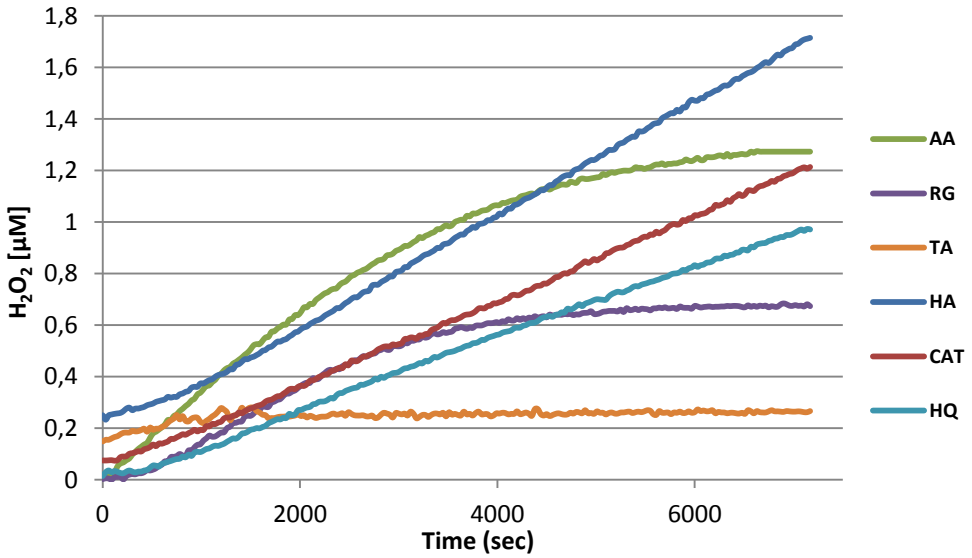

Figure 4.22. Generation of H_2O_2 by autooxidation of reductants. Lines represent the cumulative amount of H_2O_2 generated as a function of time by the autooxidation of ascorbic acid (AA), reduced glutathione (RG), tartaric acid (TA), 3-hydroxyanthranilic acid (HA), catechin (CAT) and hydroquinone (HQ). The total reaction volume was 100 µl, containing 50 µl of 2 mM reductant in 1 x reaction buffer and 50 µl Amplex Red®/HRP

solution. Values obtained in the absence of reductants were subtracted from the raw data prior to making the figure. All data points are the mean value of three replicates (i.e. three different samples were treated identical and measured at the same time), but error bars are too small to be visible.

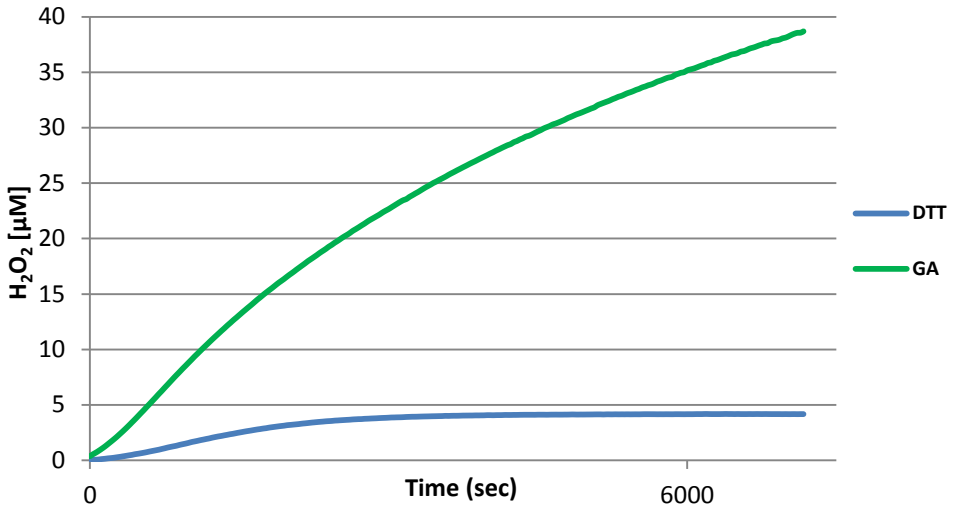

Figure 4.23. Generation of H_2O_2 by autooxidation of reductants. Lines represent the cumulative amount of H_2O_2 generated as a function of time by the autooxidation of dithiothreitol (DTT) and gallic acid (GA) under the same conditions as described legend in figure 4.22. Values obtained in the absence of reductants were subtracted from the raw data prior to making the figure. All data points are the mean value of three replicates (i.e. three different samples were treated identical and measured at the same time), but error bars are too small to be visible.

4.4.4 Generation of H_2O_2 by CBP21 variants

Formation of H_2O_2 by LPMOs (90% saturated with copper) was investigated according to section 3.11. In combination with ascorbic acid, generation of H_2O_2 by $CBP21_{WT}$ was linear over time and there also appeared to be a dose-response relationship between enzyme concentration and H_2O_2 production rate (Fig. 4.24). Based on the slope, the rate of H_2O_2 formation in each reaction was calculated (table 4.2). It must be noted that this calculation does not account for H_2O_2 putatively formed by autooxidation of free ascorbic acid. Several experiments were conducted in order to establish that the formation of H_2O_2 is the result of a reaction involving the copper ion present in CBP21. The results showed that generation of H_2O_2 by CBP21 indeed is dependent on the presence of the copper ion (Fig. 4.25 and Fig. 4.26). The figures show increased generation of H_2O_2 beyond the background of ascorbic acid, only for copper-charged CBP21.

To investigate whether H_2O_2 formation is affected by the presence of the substrate, β-chitin[B] (table 2.3) was added to the reaction mixture. The fluorimetric readout from the assay indicated that substrate particles in the reaction mixture interfere with the fluorimetric measurements, and therefore, this approach was not continued (results not shown).

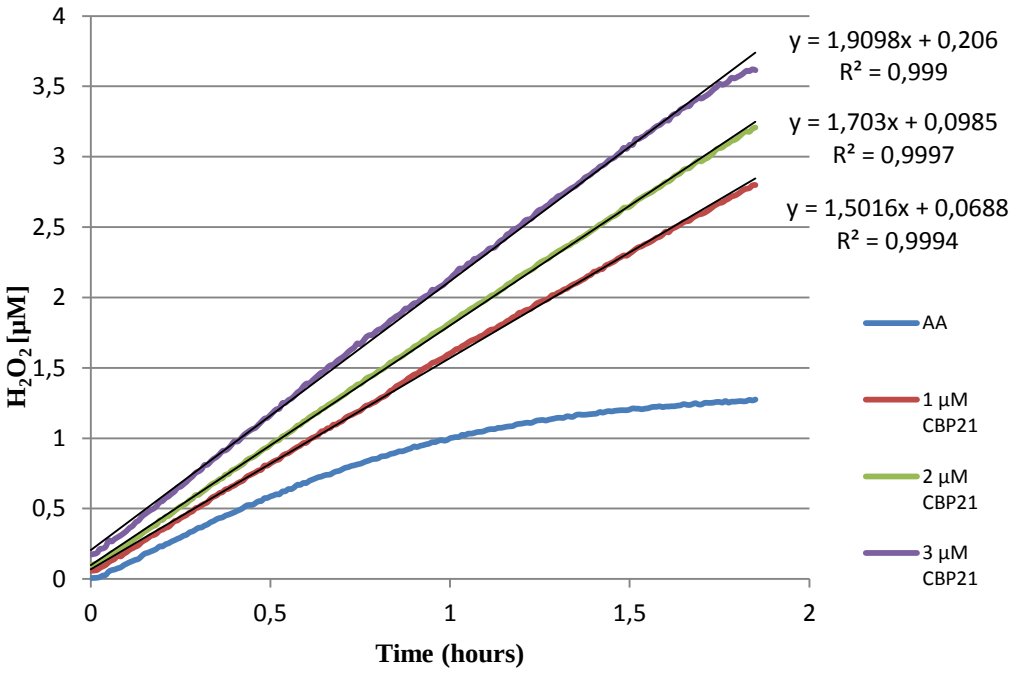

Figure 4.24. Generation of H_2O_2 by $CBP21_{WT}$. Lines represent the amount of H_2O_2 generated as a function of time by various concentrations of $CBP21_{WT}$. Negative control containing 1 x reaction buffer is subtracted from all values. Total reaction volume was 100 µl, containing 50 µl $CBP21_{WT}$ (2, 4 or 6 µM) and 2 mM reductant in 1 x reaction buffer and 50 µl Amplex Red®/HRP solution. The background activity caused by autoxidation of ascorbic acid (reaction without enzyme) generates a lower amount of H_2O_2 than the reactions with CBP21, indicating that CBP21 contributes to formation of H_2O_2. All data points are the mean value of three replicates (i.e. three different samples were treated identical and measured at the same time), but error bars are too small to be visible.

Table 4.2. Dose-response dependent generation of H_2O_2 by $CBP21_{WT}$. The rate of H_2O_2 formation is defined as µM H_2O_2 generated per second.

CBP21 concentration [µM]	H_2O_2 µM/sec
3	$1.03865*10^{-3}$
2	$9.02510*10^{-4}$
1	$8.09077*10^{-4}$

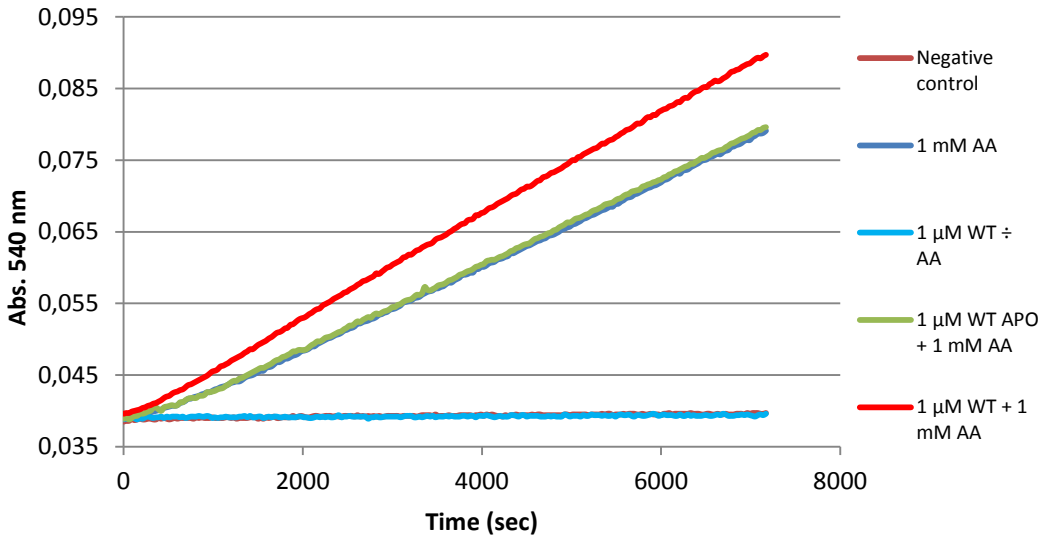

Figure 4.25. Generation of H_2O_2 by various control reactions. Lines represent the amount of H_2O_2 generated from five different control reactions; 1 x reaction buffer (negative control), 1 mM ascorbic acid (background control), 1 µM $CBP21_{WT}$ (90% copper saturated) and 1 mM ascorbic acid, 1 µM $CBP21_{WT}$ apo and 1 mM ascorbic acid, and 1 µM $CBP21_{WT}$. Note that the concentration of H_2O_2 is not determined, only the absorption (A_{540}) is shown. The light blue and the brown lines are overlapping and so are the green and the dark blue lines. All data points are the mean value of three replicates (i.e. three different samples were treated identical and measured at the same time), but error bars are too small to be visible.

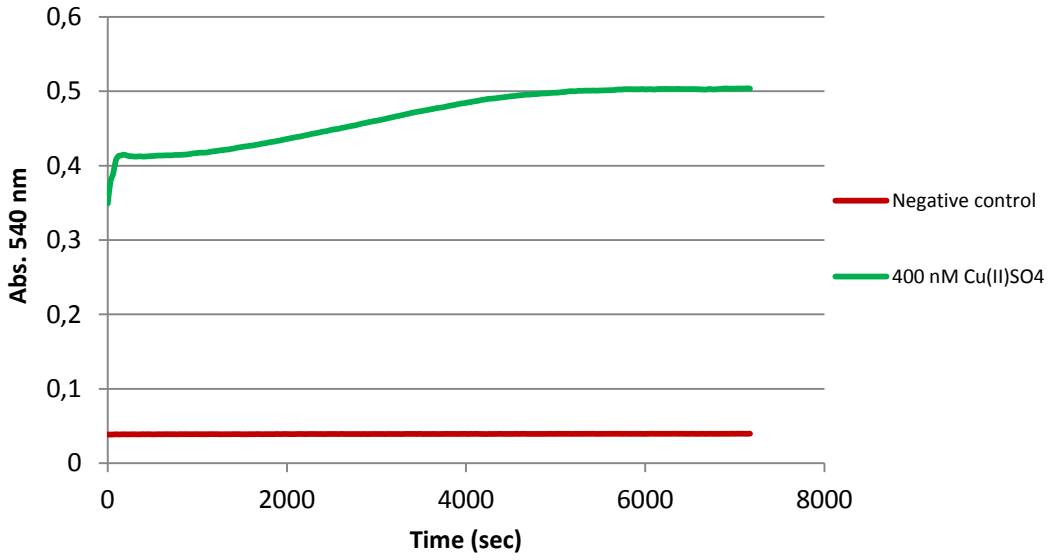

Figure 4.26. Generation of H_2O_2 by autooxidation of copper. The green line represents the amount of H_2O_2 generated by 400 nM $Cu(II)SO_4$. Note that the concentration of H_2O_2 is not determined, only the absorption (A_{540}) is shown. All data points are the mean value of three replicates (i.e. three different samples were treated identical and measured at the same time), but error bars are too small to be visible.

To determine whether mutations in or near the active site of CBP21 would affect generation of H_2O_2, all mutants were analyzed with this H_2O_2 assay and compared to the WT (Fig. 4.27). The data show that enzyme mediated H_2O_2 generation is higher than WT for $CBP21_{W178F}$, $CBP21_{T183A}$ and $CBP21_{F187Y}$, and lower than WT for $CBP21_{T111A}$. The other mutants behaved similar to $CBP21_{WT.}$ Note that $CBP21_{I180R}$, which has very low activity according to other assays (see above), produces as much H_2O_2 as the wild-type enzyme.

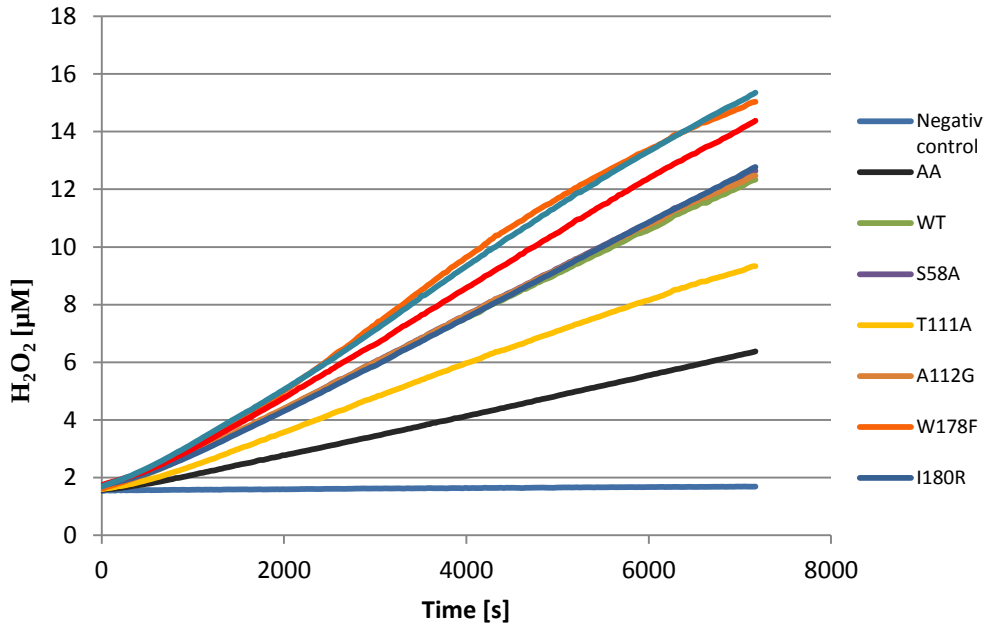

Figure 4.27. Generation of H_2O_2 by WT and mutant CBP21. Lines represent the amount of H_2O_2 generated as a function of time by WT and mutant CBP21. All CBP21 variants are 90% copper saturated**.** All data points are the mean value of three replicates measured at the same time, but error bars are not visible. The brown, dark blue, purple and the green line are overlapping. All data points are the mean value of three replicates (i.e. three different samples were treated identical and measured at the same time), but error bars are too small to be visible.

4.5 Binding assays

4.5.1 Binding studies of CBP21 variants

Binding of CBP21 to β-chitin^{A} was assessed in order to investigate if the mutated residues play a role in substrate binding. CBP21$_{WT}$ (45% bound after 2 hours) showed a considerably higher affinity towards β-chitin^{A} than all mutants (Fig.4.28). CBP21$_{S58A}$, CBP21$_{A112G}$, CBP21$_{I180R}$, CBP21$_{T183A}$ and CBP21$_{F187Y}$ showed approximately similar binding properties with approximately 30 % of the protein being bound to the substrate after two hours of incubation (table 4.3). CBP21$_{T111A}$ showed a higher affinity with almost 38 % of the protein bound to the substrate, while CBP21$_{W178A}$ showed the lowest affinity with only 26 % bound protein. The data showed that most of the binding occurs during the first 50 minutes of incubation, while equilibrium was reached after approximate 100 minutes. Figure 4.29 shows a close-up on the initial phase of the experiment revealing minor differences in the rate of binding.

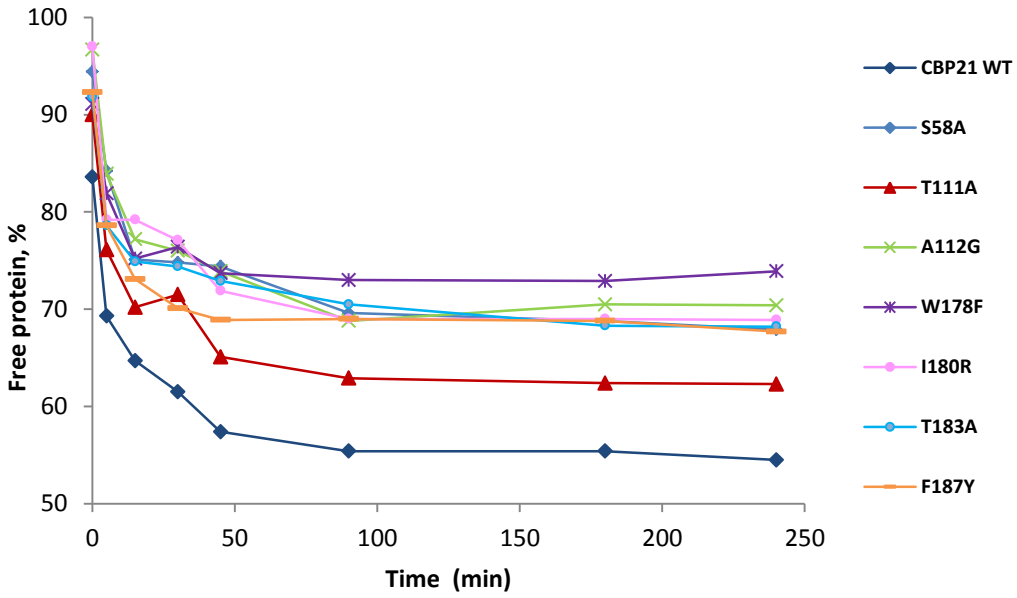

Figure 4.28. Binding of WT and mutant CBP21 to β-chitin^{A}. The data show binding of WT and mutant CBP21 to β-chitin^{A} over a time course of 240 minutes. The total reaction volume was 300 µl, containing 10 mg/ml β-chitin^{A} and 100 µg/ml protein in 50 mM sodium phosphate buffer (pH 7.0). The reaction mixtures were incubated at room temperature and rotated vertically for 240 minutes. Absorption (A_{280}) of 100 µg/ml protein in 50 mM sodium phosphate buffer (pH 7.0) was used to determine the 100 % value for each enzyme. Each data point represents the mean value of three replicates (i.e. three samples that were treated identical and measured at the same time).

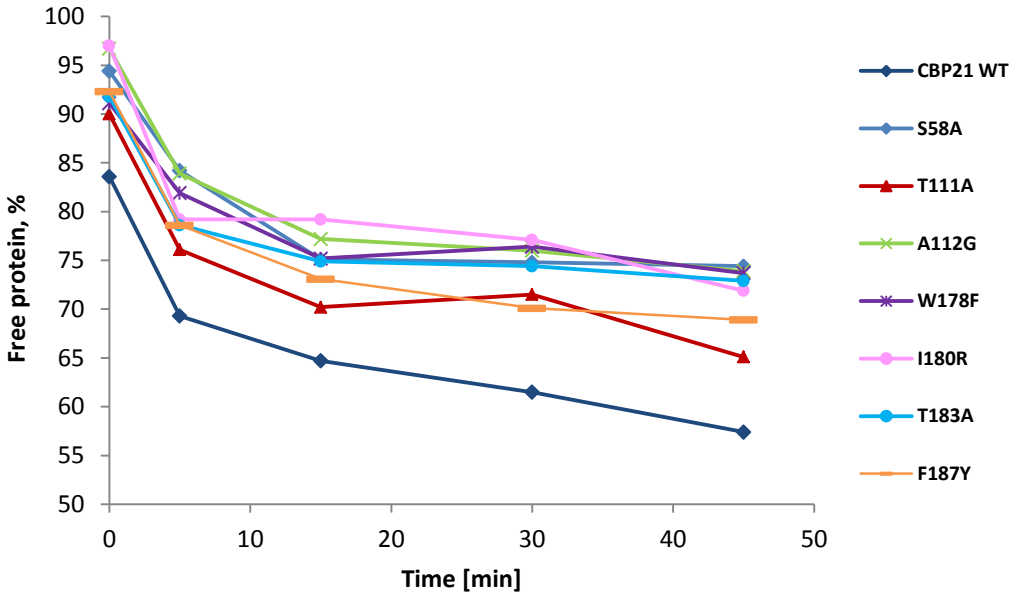

Figure 4.29. Binding of WT and mutant CBP21 to β-chitin[A]. Same data as shown in figure 4.28, but only showing data from 0 to 45 minutes.

Table 4.3. Binding of CBP21 variants to β-chitin[A]. The table shows the fraction of protein bound to the substrate after 2 hours incubation. The experimental data for this Table are shown in Figure 4.28.

CBP21	Bound protein, %
WT	45.4
T111A	37.7
F187Y	32.3
S58A	32.1
T183A	31.8
I180R	31.1
A112G	29.6
W178F	26.1

4.5.2 Binding of $CBP21_{WT}$ to β-chitin measured by isothermal titration calorimetry

Isothermal titration calorimetry (ITC) is a powerful tool to determine thermodynamic parameters of a binding event between two biomolecules, usually the binding of small molecules (e.g. a ligand) to larger macromolecules (e.g. protein). ITC was conducted according to section 3.12 by titration of 50 µM $CBP21_{WT}$ (the protein buffer was 50 mM Tris and 1.8 mM acetic acid) to β-chitin^{C}. Thermograms recorded during titration and fitted theoretical data for binding of $CBP21_{WT}$ to β-chitin^{C} are shown in figure 4.30. The ‘‘best-fit’’ parameters from the experiment are summarize in the box to the right. The calculated dissociation constant (K_d) is 0.28 µM, indicating a low binding affinity for $CBP21_{WT}$ towards the substrate.

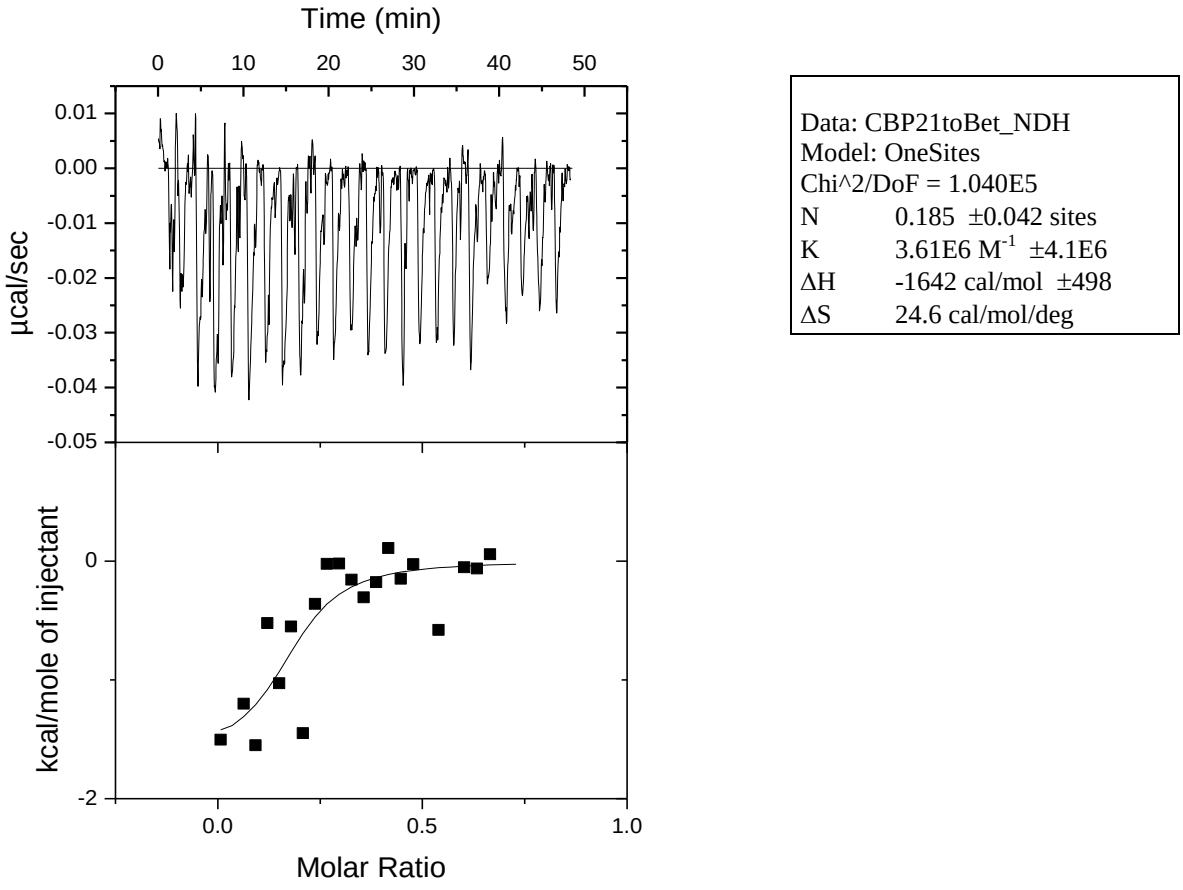

Figure 4.30. Experimental and theoretical data retrieved from the ITC experiment. The figure show the thermogram (top) and fitted data (bottom; with experimental data depicted as black squares) for binding of $CBP21_{WT}$ to β-chitin^{C}.

4.5.3 Glycan array screen of various CBM33s

Binding of CBP21, *Ll*CBM33A, *Ef* CBM33A, *Lp*CBM33(1697) and GbpA to an array of 610 soluble mammalian glycans was assayed by hybridizing Alexa Fluor® labelled variants of the protein (see section 3.8) with the glycan array. The experiment was conducted by David F. Smith and Jamie Heimburg-Molinaro at Department of Biochemistry, Emory University School of Medicine, Atalanta (GA) in USA. CBP21, *Ef*CBM33A and *Lp*CBM33(1697) showed no binding to the array while *Ll*CBM33A showed low binding, but the %CVs were very high and no obvious binding preference could be found (appendix F, Fig. F1-F4). GbpA showed higher binding and a binding preference could be observed with low %CV (Fig. 4.31). Glycans observed bound GbpA with highest intensity are listed in table 4.6 (see appendix F, table F1 for the complete structure list).

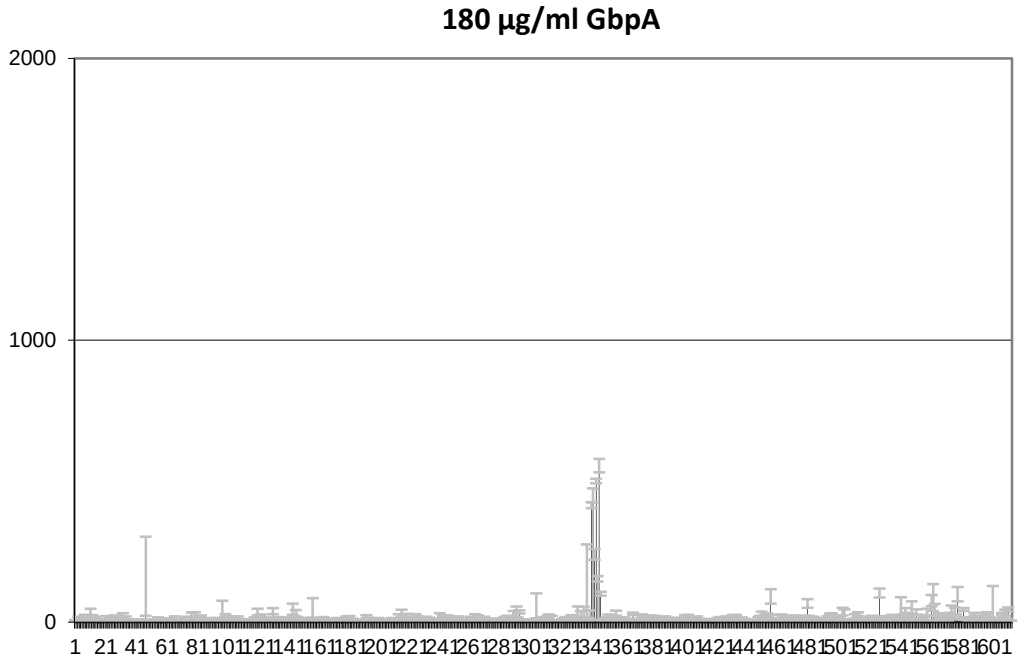

Figure 4.31. Binding of GbpA to mammalian glycans. Binding of for GbpA to a glycan array with 610 glycans. Glycans showing significant binding are listed in was found for the glycans identified in table 4.4

Table 4.4. Data for the top 10 glycans that bound with highest intensity to GbpA are listed below. Binding affinity is quantified as mean relative fluorescence units (RFU). The data presented are the average from four replicates for each glycan.

Chart Number	Structure	Average RFU	StDev	CV %
343	GlcNAca1-4Galb1-4GlcNAcb1-3Galb1-4GlcNAcb-Sp0	555	47	8
341	GlcNAca1-4Galb1-4GlcNAcb1-3Galb1-4Glcb-Sp0	501	16	3
339	GlcNAca1-4Galb1-4GlcNAcb-Sp0	449	50	11
338	GlcNAca1-4Galb1-4GlcNAcb1-3Galb1-4GlcNAcb1-3Galb1-4GlcNAcb-Sp0	414	21	5
340	GlcNAca1-4Galb1-3GlcNAcb-Sp0	240	39	16
47	(6S)GlcNAcb-Sp8	162	280	173
342	GlcNAca1-4Galb1-4GlcNAcb1-3Galb1-4(Fuca1-3)GlcNAcb1-3Galb1-4(Fuca1-3)GlcNAcb-Sp0	154	19	13
335	GalNAca1-3(Fuca1-2)Galb1-4GlcNAcb1-3Galb1-4GlcNAcb-Sp0	138	275	199
526	Neu5Aca2-3Galb1-3GlcNAcb1-2Mana-Sp0	103	31	30
344	GlcNAca1-4Galb1-3GalNAc-Sp14	101	14	13

DISCUSSION

The work described in this thesis essentially consisted of three parts: (1) a structure-function study of the chitin active LPMO CBP21 using site-directed mutagenesis; (2) development and use of assays to measure mutational effects on CBP21 activity and substrate binding, including a careful evaluation of a potentially useful novel activity assay based on generation of H_2O_2; (3) activity analysis of a serie of other CBM33-type LPMOs and analysis of possible alternative substrates for the LPMOs as well as CBP21 using glycan arrays. Some of the additional CBM33-type LPMOs were produced in this study and some were obtained in purified form from colleagues.

Evolution exerts pressure to preserve amino acids that have thermodynamic, kinetic, and functional roles. Function is conferred to a protein by a subset of residues, which in the folded state form the active site or binding sites of the protein. In order to gain more insight into binding properties and the catalytic mechanism of CBP21, seven rational designed mutants were constructed by site-directed mutagenesis. All residues that were mutated are conserved (see Table 4.1), positioned close to the active site in the folded state (see Fig. 4.2 for a graphic illustration). To be able to compare CBP21 variants, it is important that the enzymes are equally saturated with copper. Since the copper saturation of the CBP21 variants may differ after purification by chitin affinity-chromatography, all CBP21 variants were treated with EDTA to remove the copper from the enzyme. Then $Cu(II)SO_4$ was added to the apo-CBP21 to gain the desired copper saturation (90% saturated). Since Tris and normal dH_2O contain traces of copper, the protein buffer was prepared with a low concentration of Tris and the use of ion free water (TraceSELECT® Ultra water). This was done to ensure that the buffer was approximate free of copper, thus ensuring control over the copper-charge of CBP21.

Structure-function studies of CBP21

Results obtained from the binding assay show that all mutants have substantial lower affinity towards the substrate compared to the WT, indicating that the mutated residues are important for optimal substrate binding. A similar binding experiment was conducted by Vaaje-Kolstad et al (2005a), which showed that WT had a considerably higher affinity (~75% bound protein after 2 hours) than observed in this study (~35% bound protein after 2 hours). The same particle size of β-chitin was used in both experiments (80-mesh sized particles), but the same batch was probably not used. The main reason for this difference could be that the substrate used in the present study was treated differently. This emphasizes the importance of using the same batch of substrate (or other reagents) when conducting several experiments for comparison. In their 2005 study Vaaje-Kolstad et al., calculated the K_d for binding of wild-type CBP21 to β-chitin to be 1.4 μM, which reflects a somewhat lower affinity towards the substrate than data obtained from the ITC experiment in this study (the K_d was calculated to be 0.28 μM). The substrate used in the ITC experiment (see table 2.3) was in solution with dilute acetic acid. This was done to make the substrate more accessible for the enzyme. But whether this is the reason for the fivefold increase in affinity is not likely. Furthermore, since acetic acid comprises an acetyl group, the acetic acid may cause an opposite effect by occupying the putative binding-pocket on the protein surface and thereby lowering the substrate affinity (the interaction between the acetyl group and the putative binding pocket is further discussed below). Thus, if acetic acid was not used in the protein buffer and in the substrate solution, an even lower K_d may be observed. The result from the ITC experiment has "noisy" thermogram and the fitted data show low few binding events. A possible explanation for this could be that the substrate concentration was too low and that the substrate was saturated after few protein injections. More reliable data can be obtained by increasing the substrate concentration, and by doing that, increase the number of binding sites for the enzyme. It should also be mentioned that the ITC experiment had poor reproducibility, meaning that it is clearly that this assay has to be further optimized for comparing affinity between the CBP21 variants.

Quantitative analysis of product formation using UHPLC showed that the mutants generated lower amounts of oxidized products than the WT, showing that the enzyme activity is also affected by the mutations (albeit to varying extents). Lower affinity to the substrate is definitively a factor that can contribute to reduced enzyme activity for the mutants. However, when comparing the UHPLC results and the binding results between the mutants, it is obvious that several mutants with approximate same affinity have different abilities to degrade the substrate (for example compare $CBP21_{I180R}$ and $CBP21_{A112G}$ in Figures 4.20 and 4.28). This indicates that other factors than affinity affecting the activity, which is not surprising since several of the mutations are very close to the catalytic center (see Fig. 4.2).

Previously studies suggest that binding of CBP21 to chitin seems to be mediated primarily by conserved, solvent-exposed, polar side chains (Vaaje-Kolstad et al. 2005a)**.** Residues S58, T111 were primary mutated because they are thought to be part of the polar interaction with the substrate. A NMR study by Aachmann et al. (2011) indicated that residue S58 (polar), T111 (polar) and A112 (non-polar) are involved in substrate binding, which was confirmed by site-directed mutagenesis in this study. Substitution of a polar residue to a non-polar residue located at the surface close to the active site is likely to cause a negative effect on the binding event as seen for $CBP21_{S58A}$, $CBP21_{T111A}$. Interestingly, $CBP21_{T111A}$ show a considerably higher affinity to the substrate than $CBP21_{A112G}$, which is also reflected by their activity. Residue T111 and A112 are positioned close to one of the histidine that coordinates the copper ion, in sequence and in folded state. A112 is positioned closer to the active site than T111, and introduction of glycine (G) would probably introduce more conformational freedom nearby the active site, which may influence the affinity and result in lower activity for $CBP21_{A112G}$. It should be noted that many of these residues are so close to the catalytic site that effect on the activity can be caused by direct effects on the catalytic site

The copper present in CBP21 is reduced by an electron transfer who in turn activates a bound dioxygen by a reaction that is not fully understood (Vaaje-Kolstad et al. 2010). It is also unknown how the electron is transferred from the reducing agent to the copper. One suggestion is that the electron is transferred through the enzyme from the opposite side of the active site (Vaaje-Kolstad, personal communication). Two aromatic residues in the interior of the protein, W178 and F187, were mutated in order to investigate whether these residues are involved in a putative long range electron transfer through the enzyme. Because a mutation to a residue with a considerably smaller side chain, such as alanine, would probably introduce

more freedom and cause higher structural changes, the W178 and F187 were mutated to residues with a side chain of approximate same size.

Tryptophan (W) has been shown to be involved in long range electron transfer through proteins (Shih et al. 2008) and since the core of CBP21 consists of several conserved tryptophan residues (see section 1.4.1) Interestingly, $CBP21_{W178F}$ show the highest activity of the mutants, whit an activity, in terms of production of oxidized products, which amounted to almost 60% of the wild-type activity. If the electron transfer is interfered or even blocked, the mutant would probably show a dramatic decrease in activity, which is not the case. Moreover, the mutant shows the lowest affinity to the substrate. Since the mutated residue is located in the interior of the protein, the low affinity might be a result of structural changes. On the other hand the structural changes seem not to affect the catalytic ability of the mutant.

F178 was mutated to phenylalanine (F) with the intention to hinder the electron transfer through the enzyme. The mutants show almost the same affinity to the substrate as $CBP21_{S58A}$ and $CBP21_{A112G}$, but show a lower activity. Since the residue is situated in the interior, the residue is not likely involved in substrate binding interactions with the substrate. A more reasonably explanation for its low affinity and activity is structural changes and distortion of the active site. This can be supported by the increased H_2O_2 formation by the mutant (see Fig. 4.27)

An interesting theory is that a surface-pocket close to the active site may serve as a binding-pocket for one of the acetyl groups attached to C2 in chitin (see Fig. 4.2 for illustration of the pocket). In order to bind in the pocket, there need to be space and the acetyl group must probably interact with residues in or close to the pocket. Residue I180 is positioned beneath the surface-pocket and was mutated to investigate the importance of the putative binding-pocket. Since arginine (R) has a larger side chain than isoleucine (I), the side chain of arginine may occupy part of the pocket and hinder the acetyl group to interact with residues located inside and close to the putative binding-pocket . $CBP21_{I180R}$ showed approximate the same affinity to the substrate as $CBP21_{S58A}$, $CBP21_{A112G}$, $CBP21_{F187Y}$ and $CBP21_{T183A}$, but showed much lower activity compared to all CBP21 variants. If the pocket is crucial for binding, a lower affinity towards the substrate would be expected. Thus, the reason for low activity can not only be a consequence of low affinity to the substrate.

Since the side chain of arginine is pointing towards the active site, the copper ion in the active site of the protein may be distorted which could hamper hydrolysis. Arginine is one of the two amino acids that carry a positive charge. The mutation introduces a charge, which can cause repulsion between the mutated residue and adjacent residues and disturb the local structure around the active site, which in turn can affect the electron transport.

The importance of the pocket is supported by the low affinity and activity of $CBP21_{T183A}$. Residue T183 is located at the side wall of the pocket and may interact with the acetyl group. $CBP21_{T183A}$ show the same affinity to the substrate as several mutants, but show the second lowest activity of all CBP21 variants. The hydroxyl group of threonine (T) can form hydrogen bond to the acetyl group, which can have a stabilizing effect on the acetyl group when it binds to the pocket. An amino acid substitution to alanine (A) will probably result in weaker interactions between the acetyl group and the putative binding-pocket. An explanation for the low activity by $CBP21_{I180R}$ and $CBP21_{T183A}$ might be that the enzyme is not properly positioned onto the substrate due to low interactions between the acetyl group and the putative binding-pocket.

Developing a new assay based on generation of H_2O_2

To evaluate a recently published novel LPMO assay based on generation of H_2O_2 from a futile side reaction, several experiments were conducted using Amplex® Red as substrate. One of the experiments was measuring generation of H_2O_2 by autooxidation of eight reductants was investigated. Some reductants showed decrease in H_2O_2 in the late phase of the assay, indicating a limiting factor (Fig. 4.22 and Fig.23). Oxygen, reductant and Amplex Red® are "consumed" during the time course of the experiment and can all be limiting factors (see Fig. 3.1 for propose reaction scheme).

Autooxidation by most reductants leads to superoxide anion which disappears via dismutation reaction: $O^{2-} + O^{2-} + 2H^{+} \rightarrow H_2O_2 + O_2$. The reaction shows that one molecular oxygen is "consumed" during the formation of one H_2O_2 molecule. Freshwater contains approximate 250 µM dissolved oxygen. In theory, 250 µM H_2O_2 could be generated before the oxygen is exhausted in the reaction mixture. Data from this experiment show that gallic acid is the reductant that generates the most H_2O_2, but far from 250 µM, indicating that oxygen is not likely the limiting factor. The reaction stoichiometry of Amplex Red® and H_2O_2 is 1:1, meaning that 50 µM H_2O_2 can be generated before the reagent is exhausted. Neither the

oxygen, Amplex Red nor the reductant is likely to be a limiting factor in the assay. Another, maybe more reasonably explanation for the decrease in H_2O_2 formation by some reductants might be that Amplex Red® is unstable over time in the presence of specific organic compounds. According to the Kit supplier, Amplex® Red is unstable in the presence of thiols, which is a constituent of dithiothreitol (DTT), which show a decrease in H_2O_2 formation in the late phase of the assay.

Data obtained from adding various concentration of CBP21 to the reaction mixture, using ascorbic acid as a reducing agent, show that generation of H_2O_2 by CBP21 is directly proportional to the enzyme concentration (Fig. 4.24 and Table 4.2). Kittl et. al (2010) conducted a similar experiment with four copper containing LPMOs from *Neurospora crassa*, which also showed that generation of H_2O_2 by these LPMOs was directly proportional to the enzyme concentration . The total amount of H_2O_2 generated by CBP21 is increased beyond the background generated by ascorbic acid, indicating that CBP21 contributes to the formation of H_2O_2. Several control reactions were included in the assay to investigate whether the copper present in CBP21 was the result of the increased H_2O_2 formation (Fig. 4.25 and Fig 4.26) The control reaction containing $CBP21_{APO}$ and ascorbic acid generated the same amount of H_2O_2 as the control reaction containing only ascorbic acid, indicating that autooxidation of copper present in CBP21 indeed is responsible for the increased H_2O_2 formation. Since the concentration of ascorbic acid is equal in all reactions, the assay is primary measuring the presence of copper in the solution.

To determine whether mutations in or near the active site of CBP21 would affect generation of H_2O_2, all mutants were investigated and compared to the $CBP21_{WT}$. The CBP21 variants show a different ability to generate H_2O_2, suggesting that the copper present in CBP21 is more prone to autooxidation in some mutants than others.

As noted above, the H_2O_2 generation is reflecting copper in the reaction mixture. Even small amounts (400 nM) of free copper in the reaction mixture generate substantially higher amounts of H_2O_2 than all CBP21 variants (Fig. 4.26). Since all CBP21 variants are 90% copper saturated, the reaction mixtures containing CBP21 contains a substantially higher concentration of copper than the control reaction, and should by definition generate more H_2O_2. The copper present in CBP21 seems to be protected from rapid autooxidation by the enzyme. Distortion of the copper ion, due to mutation, may cause the copper ion present in CBP21 to be more exposed to autooxidation, leading to an increased generation of H_2O_2. As

previously mentioned, the low activity of $CBP21_{I180R}$ could be the result of distortion of the copper ion, but the mutant generates the same amount of H_2O_2 as $CBP21_{WT}$, indicates that the active site architecture is not affected by the mutation. Interestingly, both CBP21 variants with a mutation in the interior of the structure generate most H_2O_2. As noted previously, mutation in the interior of the protein is more likely to cause structural changes. If the copper is protected by the enzyme (i.e. the copper is not that exposed for autooxidation) a structural change may distort the copper and make it more exposed for autooxidation, hence the increased H_2O_2 concentration.

Testing additional CBM33-type LPMOs and detecting possible substrates with glycan array screen

Recent studies have demonstrated LPMO activity for several enzymes secreted by bacteria interacting with humans and there are indications that these enzymes may be related to microbe host interaction and/or virulence. Therefore, several novel CBM33-type LPMOs were tested next to CBP21: *Ef*CBM33A, *Lp*CBM33(1697), and *Ll*CBM33A and the N-terminal domain of GbpA. MALDI-TOF-MS analysis confirmed LPMO activity for all CBM33s, including all CBP21 variants (Fig 4.13. and appendix C, Fig. C3). All enzymes generated oxidized products with a dominance of even numbered products which are fully acetylated. These observations indicate cleavage of every second glycosidic bond and that cleavage happens on an ordered chain, which would be the case when the enzymes act on a chain in a crystalline context.

Moreover, MALDI-TOF spectra displayed masses similar to that of CBP21, suggesting that all enzymes oxidized the C1 (generation of δ1,5-lactone and aldonic acid). This was not unexpected since C1 oxidation is the most common mechanism among CBM33s. Cleavage of every second glycosidic bond by CBP21 variants was supported by the product profile obtained from HPLC analysis (Fig. 4.19).

The glycan array screen showed no binding of CBP21, *Ef*CBM33A, *Lp*CBM33(1697), *Ll*CBM33A. The fact that no binding was observed to soluble mammalian glycans may indicate that the enzymes have a preference towards more ordered substrates, i.e. substrates in a crystalline context such as chitin. It is of course possible that the major role of these enzymes indeed is to act on chitin (only). GbpA has previously been shown to contain an N-terminal CBM33 domain which mediates attachment of the bacteria to human intestine by

binding to GlcNAc-containing glycoconjugates (Benktander et al. 2013; Wong et al. 2012). Interstingly, GbpA-N bind to GlcNAca1-4Galb1-R (Table 4.4; chart number 343), which structure is a part of some glycoproteins on the surface of mucin that is secreted by the human gut. This finding may support the fact that the N-terminal CBM33 domain of GbpA contributes to binding of *V. cholerae* to the human intestine and facilitate colonization of the bacterium. GbpA-N was also shown to have LPMO activity in this study, but the role of this feature in the pathogenesis of *V. cholerae* is unknown.

REFERENCES

Aachmann, F. L., Eijsink, V. G. & Vaaje-Kolstad, G. (2011). 1H, 13C, 15N resonance assignment of the chitin-binding protein CBP21 from Serratia marcescens. *Biomol NMR Assign*, 5 (1): 117-9.

Beckham, G. T. & Crowley, M. F. (2011). Examination of the alpha-chitin structure and decrystallization thermodynamics at the nanoscale. *J Phys Chem B*, 115 (15): 4516-22.

Beeson, W. T., Phillips, C. M., Cate, J. H. & Marletta, M. A. (2012). Oxidative cleavage of cellulose by fungal copper-dependent polysaccharide monooxygenases. *J Am Chem Soc*, 134 (2): 890-2.

Benktander, J., Angstrom, J., Karlsson, H., Teymournejad, O., Linden, S., Lebens, M. & Teneberg, S. (2013). The repertoire of glycosphingolipids recognized by Vibrio cholerae. *PLoS One*, 8 (1): e53999.

Bhowmick, R., Ghosal, A., Das, B., Koley, H., Saha, D. R., Ganguly, S., Nandy, R. K., Bhadra, R. K. & Chatterjee, N. S. (2008). Intestinal adherence of Vibrio cholerae involves a coordinated interaction between colonization factor GbpA and mucin. *Infect Immun*, 76 (11): 4968-77.

Bourne, Y. H., B. (2001). Glycoside hydrolases and glycosyltransferases: families and functional modules. *Current Opinion in Structural Biology*, 11 (5): 593-600.

Bradford, M. M. (1976). A rapid and sensitive method for the quantitation of microgram quantities of protein utilizing the principle of protein-dye binding. *Anal Biochem*, 72: 248-54.

Brurberg, M. B., Synstad, B., Klemsdal, S. S., van Aalten, D. M. F., Sundheim, L. & Eijsink, V. G. H. (2001). Chitinases from Serratia marcescens. *Recent Research Developments in Microbiology*, 5: 187-204.

Cantarel, B. L., Coutinho, P. M., Rancurel, C., Bernard, T., Lombard, V. & Henrissat, B. (2009). The Carbohydrate-Active EnZymes database (CAZy): an expert resource for Glycogenomics. *Nucleic Acids Res*, 37 (Database issue): D233-8.

CAZy. (2013). *Carbohydrate-Active enZYmes Database*. Tilgjengelig fra: http://www.cazy.org/ (lest 02.02).

Chu, H. H., Hoang, V., Hofemeister, J. & Schrempf, H. (2001). A Bacillus amyloliquefaciens ChbB protein binds beta- and alpha-chitin and has homologues in related strains. *Microbiology*, 147 (Pt 7): 1793-803.

Davies, G. & Henrissat, B. (1995). Structures and mechanisms of glycosyl hydrolases. *Structure*, 3: 853-859.

DeLano, W. L. (2002). The PyMOL molecular graphics system.

Eijsink, V., Hoell, I. & Vaaje-Kolstada, G. (2010). Structure and function of enzymes acting on chitin and chitosan. *Biotechnol Genet Eng Rev*, 27: 331-66.

Eijsink, V. G., Vaaje-Kolstad, G., Varum, K. M. & Horn, S. J. (2008). Towards new enzymes for biofuels: lessons from chitinase research. *Trends Biotechnol*, 26 (5): 228-35.

Fennema, O. R., Parkin, K. L. & Damodaran, S. (2007). *Fennema's Food Chemistry*. 4 utg.: CRC Press

Folders, J., Tommassen, J., van Loon, L. C. & Bitter, W. (2000). Identification of a chitin-binding protein secreted by Pseudomonas aeruginosa. *J Bacteriol*, 182 (5): 1257-63.

Forsberg, Z., Vaaje-Kolstad, G., Westereng, B., Bunaes, A. C., Stenstrom, Y., MacKenzie, A., Sorlie, M., Horn, S. J. & Eijsink, V. G. (2011). Cleavage of cellulose by a CBM33 protein. *Protein Sci*, 20 (9): 1479-83.

Frederiksen, R. F., Paspaliari, D. K., Larsen, T., Storgaard, B. G., Larsen, M. H., Ingmer, H., Palcic, M. M. & Leisner, J. J. (2013). Bacterial chitinases and chitin-binding proteins as virulence factors. *Microbiology*.

Fuchs, R. L., McPherson, S. A. & Drahos, D. J. (1986). Cloning of a Serratia-Marcescens Gene Encoding Chitinase. *Applied and environmental microbiology*, 51 (3): 504-509.

Gilkes, N. R., Warren, R. A., Miller, R. C., Jr., Kilburn, D. G. (1988). Precise excision of the cellulose binding domains from two Cellulomonas fimi cellulases by a homologous protease and the effect on catalysis. *J Biol Chem*, 263 (21): 10401-7.

Gooday, G. W. (1990). Physiology of microbial degradation of chitin and chitosan. *Biodegradation*, 1: 177-190.

Henrissat, B. & Davies, G. (1997). Structural and sequence-based classification of glycoside hydrolase. *Current Opinion in Structural Biology*, 7 (5): 637-644.

Horn, S. J., Sorbotten, A., Synstad, B., Sikorski, P., Sorlie, M., Varum, K. M. & Eijsink, V. G. (2006a). Endo/exo mechanism and processivity of family 18 chitinases produced by Serratia marcescens. *FEBS J*, 273 (3): 491-503.

Horn, S. J., Sikorski, P., Cederkvist, J. B., Vaaje-Kolstad, G., Sorlie, M., Synstad, B., Vriend, G., Varum, K. M. & Eijsink, V. G. (2006c). Costs and benefits of processivity in enzymatic degradation of recalcitrant polysaccharides. *Proc Natl Acad Sci U S A*, 103 (48): 18089-94.

Horn, S. J., Vaaje-Kolstad, G., Westereng, B. & Eijsink, V. G. H. (2012). Novel enzymes for the degradation of cellulose. *Biotechnology for Biofuels*, 5 (45).

Hult, E. L., Katouno, F., Uchiyama, T., Watanabe, T. & Sugiyama, J. (2005). Molecular directionality in crystalline beta-chitin: hydrolysis by chitinases A and B from Serratia marcescens 2170. *Biochem J*, 388 (Pt 3): 851-6.

IUBMB. (2013). *Recommendations on Biochemical & Organic Nomenclature, Symbols & Terminology etc.* Tilgjengelig fra: http://www.chem.qmul.ac.uk/iubmb/ (lest 02.02).

Izquierdo, E., Horvatovich, P., Marchioni, E., Aoude-Werner, D., Sanz, Y. & Ennahar, S. (2009). 2-DE and MS analysis of key proteins in the adhesion of Lactobacillus plantarum, a first step toward early selection of probiotics based on bacterial biomarkers. *Electrophoresis*, 30 (6): 949-56.

Jang, M.-K., Kong, B.-G., Jeong, Y.-I., Lee, C. H. & Nah, J.-W. (2004). Physicochemical characterization of α-chitin, β-chitin, and γ-chitin separated from natural resources. *Journal of Polymer Science Part A: Polymer Chemistry*, 42 (14): 3423-3432.

Jayakumar, R., Prabaharan, M., Nair, S. V., Tokura, S., Tamura, H. & Selvamurugan, N. (2010). Novel carboxymethyl derivatives of chitin and chitosan materials and their biomedical applications. *Progress in Materials Science*, 55 (7): 675-709.

Johansen, B. J. (2012). *Purification and characterization of two novel polysaccharide oxidizing enzymes from Lactobacillus plantarum and Bacillus licheniformis belonging to the CBM33 family*: Universitetet for Miljø- og Biovitenskap, Institutt for Kjemi, Bioteknologi og Matvitenskap. 73 s.

Kirn, T. J., Jude, B. A. & Taylor, R. K. (2005). A colonization factor links Vibrio cholerae environmental survival and human infection. *Nature*, 438 (7069): 863-6.

Kittl, R., Kracher, D., Burgstaller, D., Haltrich, D. & Ludwig, R. (2012). Production of four Neurospora crassa lytic polysaccharide monooxygenases in Pichia pastoris monitored by a fluorimetric assay. *Biotechnol Biofuels*, 5 (1): 79.

Koivula, A., Kinnari, T., Harjunpää, V., Ruohonen, L., Teleman, A., Drakenberg, T., Rouvinen, J., Jones, T. A. & Teeri, T. T. (1998). Tryptophan 272: an essential determinant of crystalline cellulose degradation by Trichoderma reesei cellobiohydrolase Cel6A. *FEBS Letters*, 429 (3): 341-346.

Korotkov, K. V., Sandkvist, M. & Hol, W. G. J. (2012). The type II secretion system: biogenesis, molecular architecture and mechanism. *Nat Rev Micro*, 10 (5): 336-351.

Langston, J. A., Shaghasi, T., Abbate, E., Xu, F., Vlasenko, E. & Sweeney, M. D. (2011). Oxidoreductive cellulose depolymerization by the enzymes cellobiose dehydrogenase and glycoside hydrolase 61. *Appl Environ Microbiol*, 77 (19): 7007-15.

Leavitt, S. & Freire, E. (2001). Direct measurement of protein binding energetics by isothermal titration calorimetry. *Curr Opin Struct Biol*, 11 (5): 560-6.

Levasseur, A., Drula, E., Lombard, V., Coutinho, P. M. & Henrissat, B. (2013). Expansion of the enzymatic repertoire of the CAZy database to integrate auxiliary redox enzymes. *Biotechnol Biofuels*, 6 (1): 41.

Lewis, E. A. & Murphy, K. P. (2005). Isothermal titration calorimetry. *Methods Mol. Biol.*, 305: 1-16.

Liu, D., Wei, Y., Yao, P. & Jiang, L. (2006). Determination of the degree of acetylation of chitosan by UV spectrophotometry using dual standards. *Carbohydr Res*, 341 (6): 782-5.

Liu, H., Gao, Y., Yu, L. R., Jones, R. C., Elkins, C. A. & Hart, M. E. (2011). Inhibition of Staphylococcus aureus by lysostaphin-expressing Lactobacillus plantarum WCFS1 in a modified genital tract secretion medium. *Appl Environ Microbiol*, 77 (24): 8500-8.

Manos, J., Arthur, J., Rose, B., Bell, S., Tingpej, P., Hu, H., Webb, J., Kjelleberg, S., Gorrell, M. D., Bye, P., et al. (2009). Gene expression characteristics of a cystic fibrosis epidemic strain of Pseudomonas aeruginosa during biofilm and planktonic growth. *FEMS Microbiol Lett*, 292 (1): 107-14.

McCarter, J. D. W., S.G. (1994). Mechanisms of enzymatic glycoside hydrolysis. *Current Opinion in Structural Biology*, 4 (6): 885-892.

Monreal, J. & Reese, E. T. (1969). The chitinase of Serratia marcescens. *Canadian Journal of Microbiology*, 15 (7): 689-696.

Moser, F., Irwin, D., Chen, S. & Wilson, D. B. (2008). Regulation and characterization of Thermobifida fusca carbohydrate-binding module proteins E7 and E8. *Biotechnol Bioeng*, 100 (6): 1066-77.

Neish, A. S. (2009). Microbes in gastrointestinal health and disease. *Gastroenterology*, 136 (1): 65-80.

Payne, C. M., Baban, J., Horn, S. J., Backe, P. H., Arvai, A. S., Dalhus, B., Bjoras, M., Eijsink, V. G., Sorlie, M., Beckham, G. T., et al. (2012). Hallmarks of processivity in glycoside hydrolases from crystallographic and computational studies of the Serratia marcescens chitinases. *J Biol Chem*, 287 (43): 36322-30.

Phillips, C. M., Beeson, W. T., Cate, J. H. & Marletta, M. A. (2011). Cellobiose dehydrogenase and a copper-dependent polysaccharide monooxygenase potentiate cellulose degradation by Neurospora crassa. *ACS Chem Biol*, 6 (12): 1399-406.

Quinlan, R. J., Sweeney, M. D., Lo Leggio, L., Otten, H., Poulsen, J. C., Johansen, K. S., Krogh, K. B., Jorgensen, C. I., Tovborg, M., Anthonsen, A., et al. (2011). Insights into the oxidative degradation of cellulose by a copper metalloenzyme that exploits biomass components. *Proc Natl Acad Sci U S A*, 108 (37): 15079-84.

Reese, E. T., Siu, R. G. H. & Levinson, H. S. (1950). The biological degradation of soluble cellulose derivatives and its relationship to the mechanism of cellulose hydrolysis. *Journal of Bacteriology*, 59 (4): 485-497.

Rhee, S. G., Chang, T. S., Jeong, W. & Kang, D. (2010). Methods for detection and measurement of hydrogen peroxide inside and outside of cells. *Mol Cells*, 29 (6): 539-49.

Rinaudo, M. (2006). Chitin and chitosan: Properties and applications. *Progress in Polymer Science*, 31 (7): 603-632.

Sanchez, B., Gonzalez-Tejedo, C., Ruas-Madiedo, P., Urdaci, M. C. & Margolles, A. (2011). Lactobacillus plantarum extracellular chitin-binding protein and its role in the interaction between chitin, Caco-2 cells, and mucin. *Appl Environ Microbiol*, 77 (3): 1123-6.

Sanchez Ferrer, A., Santema, J. S., Hilhorst, R. & Visser, A. J. (1990). Fluorescence detection of enzymatically formed hydrogen peroxide in aqueous solution and in reversed micelles. *Anal Biochem*, 187 (1): 129-32.

Schnellmann, J., Zeltins, A., Blaak, H. & Schrempf, H. (1994). The novel lectin-like protein CHB1 is encoded by a chitin-inducible Streptomyces olivaceoviridis gene and binds specifically to crystalline α-chitin of fungi and other organisms. *Molecular Microbiology*, 13 (5): 807-819.

Shih, C., Museth, A. K., Abrahamsson, M., Blanco-Rodriguez, A. M., Di Bilio, A. J., Sudhamsu, J., Crane, B. R., Ronayne, K. L., Towrie, M., Vlcek, A., Jr., et al. (2008). Tryptophan-accelerated electron flow through proteins. *Science*, 320 (5884): 1760-2.

Shutinoski, B., Schmidt, M. A. & Heusipp, G. (2010). Transcriptional regulation of the Yts1 type II secretion system of Yersinia enterocolitica and identification of secretion substrates. *Mol Microbiol*, 75 (3): 676-91.

Sinnott, M. L. (1990). Catalytic mechanism of enzymic glycosyl transfer. *Chemical Reviews*, 90 (7): 1171-1202.

Sobhany, M. & Negishi, M. (2006). Characterization of Specific Donor Binding to α1,4-N-Acetylhexosaminyltransferase EXTL2 Using Isothermal Titration Calorimetry. I: Minoru, F. (red.) b. Volume 416 *Methods in Enzymology*, s. 3-12: Academic Press.

Solomon, E. I., Chen, P., Metz, M., Lee, S. K. & Palmer, A. E. (2001). Oxygen Binding, Activation, and Reduction to Water by Copper Proteins. *Angew Chem Int Ed Engl*, 40 (24): 4570-4590.

Spindler, K.-D., Spindler-Barth, M. & Londershausen, M. (1990). Chitin metabolism: a target for drugs against parasites. *Parasitology Research*, 76 (4): 283-288.

Suzuki, K., Suzuki, M., Taiyoji, M., Nikaidou, N. & Watanabe, T. (1998). Chitin binding protein (CBP21) in the culture supernatant of Serratia marcescens 2170. *Bioscience, Biotechnology, and Biochemistry*, 62 (1): 128-135.

Synowiecki, J. A.-K., N. A. (2003). Production, properties, and some new applications of chitin and its derivatives. *Critical Reviews in Food Science and Nutrition*, 42 (2): 145-171.

Synstad, B., Vaaje-Kolstad, G., Cederkvist, F. H., Saua, S. F., Horn, S. J., Eijsink, V. G. & Sorlie, M. (2008). Expression and characterization of endochitinase C from Serratia marcescens BJL200 and its purification by a one-step general chitinase purification method. *Biosci Biotechnol Biochem*, 72 (3): 715-23.

Sørlie, M., Zakariassen, H., Norberg, A. L. & Eijsink, V. G. H. (2012). Processivity and substrate-binding in family 18 chitinases. *Biocatalysis and Biotransformation*, 30 (3): 353-365.

Vaaje-Kolstad, G., Houston, D. R., Riemen, A. H., Eijsink, V. G. & van Aalten, D. M. (2005a). Crystal structure and binding properties of the Serratia marcescens chitin-binding protein CBP21. *J Biol Chem*, 280 (12): 11313-9.

Vaaje-Kolstad, G., Horn, S. J., van Aalten, D. M., Synstad, B. & Eijsink, V. G. (2005b). The non-catalytic chitin-binding protein CBP21 from Serratia marcescens is essential for chitin degradation. *J Biol Chem*, 280 (31): 28492-7.

Vaaje-Kolstad, G., Bunaes, A. C., Mathiesen, G. & Eijsink, V. G. H. (2009). The chitinolytic system of *Lactococcus lactiss* ssp. *lactis* comprises a nonprocessive chitinase and a chitin-binding protein that promotes the degradation of α- and β-chitin. *FEBS Journal*, 276 (8): 2402-2415.

Vaaje-Kolstad, G., Westereng, B., Horn, S. J., Liu, Z., Zhai, H., Sorlie, M. & Eijsink, V. G. (2010). An oxidative enzyme boosting the enzymatic conversion of recalcitrant polysaccharides. *Science*, 330 (6001): 219-22.

Vaaje-Kolstad, G., Bohle, L. A., Gaseidnes, S., Dalhus, B., Bjoras, M., Mathiesen, G. & Eijsink, V. G. (2012). Characterization of the chitinolytic machinery of Enterococcus faecalis V583 and high-resolution structure of its oxidative CBM33 enzyme. *J Mol Biol*, 416 (2): 239-54.

Vaaje-Kolstad, G., Horn, S. J., Sorlie, M. & Eijsink, V. G. (2013). The chitinolytic machinery of Serratia marcescens - a model system for enzymatic degradation of recalcitrant polysaccharides. *FEBS J*.

Vebo, H. C., Snipen, L., Nes, I. F. & Brede, D. A. (2009). The transcriptome of the nosocomial pathogen Enterococcus faecalis V583 reveals adaptive responses to growth in blood. *PLoS One*, 4 (11): e7660.

Vebo, H. C., Solheim, M., Snipen, L., Nes, I. F. & Brede, D. A. (2010). Comparative genomic analysis of pathogenic and probiotic Enterococcus faecalis isolates, and their transcriptional responses to growth in human urine. *PLoS One*, 5 (8): e12489.

Venil, C. K. & Lakshmanaperumalsamy, P. (2009). An Insightful Overview on Microbial Pigment, Prodigiosin. *Electronic Journal of Biology*, 5 (3): 49-61.

Vuong, T. V. W., D. B. (2010). Glycoside hydrolases: Catalytic base/nucleophile diversity. *Biotechnology and Bioengineering*, 107 (2): 195-205.

Watanabe, T., Ito, Y., Yamada, T., Hashimoto, M., Sekine, S. & Tanaka, H. (1994). The roles of the C-terminal domain and type III domains of chitinase A1 from Bacillus circulans WL-12 in chitin degradation. *J Bacteriol*, 176 (15): 4465-72.

Watanabe, T., Kimura, K., Sumiya, T., Nikaidou, N., Suzuki, K., Suzuki, M., Taiyoji, M., Ferrer, S., and Regue, M. (1997). Genetic Analysis of the Chitinase System of Serratia marcescens 2170. *Journal of bacteriology*, 179 (22): 7111–7117.

Westereng, B., Ishida, T., Vaaje-Kolstad, G., Wu, M., Eijsink, V. G., Igarashi, K., Samejima, M., Stahlberg, J., Horn, S. J. & Sandgren, M. (2011). The putative endoglucanase PcGH61D from Phanerochaete chrysosporium is a metal-dependent oxidative enzyme that cleaves cellulose. *PLoS One*, 6 (11): e27807.

Westereng, B., Agger, J. W., Horn, S. J., Vaaje-Kolstad, G., Aachmann, F. L., Stenstrom, Y. H. & Eijsink, V. G. (2013). Efficient separation of oxidized cello-oligosaccharides generated by cellulose degrading lytic polysaccharide monooxygenases. *J Chromatogr A*, 1271 (1): 144-52.

Wong, E., Vaaje-Kolstad, G., Ghosh, A., Hurtado-Guerrero, R., Konarev, P. V., Ibrahim, A. F., Svergun, D. I., Eijsink, V. G., Chatterjee, N. S. & van Aalten, D. M. (2012). The *Vibrio cholerae* colonization factor GbpA possesses a modular structure that governs binding to different host surfaces. *PLoS Pathog*, 8 (1): e1002373.

Zakariassen, H., Aam, B. B., Horn, S. J., Varum, K. M., Sorlie, M. & Eijsink, V. G. (2009). Aromatic residues in the catalytic center of chitinase A from Serratia marcescens affect processivity, enzyme activity, and biomass converting efficiency. *J Biol Chem*, 284 (16): 10610-7.

Zhou, M., Diwu, Z., Panchuk-Voloshina, N. & Haugland, R. P. (1997). A Stable Nonfluorescent Derivative of Resorufin for the Fluorometric Determination of Trace Hydrogen Peroxide: Applications in Detecting the Activity of Phagocyte NADPH Oxidase and Other Oxidases. *Analytical Biochemistry*, 253 (2): 162-168.

Zhou, W., Irwin, D. C., Escovar-Kousen, J. & Wilson, D. B. (2004). Kinetic Studies of Thermobifida fusca Cel9A Active Site Mutant Enzymes. *Biochemistry*, 43 (30): 9655-9663.

Appendix A

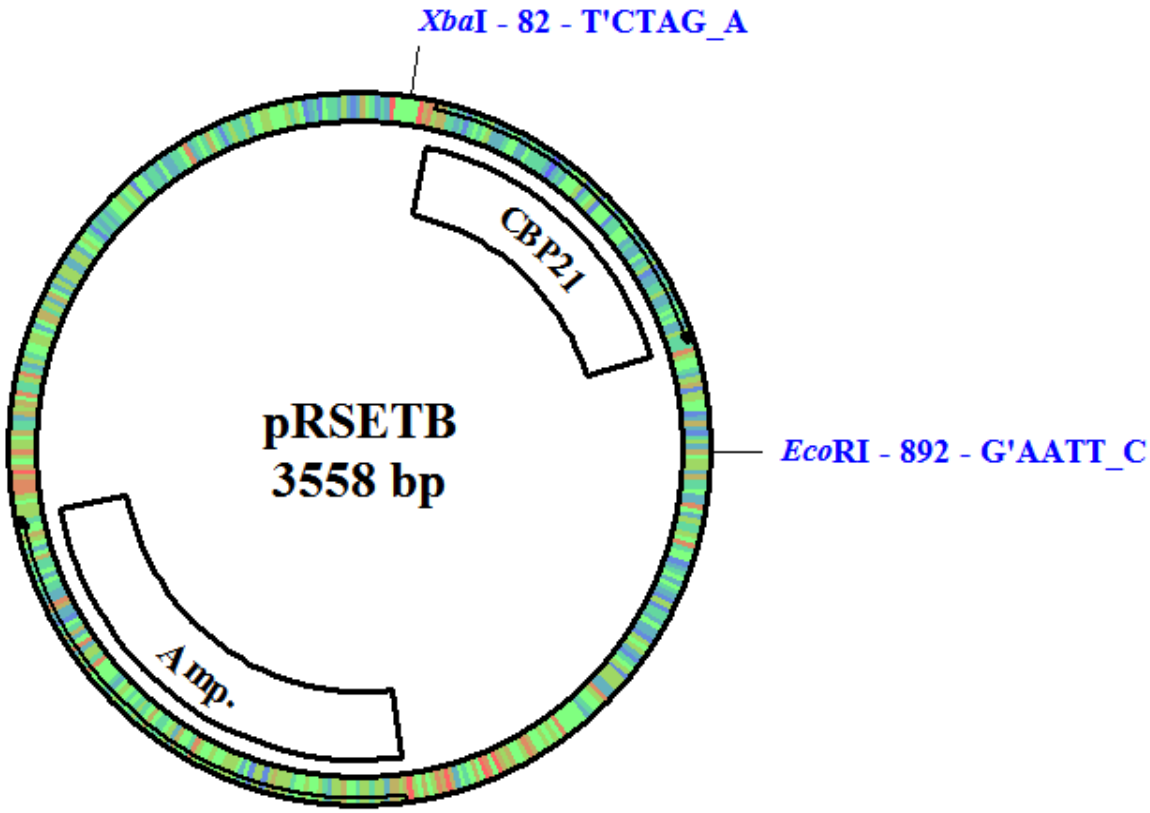

Figure A1. Vector map of pRSETB/*cbp21*. The figure shows the total size of the vector and the positions of the ampicillin resistance gene and the *cbp21* gene, including restriction sites for EcoRI and XbaI. The image was generated using pDRAW32.

Appendix B

a)

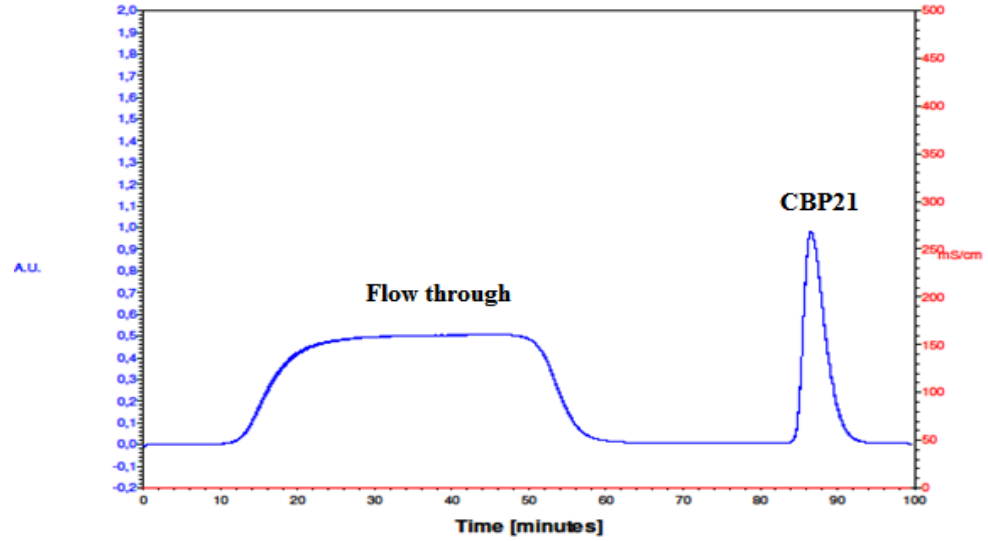

b)

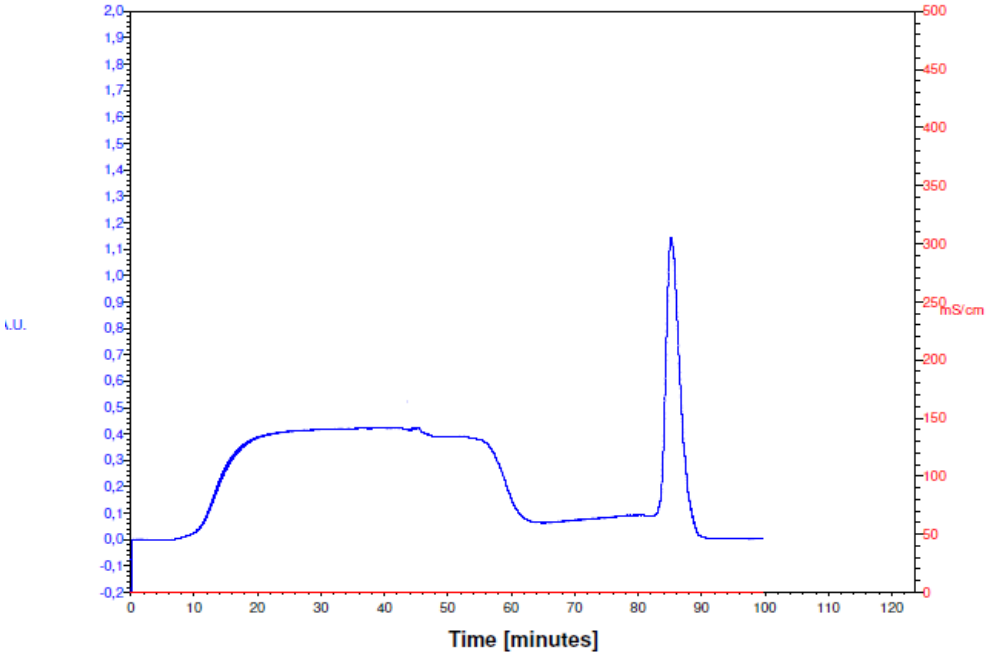

Figure B1. Chromatogram recorded during purification of CBP21 and *Ef*CBM33A by chitin-affinity chromatography. CBP21 (a) and *Ef*CBM33A (b) were purified from approximate 20 ml periplasmic extract using chitin beads as chromatographic medium. The periplasmic extract was loaded onto the column with a flow rate of 1.5 ml/sec. At 20 minutes (when no more periplasmic extract was left), the buffer was changed to 20 mM Tris-HCl, pH8. At approximately 65 minutes, the buffer was changed to 20 mM acetic acid pH 3.6 (elution buffer) and bound protein was eluted. The flow through is protein that did not bind to the chitin beads, while peak number two represents purified protein.

Appendix C

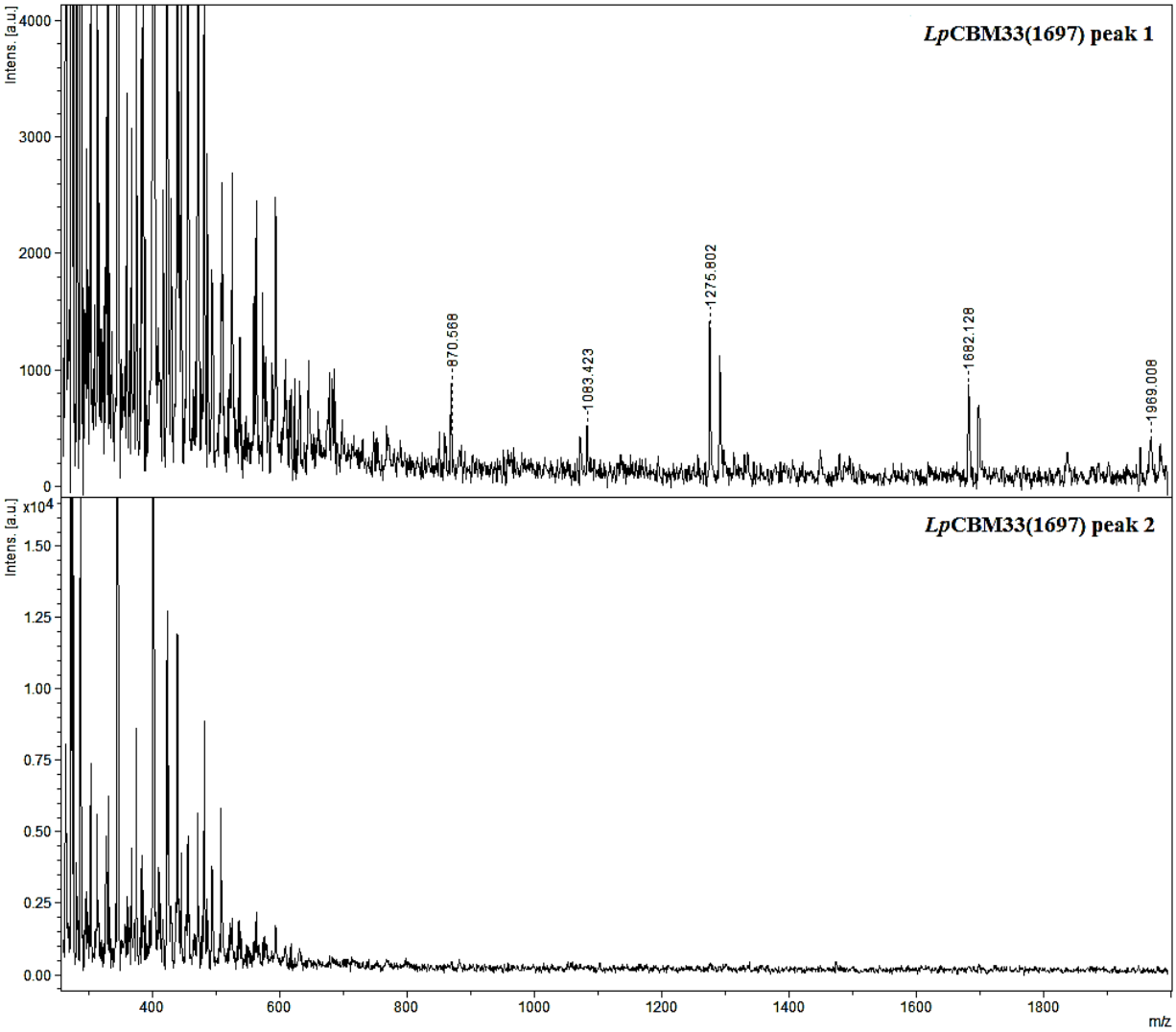

Figure C1. MALDI-TOF MS spectra of *Lp*CBM33(1697). The upper spectrum shows oxidized chitooligosaccharides of various DP`s generated when 2 mg/ml β-chitin^{A} was incubated with 2 µl sample from peak 1 (pooled fractions from peak 1 in the IEC chromatogram; see section 4.3.2, Fig.4.7) and 1 mM ascorbic acid in 50 mM Bis-Tris pH 8.0 for 16 hours at 37°C and 900 rpm. The peaks in the upper spectrum are labelled with their respective m/z values, which reflect the DP; DP4ox (m/z 870), $DP6_{ox}$ (m/z 1275) and $DP8_{ox}$ (m/z 1682). The lower spectrum shows that no oxidized products was generated when 2 µl sample from peak 2 was incubated under same conditions as described above, suggesting *Lp*CBM33(1697) is only present in peak 1.

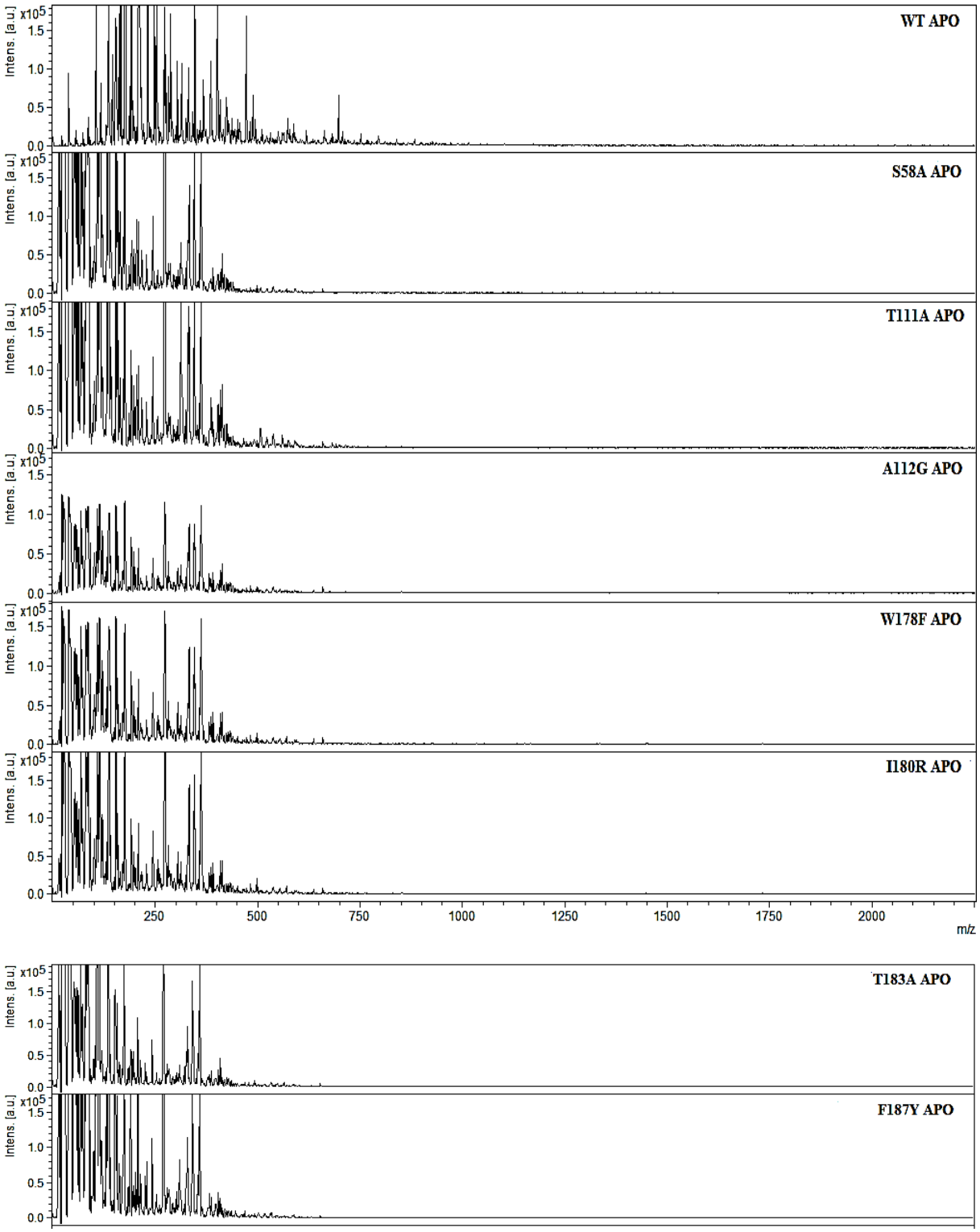

Figure C2. MALDI-TOF MS spectra of the apo form of CBP21 variants. The spectra show that no oxidized chitooligosaccharides were generated when 2 mg/ml β-chitin[A] was incubated with 1 µM EDTA-treated CBP21 and 1 mM ascorbic acid in 50 mM Bis-Tris pH 8.0 at 37°C and 900 rpm for ~16hours.

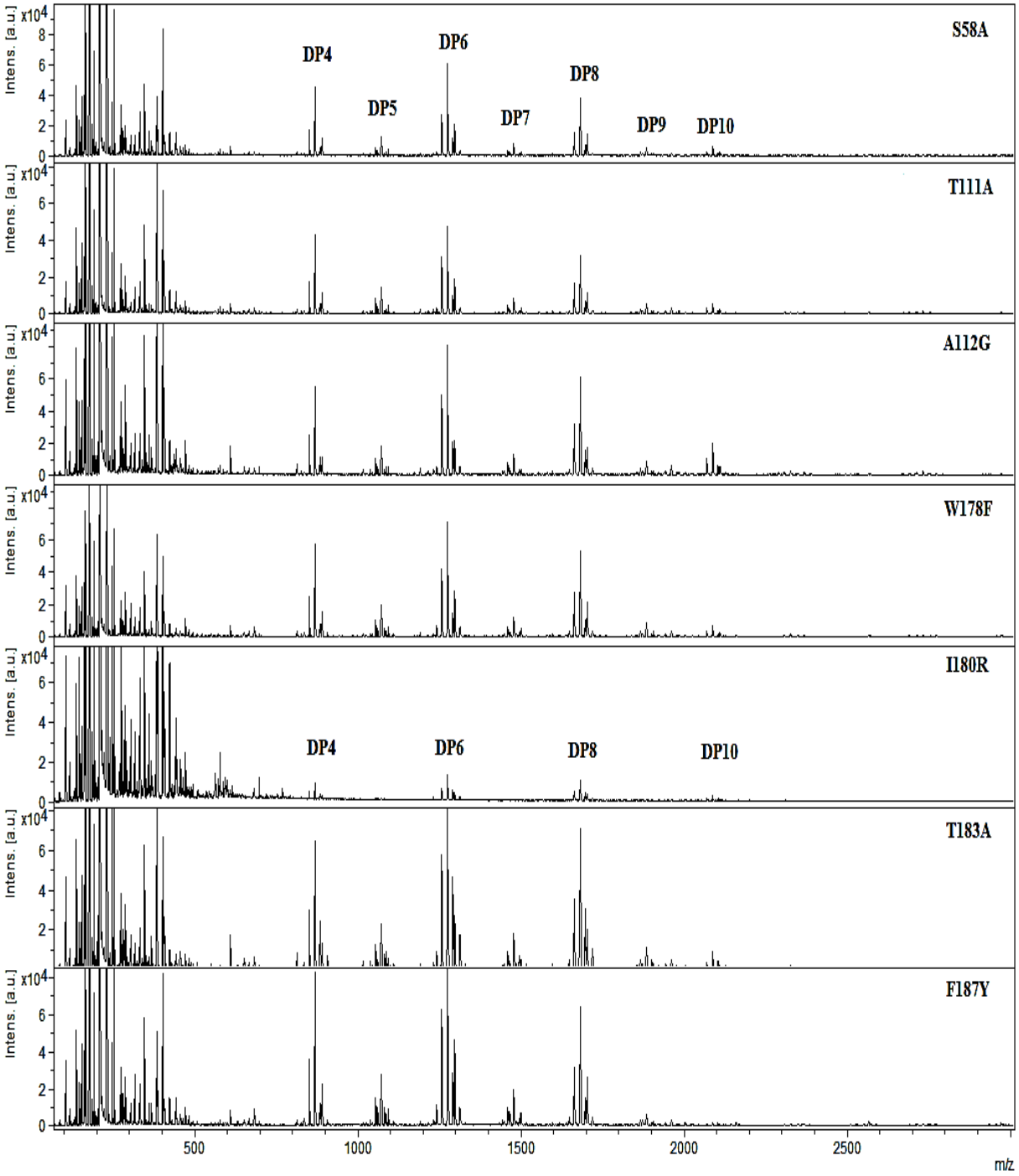

Figure C3. MALDI-TOF MS spectra of $CBP21_{WT}$ and mutants. The figure shows that all CBP21 variants (90% copper saturated) generate oxidized chitooligosaccharides of various DP were when 2 mg/ml β-chitin^{A} was incubated with 1 µM enzyme (90 % saturated with copper) and 1 mM ascorbic acid in 50 mM Bis-Tris pH 8.0 at 37°C and 900 rpm for ~16 hours.

Appendix D

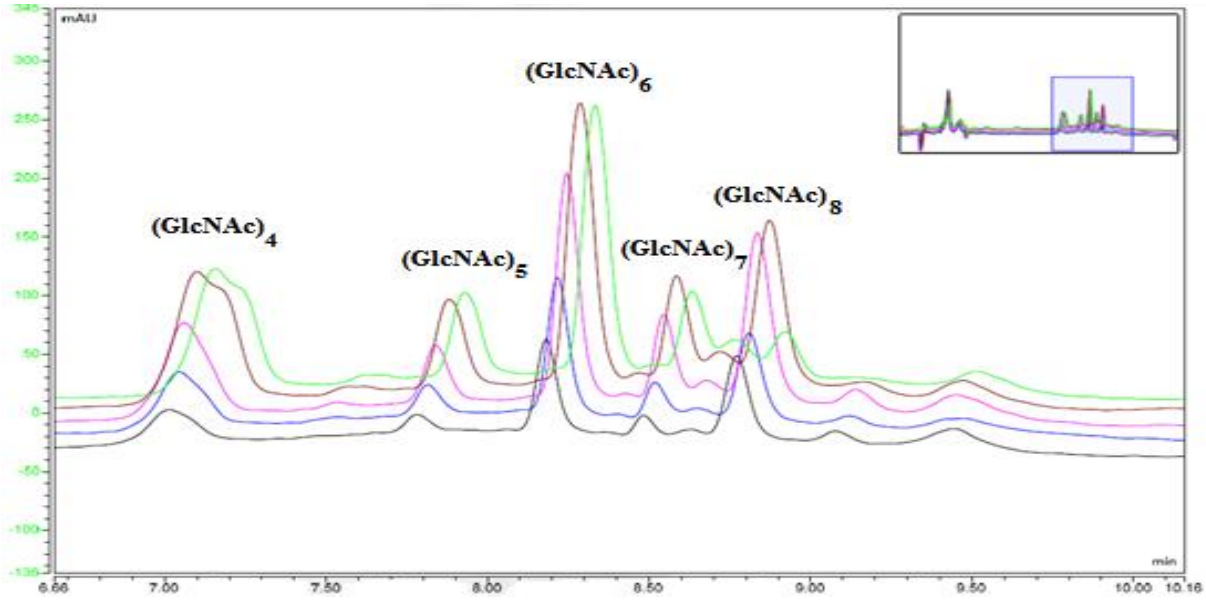

Figure D1. Recorded chromatogram during separation of oxidized products generated by CBP21$_{WT}$. The figure shows a typical chromatogram recorded during the experiment and shows the elution time (X-axis) of DP4$_{ox}$ -DP8$_{ox}$ after sample injection. DP4$_{ox}$ eluted after 6.9 minutes, DP5$_{ox}$ eluted after 7.7 minutes, DP6$_{ox}$ eluted after 8.1 minutes, DP7$_{ox}$ eluted after 8.4 minutes and DP8$_{ox}$ eluted after 8.7 minutes. The colours represent the time of measurement; black (20 minutes), blue (40 minutes), magenta (60 minutes), brown (80 minutes) and green (100 minutes). Note the drop in DP7$_{ox}$ and DP8$_{ox}$ after at 100 minutes (green line).

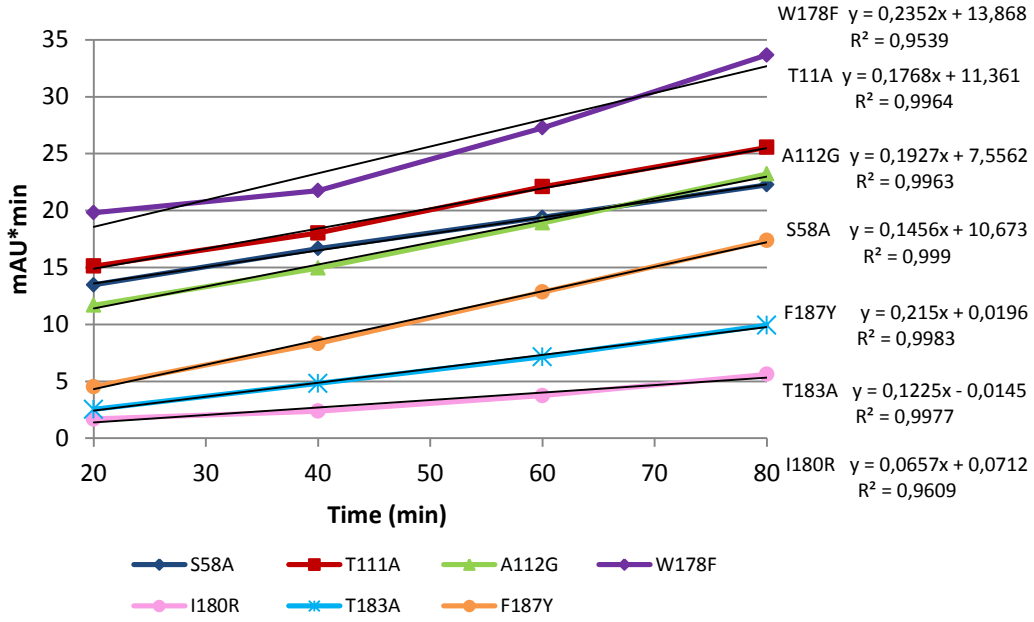

Figure D2. Oxidized products generated by CBP21 mutants from 20 to 80 minutes. The figure shows the amount of oxidized products generated at 20, 40, 60 and 80 minutes. The equations displayed on the chart were used to calculate chitin turnover between 20-80 minutes for each mutant respectively.

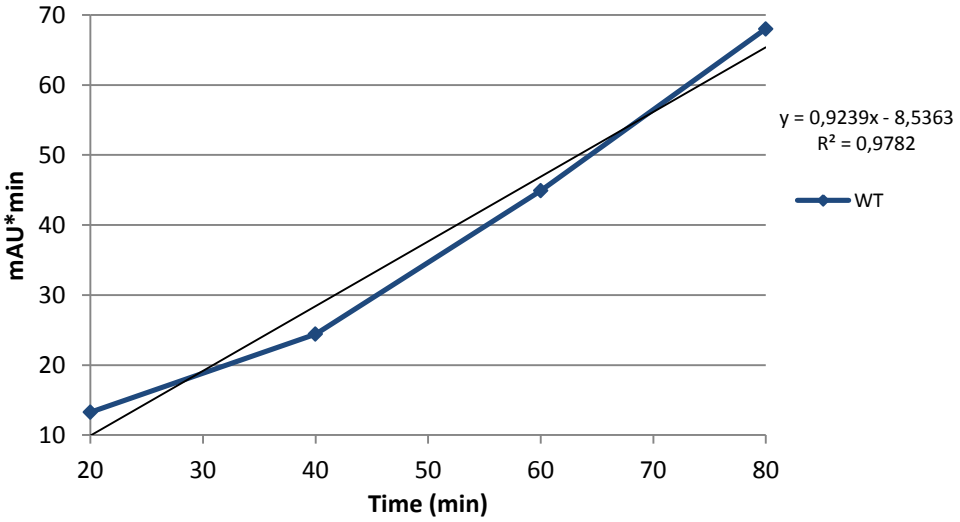

Figure D3. Oxidized products generated by CBP21$_{WT}$ from 20 to 80 minutes. The figure shows the amount of oxidized products generated at 20, 40, 60 and 80 minutes. The equation displayed on the chart was used to calculate chitin turnover between 20-80 minutes.

Appendix E

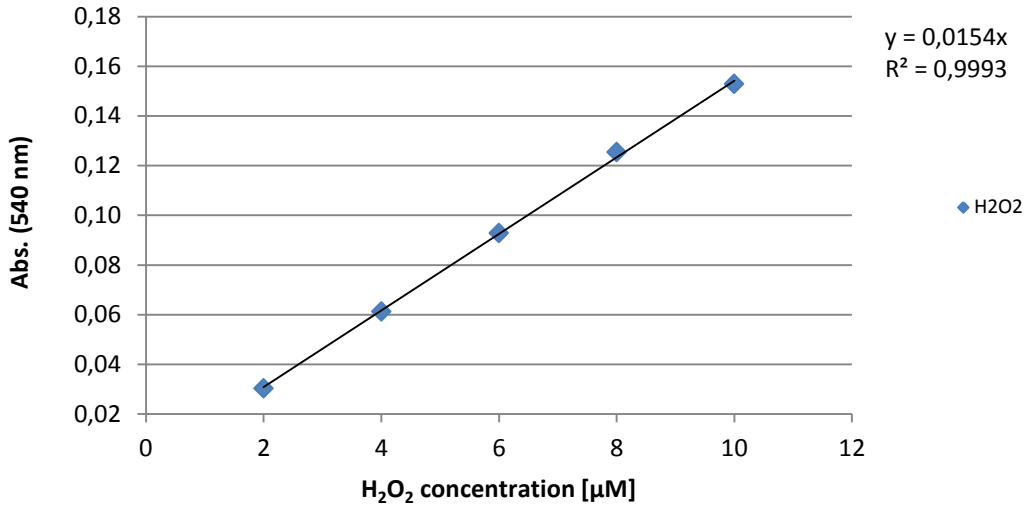

Figure E1. H_2O_2 standard curve. In order to convert the fluorimetric readouts to H_2O_2 concentrations, various concentrations (2, 4, 6, 8, and 10 µM) of H_2O_2 in 1 x reaction buffer was measured (A_{540}) using Amplex Red®/HRP. A control reaction containing 1 x reaction buffer was included and the readouts of this reaction were subtracted from the fluorimetric values in order to determine the exact absorption from H_2O_2. The equation at the top right corner in the graph was used to convert fluorimetric values to H_2O_2 concentration in all H_2O_2 experiments.

Appendix F

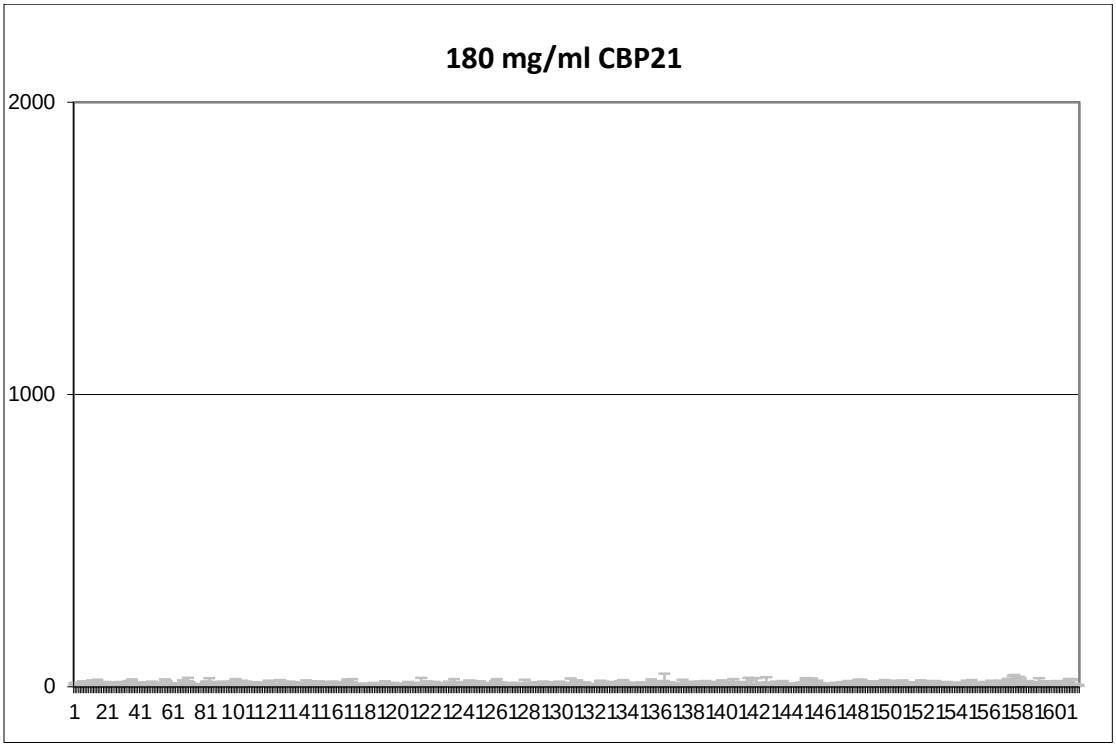

Figure F1. Binding of CBP21 to mammalian glycans.

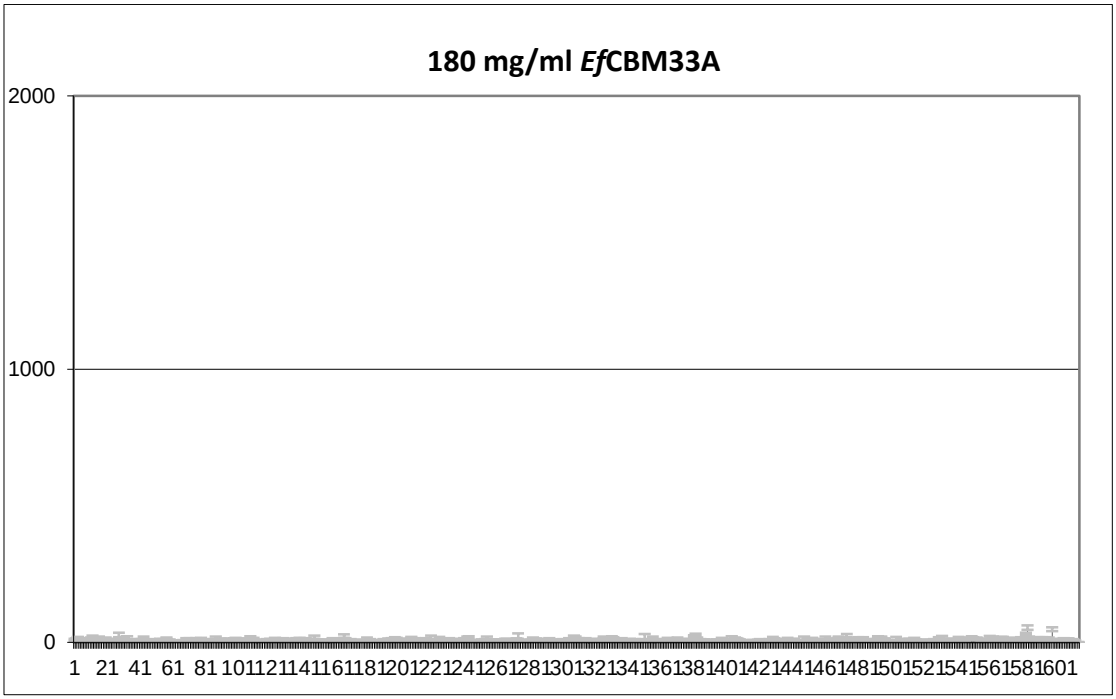

Figure F2. Binding of *Ef*CBM33A to mammalian glycans.

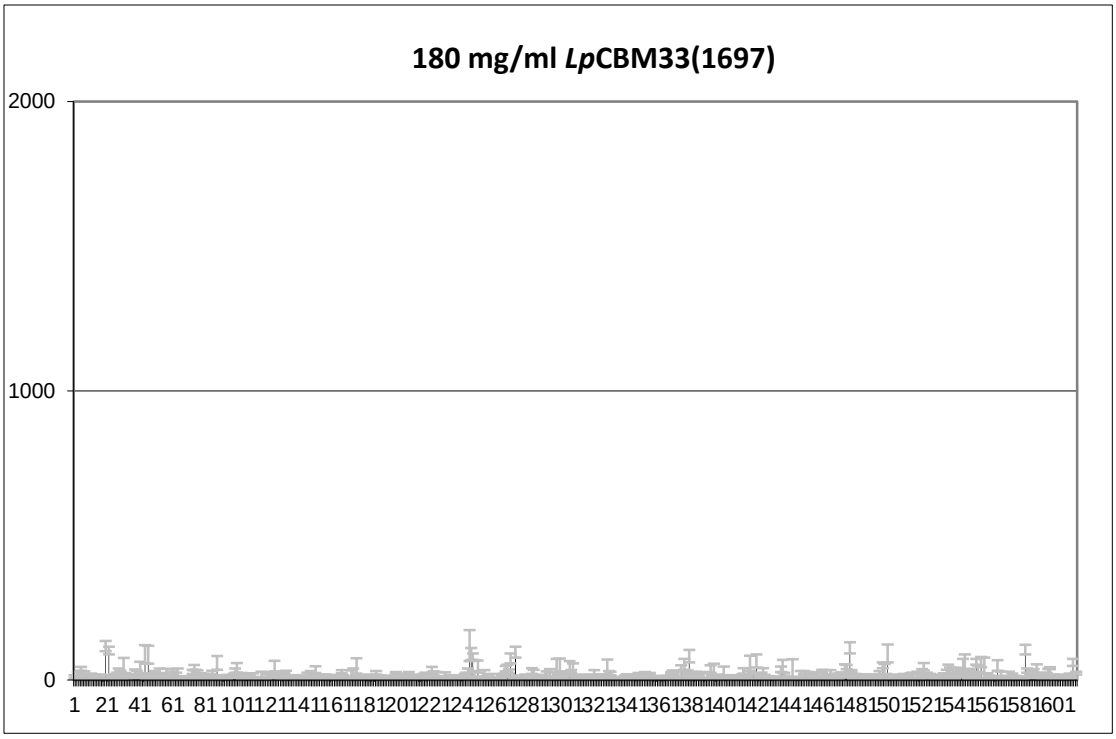

Figure F3. Binding of *Lp*CBM33(1697) to mammalian glycans.

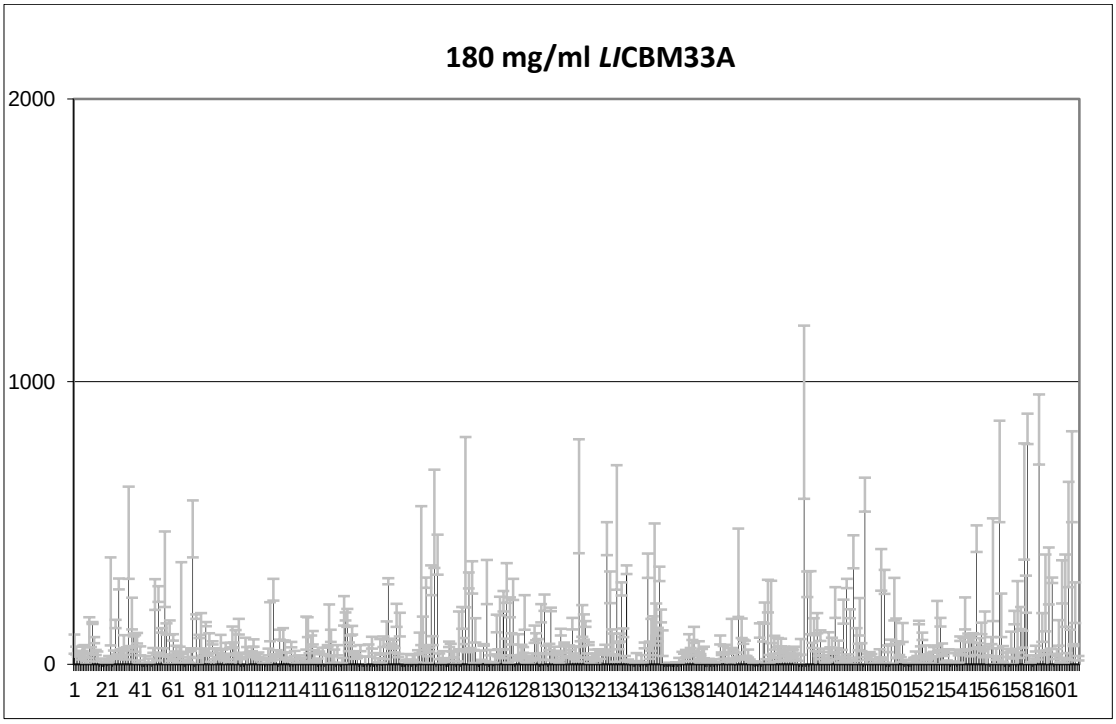

Figure F4. Binding of *Ll*CBM33A to mammalian glycans.

Table F1. Complete structure list of mammalian glycans used in the glycan array.

Chart Number	Structure
1	Gala-Sp8
2	Glca-Sp8
3	Mana-Sp8
4	GalNAca-Sp8
5	GalNAca-Sp15
6	Fuca-Sp8
7	Fuca-Sp9
8	Rhaa-Sp8
9	Neu5Aca-Sp8
10	Neu5Aca-Sp11
11	Neu5Acb-Sp8
12	Galb-Sp8
13	Glcb-Sp8
14	Manb-Sp8
15	GalNAcb-Sp8
16	GlcNAcb-Sp0
17	GlcNAcb-Sp8
18	GlcN(Gc)b-Sp8
19	Galb1-4GlcNAcb1-6(Galb1-4GlcNAcb1-3)GalNAca-Sp8
20	Galb1-4GlcNAcb1-6(Galb1-4GlcNAcb1-3)GalNAc-Sp14
21	GlcNAcb1-6(GlcNAcb1-4)(GlcNAcb1-3)GlcNAc-Sp8
22	6S(3S)Galb1-4(6S)GlcNAcb-Sp0
23	6S(3S)Galb1-4GlcNAcb-Sp0
24	(3S)Galb1-4(Fuca1-3)(6S)Glc-Sp0
25	(3S)Galb1-4Glcb-Sp8
26	(3S)Galb1-4(6S)Glcb-Sp0
27	(3S)Galb1-4(6S)Glcb-Sp8
28	(3S)Galb1-3(Fuca1-4)GlcNAcb-Sp8
29	(3S)Galb1-3GalNAca-Sp8
30	(3S)Galb1-3GlcNAcb-Sp0
31	(3S)Galb1-3GlcNAcb-Sp8
32	(3S)Galb1-4(Fuca1-3)GlcNAc-Sp0
33	(3S)Galb1-4(Fuca1-3)GlcNAc-Sp8
34	(3S)Galb1-4(6S)GlcNAcb-Sp0
35	(3S)Galb1-4(6S)GlcNAcb-Sp8
36	(3S)Galb1-4GlcNAcb-Sp0
37	(3S)Galb1-4GlcNAcb-Sp8
38	(3S)Galb-Sp8
39	(6S)(4S)Galb1-4GlcNAcb-Sp0
40	(4S)Galb1-4GlcNAcb-Sp8
41	(6P)Mana-Sp8
42	(6S)Galb1-4Glcb-Sp0
43	(6S)Galb1-4Glcb-Sp8
44	(6S)Galb1-4GlcNAcb-Sp8
45	(6S)Galb1-4(6S)Glcb-Sp8
46	Neu5Aca2-3(6S)Galb1-4GlcNAcb-Sp8

47	(6S)GlcNAcb-Sp8
48	Neu5,9Ac_2a-Sp8
49	Neu5,9Ac2a2-6Galb1-4GlcNAcb-Sp8
50	Mana1-6(Mana1-3)Manb1-4GlcNAcb1-4GlcNAcb-Sp12
51	Mana1-6(Mana1-3)Manb1-4GlcNAcb1-4GlcNAcb-Sp13
52	GlcNAcb1-2Mana1-6(GlcNAcb1-2Mana1-3)Manb1-4GlcNAcb1-4GlcNAcb-Sp12
53	GlcNAcb1-2Mana1-6(GlcNAcb1-2Mana1-3)Manb1-4GlcNAcb1-4GlcNAcb-Sp13
54	Galb1-4GlcNAcb1-2Mana1-6(Galb1-4GlcNAcb1-2Mana1-3)Manb1-4GlcNAcb1-4GlcNAcb-Sp12
55	Neu5Aca2-6Galb1-4GlcNAcb1-2Mana1-6(Neu5Aca2-6Galb1-4GlcNAcb1-2Mana1-3)Manb1-4GlcNAcb1-4GlcNAcb-Sp12
56	Neu5Aca2-6Galb1-4GlcNAcb1-2Mana1-6(Neu5Aca2-6Galb1-4GlcNAcb1-2Man-a1-3)Manb1-4GlcNAcb1-4GlcNAcb-Sp21
57	Neu5Aca2-6Galb1-4GlcNAcb1-2Mana1-6(Neu5Aca2-6Galb1-4GlcNAcb1-2Mana1-3)Manb1-4GlcNAcb1-4GlcNAcb-Sp24
58	Fuca1-2Galb1-3GalNAcb1-3Gala-Sp9
59	Fuca1-2Galb1-3GalNAcb1-3Gala1-4Galb1-4Glcb-Sp9
60	Fuca1-2Galb1-3(Fuca1-4)GlcNAcb-Sp8
61	Fuca1-2Galb1-3GalNAca-Sp8
62	Fuca1-2Galb1-3GalNAca-Sp14
63	Fuca1-2Galb1-3GalNAcb1-4(Neu5Aca2-3)Galb1-4Glcb-Sp0
64	Fuca1-2Galb1-3GalNAcb1-4(Neu5Aca2-3)Galb1-4Glcb-Sp9
65	Fuca1-2Galb1-3GlcNAcb1-3Galb1-4Glcb-Sp8
66	Fuca1-2Galb1-3GlcNAcb1-3Galb1-4Glcb-Sp10
67	Fuca1-2Galb1-3GlcNAcb-Sp0
68	Fuca1-2Galb1-3GlcNAcb-Sp8
69	Fuca1-2Galb1-4(Fuca1-3)GlcNAcb1-3Galb1-4(Fuca1-3)GlcNAcb-Sp0
70	Fuca1-2Galb1-4(Fuca1-3)GlcNAcb1-3Galb1-4(Fuca1-3)GlcNAcb1-3Galb1-4(Fuca1-3)GlcNAcb-Sp0
71	Fuca1-2Galb1-4(Fuca1-3)GlcNAcb-Sp0
72	Fuca1-2Galb1-4(Fuca1-3)GlcNAcb-Sp8
73	Fuca1-2Galb1-4GlcNAcb1-3Galb1-4GlcNAcb-Sp0
74	Fuca1-2Galb1-4GlcNAcb1-3Galb1-4GlcNAcb1-3Galb1-4GlcNAcb-Sp0
75	Fuca1-2Galb1-4GlcNAcb-Sp0
76	Fuca1-2Galb1-4GlcNAcb-Sp8
77	Fuca1-2Galb1-4Glcb-Sp0
78	Fuca1-2Galb-Sp8
79	Fuca1-3GlcNAcb-Sp8
80	Fuca1-4GlcNAcb-Sp8
81	Fucb1-3GlcNAcb-Sp8
82	GalNAca1-3(Fuca1-2)Galb1-3GlcNAcb-Sp0
83	GalNAca1-3(Fuca1-2)Galb1-4(Fuca1-3)GlcNAcb-Sp0
84	(3S)Galb1-4(Fuca1-3)Glcb-Sp0
85	GalNAca1-3(Fuca1-2)Galb1-4GlcNAcb-Sp0
86	GalNAca1-3(Fuca1-2)Galb1-4GlcNAcb-Sp8
87	GalNAca1-3(Fuca1-2)Galb1-4Glcb-Sp0
88	GlcNAcb1-3Galb1-3GalNAca-Sp8
89	GalNAca1-3(Fuca1-2)Galb-Sp8
90	GalNAca1-3(Fuca1-2)Galb-Sp18
91	GalNAca1-3GalNAcb-Sp8

92	GalNAca1-3Galb-Sp8
93	GalNAca1-4(Fuca1-2)Galb1-4GlcNAcb-Sp8
94	GalNAcb1-3GalNAca-Sp8
95	GalNAcb1-3(Fuca1-2)Galb-Sp8
96	GalNAcb1-3Gala1-4Galb1-4GlcNAcb-Sp0
97	GalNAcb1-4(Fuca1-3)GlcNAcb-Sp0
98	GalNAcb1-4GlcNAcb-Sp0
99	GalNAcb1-4GlcNAcb-Sp8
100	Gala1-2Galb-Sp8
101	Gala1-3(Fuca1-2)Galb1-3GlcNAcb-Sp0
102	Gala1-3(Fuca1-2)Galb1-3GlcNAcb-Sp8
103	Gala1-3(Fuca1-2)Galb1-4(Fuca1-3)GlcNAcb-Sp0
104	Gala1-3(Fuca1-2)Galb1-4(Fuca1-3)GlcNAcb-Sp8
105	Gala1-3(Fuca1-2)Galb1-4GlcNAc-Sp0
106	Gala1-3(Fuca1-2)Galb1-4Glcb-Sp0
107	Gala1-3(Fuca1-2)Galb-Sp8
108	Gala1-3(Fuca1-2)Galb-Sp18
109	Gala1-4(Gala1-3)Galb1-4GlcNAcb-Sp8
110	Gala1-3GalNAca-Sp8
111	Gala1-3GalNAca-Sp16
112	Gala1-3GalNAcb-Sp8
113	Gala1-3Galb1-4(Fuca1-3)GlcNAcb-Sp8
114	Gala1-3Galb1-3GlcNAcb-Sp0
115	Gala1-3Galb1-4GlcNAcb-Sp8
116	Gala1-3Galb1-4Glcb-Sp0
117	Gala1-3Galb1-4Glc-Sp10
118	Gala1-3Galb-Sp8
119	Gala1-4(Fuca1-2)Galb1-4GlcNAcb-Sp8
120	Gala1-4Galb1-4GlcNAcb-Sp0
121	Gala1-4Galb1-4GlcNAcb-Sp8
122	Gala1-4Galb1-4Glcb-Sp0
123	Gala1-4GlcNAcb-Sp8
124	Gala1-6Glcb-Sp8
125	Galb1-2Galb-Sp8
126	Galb1-3(Fuca1-4)GlcNAcb1-3Galb1-4(Fuca1-3)GlcNAcb-Sp0
127	Galb1-3GlcNAcb1-3Galb1-4(Fuca1-3)GlcNAcb-Sp0
128	Galb1-3(Fuca1-4)GlcNAc-Sp0
129	Galb1-3(Fuca1-4)GlcNAc-Sp8
130	Fuca1-4(Galb1-3)GlcNAcb-Sp8
131	Galb1-4GlcNAcb1-6GalNAca-Sp8
132	Galb1-4GlcNAcb1-6GalNAc-Sp14
133	GlcNAcb1-6(Galb1-3)GalNAca-Sp8
134	GlcNAcb1-6(Galb1-3)GalNAca-Sp14
135	Neu5Aca2-6(Galb1-3)GalNAca-Sp8
136	Neu5Aca2-6(Galb1-3)GalNAca-Sp14
137	Neu5Acb2-6(Galb1-3)GalNAca-Sp8
138	Neu5Aca2-6(Galb1-3)GlcNAcb1-4Galb1-4Glcb-Sp10
139	Galb1-3GalNAca-Sp8
140	Galb1-3GalNAca-Sp14
141	Galb1-3GalNAca-Sp16

142	Galb1-3GalNAcb-Sp8
143	Galb1-3GalNAcb1-3Gala1-4Galb1-4Glcb-Sp0
144	Galb1-3GalNAcb1-4(Neu5Aca2-3)Galb1-4Glcb-Sp0
145	Galb1-3GalNAcb1-4Galb1-4Glcb-Sp8
146	Galb1-3Galb-Sp8
147	Galb1-3GlcNAcb1-3Galb1-4GlcNAcb-Sp0
148	Galb1-3GlcNAcb1-3Galb1-4Glcb-Sp10
149	Galb1-3GlcNAcb-Sp0
150	Galb1-3GlcNAcb-Sp8
151	Galb1-4(Fuca1-3)GlcNAcb-Sp0
152	Galb1-4(Fuca1-3)GlcNAcb-Sp8
153	Galb1-4(Fuca1-3)GlcNAcb1-3Galb1-4(Fuca1-3)GlcNAcb-Sp0
154	Galb1-4(Fuca1-3)GlcNAcb1-3Galb1-4(Fuca1-3)GlcNAcb1-3Galb1-4(Fuca1-3)GlcNAcb-Sp0
155	Galb1-4(6S)Glcb-Sp0
156	Galb1-4(6S)Glcb-Sp8
157	Galb1-4GalNAca1-3(Fuca1-2)Galb1-4GlcNAcb-Sp8
158	Galb1-4GalNAcb1-3(Fuca1-2)Galb1-4GlcNAcb-Sp8
159	Galb1-4GlcNAcb1-3GalNAca-Sp8
160	Galb1-4GlcNAcb1-3GalNAc-Sp14
161	Galb1-4GlcNAcb1-3Galb1-4(Fuca1-3)GlcNAcb1-3Galb1-4(Fuca1-3)GlcNAcb-Sp0
162	Galb1-4GlcNAcb1-3Galb1-4GlcNAcb1-3Galb1-4GlcNAcb-Sp0
163	Galb1-4GlcNAcb1-3Galb1-4GlcNAcb-Sp0
164	Galb1-4GlcNAcb1-3Galb1-4Glcb-Sp0
165	Galb1-4GlcNAcb1-3Galb1-4Glcb-Sp8
166	Galb1-4GlcNAcb1-6(Galb1-3)GalNAca-Sp8
167	Galb1-4GlcNAcb1-6(Galb1-3)GalNAc-Sp14
168	Galb1-4GlcNAcb-Sp0
169	Galb1-4GlcNAcb-Sp8
170	Galb1-4GlcNAcb-Sp23
171	Galb1-4Glcb-Sp0
172	Galb1-4Glcb-Sp8
173	GlcNAca1-3Galb1-4GlcNAcb-Sp8
174	GlcNAca1-6Galb1-4GlcNAcb-Sp8
175	GlcNAcb1-2Galb1-3GalNAca-Sp8
176	GlcNAcb1-6(GlcNAcb1-3)GalNAca-Sp8
177	GlcNAcb1-6(GlcNAcb1-3)GalNAca-Sp14
178	GlcNAcb1-6(GlcNAcb1-3)Galb1-4GlcNAcb-Sp8
179	GlcNAcb1-3GalNAca-Sp8
180	GlcNAcb1-3GalNAca-Sp14
181	GlcNAcb1-3Galb-Sp8
182	GlcNAcb1-3Galb1-4GlcNAcb-Sp0
183	GlcNAcb1-3Galb1-4GlcNAcb-Sp8
184	GlcNAcb1-3Galb1-4GlcNAcb1-3Galb1-4GlcNAcb-Sp0
185	GlcNAcb1-3Galb1-4Glcb-Sp0
186	GlcNAcb1-4-MDPLys
187	GlcNAcb1-6(GlcNAcb1-4)GalNAca-Sp8
188	GlcNAcb1-4Galb1-4GlcNAcb-Sp8
189	GlcNAcb1-4GlcNAcb1-4GlcNAcb1-4GlcNAcb1-4GlcNAcb1-4GlcNAcb1-Sp8
190	GlcNAcb1-4GlcNAcb1-4GlcNAcb1-4GlcNAcb1-4GlcNAcb1-Sp8
191	GlcNAcb1-4GlcNAcb1-4GlcNAcb-Sp8

192	GlcNAcb1-6GalNAca-Sp8
193	GlcNAcb1-6GalNAca-Sp14
194	GlcNAcb1-6Galb1-4GlcNAcb-Sp8
195	Glca1-4Glcb-Sp8
196	Glca1-4Glca-Sp8
197	Glca1-6Glca1-6Glcb-Sp8
198	Glcb1-4Glcb-Sp8
199	Glcb1-6Glcb-Sp8
200	G-ol-Sp8
201	GlcAa-Sp8
202	GlcAb-Sp8
203	GlcAb1-3Galb-Sp8
204	GlcAb1-6Galb-Sp8
205	KDNa2-3Galb1-3GlcNAcb-Sp0
206	KDNa2-3Galb1-4GlcNAcb-Sp0
207	Mana1-2Mana1-2Mana1-3Mana-Sp9
208	Mana1-2Mana1-6(Mana1-2Mana1-3)Mana-Sp9
209	Mana1-2Mana1-3Mana-Sp9
210	Mana1-6(Mana1-2Mana1-3)Mana1-6(Mana1-2Mana1-3)Manb1-4GlcNAcb1-4GlcNAcb-Sp12
211	Mana1-2Mana1-6(Mana1-3)Mana1-6(Mana1-2Mana1-2Mana1-3)Manb1-4GlcNAcb1-4GlcNAcb-Sp12
212	Mana1-2Mana1-6(Mana1-2Mana1-3)Mana1-6(Mana1-2Mana1-2Mana1-3)Manb1-4GlcNAcb1-4GlcNAcb-Sp12
213	Mana1-6(Mana1-3)Mana-Sp9
214	Mana1-2Mana1-2Mana1-6(Mana1-3)Mana-Sp9
215	Mana1-6(Mana1-3)Mana1-6(Mana1-2Mana1-3)Manb1-4GlcNAcb1-4GlcNAcb-Sp12
216	Mana1-6(Mana1-3)Mana1-6(Mana1-3)Manb1-4GlcNAcb1-4GlcNAcb-Sp12
217	Manb1-4GlcNAcb-Sp0
218	Neu5Aca2-3Galb1-4GlcNAcb1-3Galb1-4(Fuca1-3)GlcNAcb-Sp0
219	(3S)Galb1-4(Fuca1-3)(6S)GlcNAcb-Sp8
220	Fuca1-2(6S)Galb1-4GlcNAcb-Sp0
221	Fuca1-2Galb1-4(6S)GlcNAcb-Sp8
222	Fuca1-2(6S)Galb1-4(6S)Glcb-Sp0
223	Neu5Aca2-3Galb1-3GalNAca-Sp8
224	Neu5Aca2-3Galb1-3GalNAca-Sp14
225	GalNAcb1-4(Neu5Aca2-8Neu5Aca2-8Neu5Aca2-8Neu5Aca2-3)Galb1-4Glcb-Sp0
226	GalNAcb1-4(Neu5Aca2-8Neu5Aca2-8Neu5Aca2-3)Galb1-4Glcb-Sp0
227	Neu5Aca2-8Neu5Aca2-8Neu5Aca2-3Galb1-4Glcb-Sp0
228	GalNAcb1-4(Neu5Aca2-8Neu5Aca2-3)Galb1-4Glcb-Sp0
229	Neu5Aca2-8Neu5Aca2-8Neu5Aca-Sp8
230	Neu5Aca2-3(6S)Galb1-4(Fuca1-3)GlcNAcb-Sp8
231	GalNAcb1-4(Neu5Aca2-3)Galb1-4GlcNAcb-Sp0
232	GalNAcb1-4(Neu5Aca2-3)Galb1-4GlcNAcb-Sp8
233	GalNAcb1-4(Neu5Aca2-3)Galb1-4Glcb-Sp0
234	Neu5Aca2-3Galb1-3GalNAcb1-4(Neu5Aca2-3)Galb1-4Glcb-Sp0
235	Neu5Aca2-6(Neu5Aca2-3)GalNAca-Sp8
236	Neu5Aca2-3GalNAca-Sp8
237	Neu5Aca2-3GalNAcb1-4GlcNAcb-Sp0
238	Neu5Aca2-3Galb1-3(6S)GlcNAc-Sp8

239	Neu5Aca2-3Galb1-3(Fuca1-4)GlcNAcb-Sp8
240	Neu5Aca2-3Galb1-3(Fuca1-4)GlcNAcb1-3Galb1-4(Fuca1-3)GlcNAcb-Sp0
241	Neu5Aca2-3Galb1-4(Neu5Aca2-3Galb1-3)GlcNAcb-Sp8
242	Neu5Aca2-3Galb1-3(6S)GalNAca-Sp8
243	Neu5Aca2-6(Neu5Aca2-3Galb1-3)GalNAca-Sp8
244	Neu5Aca2-6(Neu5Aca2-3Galb1-3)GalNAca-Sp14
245	Neu5Aca2-3Galb-Sp8
246	Neu5Aca2-3Galb1-3GalNAcb1-3Gala1-4Galb1-4Glcb-Sp0
247	Neu5Aca2-3Galb1-3GlcNAcb1-3Galb1-4GlcNAcb-Sp0
248	Fuca1-2(6S)Galb1-4Glcb-Sp0
249	Neu5Aca2-3Galb1-3GlcNAcb-Sp0
250	Neu5Aca2-3Galb1-3GlcNAcb-Sp8
251	Neu5Aca2-3Galb1-4(6S)GlcNAcb-Sp8
252	Neu5Aca2-3Galb1-4(Fuca1-3)(6S)GlcNAcb-Sp8
253	Neu5Aca2-3Galb1-4(Fuca1-3)GlcNAcb1-3Galb1-4(Fuca1-3)GlcNAcb1-3Galb1-4(Fuca1-3)GlcNAcb-Sp0
254	Neu5Aca2-3Galb1-4(Fuca1-3)GlcNAcb-Sp0
255	Neu5Aca2-3Galb1-4(Fuca1-3)GlcNAcb-Sp8
256	Neu5Aca2-3Galb1-4(Fuca1-3)GlcNAcb1-3Galb-Sp8
257	Neu5Aca2-3Galb1-4(Fuca1-3)GlcNAcb1-3Galb1-4GlcNAcb-Sp8
258	Neu5Aca2-3Galb1-4GlcNAcb1-3Galb1-4GlcNAcb1-3Galb1-4GlcNAcb-Sp0
259	Neu5Aca2-3Galb1-4GlcNAcb-Sp0
260	Neu5Aca2-3Galb1-4GlcNAcb-Sp8
261	Neu5Aca2-3Galb1-4GlcNAcb1-3Galb1-4GlcNAcb-Sp0
262	Fuca1-2Galb1-4(6S)Glcb-Sp0
263	Neu5Aca2-3Galb1-4Glcb-Sp0
264	Neu5Aca2-3Galb1-4Glcb-Sp8
265	Neu5Aca2-6GalNAca-Sp8
266	Neu5Aca2-6GalNAcb1-4GlcNAcb-Sp0
267	Neu5Aca2-6Galb1-4(6S)GlcNAcb-Sp8
268	Neu5Aca2-6Galb1-4GlcNAcb-Sp0
269	Neu5Aca2-6Galb1-4GlcNAcb-Sp8
270	Neu5Aca2-6Galb1-4GlcNAcb1-3Galb1-4(Fuca1-3)GlcNAcb1-3Galb1-4(Fuca1-3)GlcNAcb-Sp0
271	Neu5Aca2-6Galb1-4GlcNAcb1-3Galb1-4GlcNAcb-Sp0
272	Neu5Aca2-6Galb1-4Glcb-Sp0
273	Neu5Aca2-6Galb1-4Glcb-Sp8
274	Neu5Aca2-6Galb-Sp8
275	Neu5Aca2-8Neu5Aca-Sp8
276	Neu5Aca2-8Neu5Aca2-3Galb1-4Glcb-Sp0
277	Galb1-3(Fuca1-4)GlcNAcb1-3Galb1-3(Fuca1-4)GlcNAcb-Sp0
278	Neu5Acb2-6GalNAca-Sp8
279	Neu5Acb2-6Galb1-4GlcNAcb-Sp8
280	Neu5Gca2-3Galb1-3(Fuca1-4)GlcNAcb-Sp0
281	Neu5Gca2-3Galb1-3GlcNAcb-Sp0
282	Neu5Gca2-3Galb1-4(Fuca1-3)GlcNAcb-Sp0
283	Neu5Gca2-3Galb1-4GlcNAcb-Sp0
284	Neu5Gca2-3Galb1-4Glcb-Sp0
285	Neu5Gca2-6GalNAca-Sp0
286	Neu5Gca2-6Galb1-4GlcNAcb-Sp0

287	Neu5Gca-Sp8
288	Neu5Aca2-3Galb1-4GlcNAcb1-6(Galb1-3)GalNAca-Sp14
289	Galb1-3GlcNAcb1-3Galb1-3GlcNAcb-Sp0
290	Galb1-4(Fuca1-3)(6S)GlcNAcb-Sp0
291	Galb1-4(Fuca1-3)(6S)Glcb-Sp0
292	Galb1-4(Fuca1-3)GlcNAcb1-3Galb1-3(Fuca1-4)GlcNAcb-Sp0
293	Galb1-4GlcNAcb1-3Galb1-3GlcNAcb-Sp0
294	Neu5Aca2-3Galb1-3GlcNAcb1-3Galb1-3GlcNAcb-Sp0
295	Neu5Aca2-3Galb1-4GlcNAcb1-3Galb1-3GlcNAcb-Sp0
296	4S(3S)Galb1-4GlcNAcb-Sp0
297	(6S)Galb1-4(6S)GlcNAcb-Sp0
298	(6P)Glcb-Sp10
299	Neu5Aca2-3Galb1-4(Fuca1-3)GlcNAcb1-6(Galb1-3)GalNAca-Sp14
300	Galb1-3Galb1-4GlcNAcb-Sp8
301	Neu5Aca2-6Galb1-4GlcNAcb1-2Mana1-6(Galb1-4GlcNAcb1-2Mana1-3)Manb1-4GlcNAcb1-4GlcNAcb-Sp12
302	Galb1-4GlcNAcb1-6(Galb1-4GlcNAcb1-3)Galb1-4GlcNAc-Sp0
303	GlcNAcb1-6(Galb1-4GlcNAcb1-3)Galb1-4GlcNAc-Sp0
304	Galb1-4GlcNAca1-6Galb1-4GlcNAcb-Sp0
305	Galb1-4GlcNAcb1-6Galb1-4GlcNAcb-Sp0
306	GalNAcb1-3Galb-Sp8
307	GlcAb1-3GlcNAcb-Sp8
308	Neu5Aca2-6Galb1-4GlcNAcb1-2Mana1-6(GlcNAcb1-2Mana1-3)Manb1-4GlcNAcb1-4GlcNAcb-Sp12
309	GlcNAcb1-3Man-Sp10
310	GlcNAcb1-4GlcNAcb-Sp10
311	GlcNAcb1-4GlcNAcb-Sp12
312	MurNAcb1-4GlcNAcb-Sp10
313	Mana1-6Manb-Sp10
314	Mana1-6(Mana1-3)Mana1-6(Mana1-3)Manb-Sp10
315	Mana1-2Mana1-6(Mana1-3)Mana1-6(Mana1-2Mana1-2Mana1-3)Mana-Sp9
316	Mana1-2Mana1-6(Mana1-2Mana1-3)Mana1-6(Mana1-2Mana1-2Mana1-3)Mana-Sp9
317	Neu5Aca2-3Galb1-4GlcNAcb1-6(Neu5Aca2-3Galb1-3)GalNAca-Sp14
318	Neu5Aca2-6Galb1-4GlcNAcb1-2Mana1-6(Neu5Aca2-3Galb1-4GlcNAcb1-2Mana1-3)Manb1-4GlcNAcb1-4GlcNAcb-Sp12
319	Galb1-4GlcNAcb1-2Mana1-6(Neu5Aca2-6Galb1-4GlcNAcb1-2Mana1-3)Manb1-4GlcNAcb1-4GlcNAcb-Sp12
320	GlcNAcb1-2Mana1-6(Neu5Aca2-6Galb1-4GlcNAcb1-2Mana1-3)Manb1-4GlcNAcb1-4GlcNAcb-Sp12
321	Neu5Aca2-8Neu5Acb-Sp17
322	Neu5Aca2-8Neu5Aca2-8Neu5Acb-Sp8
323	Neu5Gcb2-6Galb1-4GlcNAc-Sp8
324	Galb1-3GlcNAcb1-2Mana1-6(Galb1-3GlcNAcb1-2Mana1-3)Manb1-4GlcNAcb1-4GlcNAcb-Sp19
325	Neu5Aca2-3Galb1-4GlcNAcb1-2Mana1-6(Neu5Aca2-3Galb1-4GlcNAcb1-2Mana1-3)Manb1-4GlcNAcb1-4GlcNAcb-Sp12
326	Neu5Aca2-3Galb1-4GlcNAcb1-2Mana1-6(Neu5Aca2-6Galb1-4GlcNAcb1-2Mana1-3)Manb1-4GlcNAcb1-4GlcNAcb-Sp12
327	Galb1-4(Fuca1-3)GlcNAcb1-2Mana1-6(Galb1-4(Fuca1-3)GlcNAcb1-2Mana1-3)Manb1-4GlcNAcb1-4GlcNAcb-Sp20

328	Neu5,9Ac2a2-3Galb1-4GlcNAcb-Sp0
329	Neu5,9Ac2a2-3Galb1-3GlcNAcb-Sp0
330	Neu5Aca2-6Galb1-4GlcNAcb1-3Galb1-3GlcNAcb-Sp0
331	Neu5Aca2-3Galb1-3(Fuca1-4)GlcNAcb1-3Galb1-3(Fuca1-4)GlcNAcb-Sp0
332	Neu5Aca2-6Galb1-4GlcNAcb1-3Galb1-4GlcNAcb1-3Galb1-4GlcNAcb-Sp0
333	Gala1-4Galb1-4GlcNAcb1-3Galb1-4Glcb-Sp0
334	GalNAcb1-3Gala1-4Galb1-4GlcNAcb1-3Galb1-4Glcb-Sp0
335	GalNAca1-3(Fuca1-2)Galb1-4GlcNAcb1-3Galb1-4GlcNAcb-Sp0
336	GalNAca1-3(Fuca1-2)Galb1-4GlcNAcb1-3Galb1-4GlcNAcb1-3Galb1-4GlcNAcb-Sp0
337	Neu5Aca2-3Galb1-4(Fuca1-3)GlcNAcb1-6(Neu5Aca2-3Galb1-3)GalNAc-Sp14
338	GlcNAca1-4Galb1-4GlcNAcb1-3Galb1-4GlcNAcb1-3Galb1-4GlcNAcb-Sp0
339	GlcNAca1-4Galb1-4GlcNAcb-Sp0
340	GlcNAca1-4Galb1-3GlcNAcb-Sp0
341	GlcNAca1-4Galb1-4GlcNAcb1-3Galb1-4Glcb-Sp0
342	GlcNAca1-4Galb1-4GlcNAcb1-3Galb1-4(Fuca1-3)GlcNAcb1-3Galb1-4(Fuca1-3)GlcNAcb-Sp0
343	GlcNAca1-4Galb1-4GlcNAcb1-3Galb1-4GlcNAcb-Sp0
344	GlcNAca1-4Galb1-3GalNAc-Sp14
345	Neu5Aca2-6Galb1-4GlcNAcb1-2Mana1-6(Mana1-3)Manb1-4GlcNAcb1-4GlcNAc-Sp12
346	Mana1-6(Neu5Aca2-6Galb1-4GlcNAcb1-2Mana1-3)Manb1-4GlcNAcb1-4GlcNAc-Sp12
347	Neu5Aca2-6Galb1-4GlcNAcb1-2Mana1-6Manb1-4GlcNAcb1-4GlcNAc-Sp12
348	Neu5Aca2-6Galb1-4GlcNAcb1-2Mana1-3Manb1-4GlcNAcb1-4GlcNAc-Sp12
349	Galb1-4GlcNAcb1-2Mana1-3Manb1-4GlcNAcb1-4GlcNAc-Sp12
350	Galb1-4GlcNAcb1-2Mana1-6Manb1-4GlcNAcb1-4GlcNAc-Sp12
351	Mana1-6(Galb1-4GlcNAcb1-2Mana1-3)Manb1-4GlcNAcb1-4GlcNAcb-Sp12
352	GlcNAcb1-2Mana1-6(GlcNAcb1-2Mana1-3)Manb1-4GlcNAcb1-4(Fuca1-6)GlcNAcb-Sp22
353	Galb1-4GlcNAcb1-2Mana1-6(Galb1-4GlcNAcb1-2Mana1-3)Manb1-4GlcNAcb1-4(Fuca1-6)GlcNAcb-Sp22
354	Galb1-3GlcNAcb1-2Mana1-6(Galb1-3GlcNAcb1-2Mana1-3)Manb1-4GlcNAcb1-4(Fuca1-6)GlcNAcb-Sp22
355	(6S)GlcNAcb1-3Galb1-4GlcNAcb-Sp0
356	KDNa2-3Galb1-4(Fuca1-3)GlcNAc-Sp0
357	KDNa2-6Galb1-4GlcNAc-Sp0
358	KDNa2-3Galb1-4Glc-Sp0
359	KDNa2-3Galb1-3GalNAca-Sp14
360	Fuca1-2Galb1-3GlcNAcb1-2Mana1-6(Fuca1-2Galb1-3GlcNAcb1-2Mana1-3)Manb1-4GlcNAcb1-4GlcNAcb-Sp20
361	Fuca1-2Galb1-4GlcNAcb1-2Mana1-6(Fuca1-2Galb1-4GlcNAcb1-2Mana1-3)Manb1-4GlcNAcb1-4GlcNAcb-Sp20
362	Fuca1-2Galb1-4(Fuca1-3)GlcNAcb1-2Mana1-6(Fuca1-2Galb1-4(Fuca1-3)GlcNAcb1-2Mana1-3)Manb1-4GlcNAcb1-4GlcNAb-Sp20
363	Gala1-3Galb1-4GlcNAcb1-2Mana1-6(Gala1-3Galb1-4GlcNAcb1-2Mana1-3)Manb1-4GlcNAcb1-4GlcNAcb-Sp20
364	Galb1-4GlcNAcb1-2Mana1-6(Mana1-3)Manb1-4GlcNAcb1-4GlcNAcb-Sp12
365	Fuca1-4(Galb1-3)GlcNAcb1-2Mana1-6(Fuca1-4(Galb1-3)GlcNAcb1-2Mana1-3)Manb1-4GlcNAcb1-4(Fuca1-6)GlcNAcb-Sp22
366	Neu5Aca2-6GlcNAcb1-4GlcNAc-Sp21
367	Neu5Aca2-6GlcNAcb1-4GlcNAcb1-4GlcNAc-Sp21
368	Galb1-4(Fuca1-3)GlcNAcb1-6(Fuca1-2Galb1-4GlcNAcb1-3)Galb1-4Glc-Sp21

369	Galb1-4GlcNAcb1-2Mana1-6(Galb1-4GlcNAcb1-4(Galb1-4GlcNAcb1-2)Mana1-3)Manb1-4GlcNAcb1-4GlcNAc-Sp21
370	GalNAca1-3(Fuca1-2)Galb1-4GlcNAcb1-2Mana1-6(GalNAca1-3(Fuca1-2)Galb1-4GlcNAcb1-2Mana1-3)Manb1-4GlcNAcb1-4GlcNAcb-Sp20
371	Gala1-3(Fuca1-2)Galb1-4GlcNAcb1-2Mana1-6(Gala1-3(Fuca1-2)Galb1-4GlcNAcb1-2Mana1-3)Manb1-4GlcNAcb1-4GlcNAcb-Sp20
372	Gala1-3Galb1-4(Fuca1-3)GlcNAcb1-2Mana1-6(Gala1-3Galb1-4(Fuca1-3)GlcNAcb1-2Mana1-3)Manb1-4GlcNAcb1-4GlcNAcb-Sp20
373	GalNAca1-3(Fuca1-2)Galb1-3GlcNAcb1-2Mana1-6(GalNAca1-3(Fuca1-2)Galb1-3GlcNAcb1-2Mana1-3)Manb1-4GlcNAcb1-4GlcNAcb-Sp20
374	Gala1-3(Fuca1-2)Galb1-3GlcNAcb1-2Mana1-6(Gala1-3(Fuca1-2)Galb1-3GlcNAcb1-2Mana1-3)Manb1-4GlcNAcb1-4GlcNAcb-Sp20
375	Fuca1-4(Fuca1-2Galb1-3)GlcNAcb1-2Mana1-3(Fuca1-4(Fuca1-2Galb1-3)GlcNAcb1-2Mana1-3)Manb1-4GlcNAcb1-4GlcNAcb-Sp19
376	Neu5Aca2-3Galb1-4GlcNAcb1-3GalNAc-Sp14
377	Neu5Aca2-6Galb1-4GlcNAcb1-3GalNAc-Sp14
378	Neu5Aca2-3Galb1-4(Fuca1-3)GlcNAcb1-3GalNAca-Sp14
379	GalNAcb1-4GlcNAcb1-2Mana1-6(GalNAcb1-4GlcNAcb1-2Mana1-3)Manb1-4GlcNAcb1-4GlcNAc-Sp12
380	Galb1-3GalNAca1-3(Fuca1-2)Galb1-4Glc-Sp0
381	Galb1-3GalNAca1-3(Fuca1-2)Galb1-4GlcNAc-Sp0
382	Galb1-3GlcNAcb1-3Galb1-4GlcNAcb1-6(Galb1-3GlcNAcb1-3)Galb1-4Glcb-Sp0
383	Galb1-4(Fuca1-3)GlcNAcb1-6(Galb1-3GlcNAcb1-3)Galb1-4Glc-Sp21
384	Galb1-4GlcNAcb1-6(Fuca1-4(Fuca1-2Galb1-3)GlcNAcb1-3)Galb1-4Glc-Sp21
385	Galb1-4(Fuca1-3)GlcNAcb1-6(Fuca1-4(Fuca1-2Galb1-3)GlcNAcb1-3)Galb1-4Glc-Sp21
386	Galb1-3GlcNAcb1-3Galb1-4(Fuca1-3)GlcNAcb1-6(Galb1-3GlcNAcb1-3)Galb1-4Glc-Sp21
387	Galb1-4GlcNAcb1-6(Galb1-4GlcNAcb1-2)Mana1-6(Galb1-4GlcNAcb1-4(Galb1-4GlcNAcb1-2)Mana1-3)Manb1-4GlcNAcb1-4GlcNAcb-Sp21
388	GlcNAcb1-2Mana1-6(GlcNAcb1-4(GlcNAcb1-2)Mana1-3)Manb1-4GlcNAcb1-4GlcNAc-Sp21
389	Fuca1-2Galb1-3GalNAca1-3(Fuca1-2)Galb1-4Glcb-Sp0
390	Fuca1-2Galb1-3GalNAca1-3(Fuca1-2)Galb1-4GlcNAcb-Sp0
391	Galb1-3GlcNAcb1-3GalNAca-Sp14
392	GalNAcb1-4(Neu5Aca2-3)Galb1-4GlcNAcb1-3GalNAca-Sp14
393	GalNAca1-3(Fuca1-2)Galb1-3GalNAca1-3(Fuca1-2)Galb1-4GlcNAcb-Sp0
394	Gala1-3Galb1-3GlcNAcb1-2Mana1-6(Gala1-3Galb1-3GlcNAcb1-2Mana1-3)Manb1-4GlcNAcb1-4GlcNAc-Sp19
395	Gala1-3Galb1-3(Fuca1-4)GlcNAcb1-2Mana1-6(Gala1-3Galb1-3(Fuca1-4)GlcNAcb1-2Mana1-3)Manb1-4GlcNAcb1-4GlcNAc-Sp19
396	Neu5Aca2-3Galb1-3GlcNAcb1-2Mana1-6(Neu5Aca2-3Galb1-3GlcNAcb1-2Mana1-3)Manb1-4GlcNAcb1-4GlcNAc-Sp19
397	GlcNAcb1-2Mana1-6(Galb1-4GlcNAcb1-2Mana1-3)Manb1-4GlcNAcb1-4GlcNAc-Sp12
398	Galb1-4GlcNAcb1-2Mana1-6(GlcNAcb1-2Mana1-3)Manb1-4GlcNAcb1-4GlcNAc-Sp12
399	Neu5Aca2-3Galb1-3GlcNAcb1-3GalNAca-Sp14
400	Fuca1-2Galb1-4GlcNAcb1-3GalNAca-Sp14
401	Galb1-4(Fuca1-3)GlcNAcb1-3GalNAca-Sp14
402	GalNAca1-3GalNAcb1-3Gala1-4Galb1-4GlcNAcb-Sp0
403	Gala1-4Galb1-3GlcNAcb1-2Mana1-6(Gala1-4Galb1-3GlcNAcb1-2Mana1-3)Manb1-4GlcNAcb1-4GlcNAcb-Sp19
404	Gala1-4Galb1-4GlcNAcb1-2Mana1-6(Gala1-4Galb1-4GlcNAcb1-2Mana1-3)Manb1-

	4GlcNAcb1-4GlcNAcb-Sp24
405	Gala1-3Galb1-4GlcNAcb1-3GalNAca-Sp14
406	Galb1-3GlcNAcb1-6Galb1-4GlcNAcb-Sp0
407	Galb1-3GlcNAca1-6Galb1-4GlcNAcb-Sp0
408	GalNAcb1-3Gala1-6Galb1-4Glcb-Sp8
409	Gala1-3(Fuca1-2)Galb1-4(Fuca1-3)Glcb-Sp21
410	Galb1-4GlcNAcb1-6(Neu5Aca2-6Galb1-3GlcNAcb1-3)Galb1-4Glc-Sp21
411	Galb1-3GalNAcb1-4(Neu5Aca2-8Neu5Aca2-3)Galb1-4Glcb-Sp0
412	Neu5Aca2-3Galb1-3GalNAcb1-4(Neu5Aca2-8Neu5Aca2-3)Galb1-4Glcb-Sp0
413	Gala1-3(Fuca1-2)Galb1-4GlcNAcb1-3GalNAca-Sp14
414	GalNAca1-3(Fuca1-2)Galb1-4GlcNAcb1-3GalNAca-Sp14
415	GalNAca1-3GalNAcb1-3Gala1-4Galb1-4Glcb-Sp0
416	Fuca1-2Galb1-4(Fuca1-3)GlcNAcb1-3GalNAca-Sp14
417	Gala1-3(Fuca1-2)Galb1-4(Fuca1-3)GlcNAcb1-3GalNAc-Sp14
418	GalNAca1-3(Fuca1-2)Galb1-4(Fuca1-3)GlcNAcb1-3GalNAc-Sp14
419	Galb1-4(Fuca1-3)GlcNAcb1-2Mana1-6(Galb1-4(Fuca1-3)GlcNAcb1-2Mana1-3)Manb1-4GlcNAcb1-4(Fuca1-6)GlcNAcb-Sp22
420	Fuca1-2Galb1-4GlcNAcb1-2Mana1-6(Fuca1-2Galb1-4GlcNAcb1-2Mana1-3)Manb1-4GlcNAcb1-4(Fuca1-6)GlcNAcb-Sp22
421	GlcNAcb1-2(GlcNAcb1-6)Mana1-6(GlcNAcb1-2Mana1-3)Manb1-4GlcNAcb1-4GlcNAcb-Sp19
422	Fuca1-2Galb1-3GlcNAcb1-3GalNAc-Sp14
423	Gala1-3(Fuca1-2)Galb1-3GlcNAcb1-3GalNAc-Sp14
424	GalNAca1-3(Fuca1-2)Galb1-3GlcNAcb1-3GalNAc-Sp14
425	Gala1-3Galb1-3GlcNAcb1-3GalNAc-Sp14
426	Fuca1-2Galb1-3GlcNAcb1-2Mana1-6(Fuca1-2Galb1-3GlcNAcb1-2Mana1-3)Manb1-4GlcNAcb1-4(Fuca1-6)GlcNAcb-Sp22
427	Gala1-3(Fuca1-2)Galb1-4GlcNAcb1-2Mana1-6(Gala1-3(Fuca1-2)Galb1-4GlcNAcb1-2Mana1-3)Manb1-4GlcNAcb1-4(Fuca1-6)GlcNAcb-Sp22
428	Galb1-3GlcNAcb1-6(Galb1-3GlcNAcb1-2)Mana1-6(Galb1-3GlcNAcb1-2Mana1-3)Manb1-4GlcNAcb1-4GlcNAcb-Sp19
429	Galb1-4GlcNAcb1-6(Fuca1-2Galb1-3GlcNAcb1-3)Galb1-4Glc-Sp21
430	Fuca1-3GlcNAcb1-6(Galb1-4GlcNAcb1-3)Galb1-4Glc-Sp21
431	GlcNAcb1-2Mana1-6(GlcNAcb1-4)(GlcNAcb1-2Mana1-3)Manb1-4GlcNAcb1-4GlcNAc-Sp21
432	GlcNAcb1-2Mana1-6(GlcNAcb1-4)(GlcNAcb1-4(GlcNAcb1-2)Mana1-3)Manb1-4GlcNAcb1-4GlcNAc-Sp21
433	GlcNAcb1-6(GlcNAcb1-2)Mana1-6(GlcNAcb1-4)(GlcNAcb1-2Mana1-3)Manb1-4GlcNAcb1-4GlcNAc-Sp21
434	GlcNAcb1-6(GlcNAcb1-2)Mana1-6(GlcNAcb1-4)(GlcNAcb1-4(GlcNAcb1-2)Mana1-3)Manb1-4GlcNAcb1-4GlcNAc-Sp21
435	Galb1-4GlcNAcb1-2Mana1-6(GlcNAcb1-4)(Galb1-4GlcNAcb1-2Mana1-3)Manb1-4GlcNAcb1-4GlcNAc-Sp21
436	Galb1-4GlcNAcb1-2Mana1-6(GlcNAcb1-4)(Galb1-4GlcNAcb1-4(Galb1-4GlcNAcb1-2)Mana1-3)Manb1-4GlcNAcb1-4GlcNAc-Sp21
437	Galb1-4GlcNAcb1-6(Galb1-4GlcNAcb1-2)Mana1-6(GlcNAcb1-4)(Galb1-4GlcNAcb1-2Mana1-3)Manb1-4GlcNAcb1-4GlcNAc-Sp21
438	Galb1-4GlcNAcb1-6(Galb1-4GlcNAcb1-2)Mana1-6(GlcNAcb1-4)(Galb1-4GlcNAcb1-4(Galb1-4GlcNAcb1-2)Mana1-3)Manb1-4GlcNAcb1-4GlcNAc-Sp21
439	Galb1-4Galb-Sp10

440	Galb1-6Galb-Sp10
441	Neu5Aca2-3Galb1-4GlcNAcb1-3Galb-Sp8
442	GalNAcb1-6GalNAcb-Sp8
443	(6S)Galb1-3GlcNAcb-Sp0
444	(6S)Galb1-3(6S)GlcNAc-Sp0
445	Fuca1-2Galb1-4 GlcNAcb1-2Mana1-6(Fuca1-2Galb1-4GlcNAcb1-2(Fuca1-2Galb1-4GlcNAcb1-4)Mana1-3)Manb1-4GlcNAcb1-4GlcNAcb-Sp12
446	Fuca1-2Galb1-4(Fuca1-3)GlcNAcb1-2Mana1-6(Fuca1-2Galb1-4(Fuca1-3)GlcNAcb1-4(Fuca1-2Galb1-4(Fuca1-3)GlcNAcb1-2)Mana1-3)Manb1-4GlcNAcb1-4GlcNAcb-Sp12
447	Galb1-4(Fuca1-3)GlcNAcb1-6GalNAc-Sp14
448	Galb1-4GlcNAcb1-2Mana-Sp0
449	Fuca1-2Galb1-4GlcNAcb1-6(Fuca1-2Galb1-4GlcNAcb1-3)GalNAc-Sp14
450	Gala1-3(Fuca1-2)Galb1-4GlcNAcb1-6(Gala1-3(Fuca1-2)Galb1-4GlcNAcb1-3)GalNAc-Sp14
451	GalNAca1-3(Fuca1-2)Galb1-4GlcNAcb1-6(GalNAca1-3(Fuca1-2)Galb1-4GlcNAcb1-3)GalNAc-Sp14
452	Neu5Aca2-8Neu5Aca2-3Galb1-3GalNAcb1-4(Neu5Aca2-8Neu5Aca2-3)Galb1-4Glcb-Sp0
453	GalNAcb1-4Galb1-4Glcb-Sp0
454	GalNAca1-3(Fuca1-2)Galb1-4GlcNAcb1-2Mana1-6(GalNAca1-3(Fuca1-2)Galb1-4GlcNAcb1-2Mana1-3)Manb1-4GlcNAcb1-4(Fuca1-6)GlcNAcb-Sp22
455	Gala1-3(Fuca1-2)Galb1-3GlcNAcb1-2Mana1-6(Gala1-3(Fuca1-2)Galb1-3GlcNAcb1-2Mana1-3)Manb1-4GlcNAcb1-4(Fuca1-6)GlcNAcb-Sp22
456	Neu5Aca2-6Galb1-4GlcNAcb1-6(Fuca1-2Galb1-3GlcNAcb1-3)Galb1-4Glc-Sp21
457	GalNAca1-3(Fuca1-2)Galb1-3GlcNAcb1-2Mana1-6(GalNAca1-3(Fuca1-2)Galb1-3GlcNAcb1-2Mana1-3)Manb1-4GlcNAcb1-4(Fuca1-6)GlcNAcb-Sp22
458	Galb1-4GlcNAcb1-6(Galb1-4GlcNAcb1-2)Mana1-6(Galb1-4GlcNAcb1-2Mana1-3)Manb1-4GlcNAcb1-4GlcNAcb-Sp19
459	Neu5Aca2-3Galb1-4GlcNAcb1-2Mana1-6(GlcNAcb1-4)(Neu5Aca2-3Galb1-4GlcNAcb1-2Mana1-3)Manb1-4GlcNAcb1-4GlcNAcb-Sp21
460	Neu5Aca2-3Galb1-4GlcNAcb1-4Mana1-6(GlcNAcb1-4)(Neu5Aca2-3Galb1-4GlcNAcb1-4(Neu5Aca2-3Galb1-4GlcNAcb1-2)Mana1-3)Manb1-4GlcNAcb1-4GlcNAcb-Sp21
461	Neu5Aca2-3Galb1-4GlcNAcb1-6(Neu5Aca2-3Galb1-4GlcNAcb1-2)Mana1-6(GlcNAcb1-4)(Neu5Aca2-3Galb1-4GlcNAcb1-2Mana1-3)Manb1-4GlcNAcb1-4GlcNAcb-Sp21
462	Neu5Aca2-3Galb1-4GlcNAcb1-6(Neu5Aca2-3Galb1-4GlcNAcb1-2)Mana1-6(GlcNAcb1-4)(Neu5Aca2-3Galb1-4GlcNAcb1-4(Neu5Aca2-3Galb1-4GlcNAcb1-2)Mana1-3)Manb1-4GlcNAcb1-4GlcNAcb-Sp21
463	Neu5Aca2-6Galb1-4GlcNAcb1-2Mana1-6(GlcNAcb1-4)(Neu5Aca2-6Galb1-4GlcNAcb1-2Mana1-3)Manb1-4GlcNAcb1-4GlcNAcb-Sp21
464	Neu5Aca2-6Galb1-4GlcNAcb1-4Mana1-6(GlcNAcb1-4)(Neu5Aca2-6Galb1-4GlcNAcb1-4(Neu5Aca2-6Galb1-4GlcNAcb1-2)Mana1-3)Manb1-4GlcNAcb1-4GlcNAcb-Sp21
465	Neu5Aca2-6Galb1-4GlcNAcb1-6(Neu5Aca2-6Galb1-4GlcNAcb1-2)Mana1-6(GlcNAcb1-4)(Neu5Aca2-6Galb1-4GlcNAcb1-2Mana1-3)Manb1-4GlcNAcb1-4GlcNAcb-Sp21
466	Neu5Aca2-6Galb1-4GlcNAcb1-6(Neu5Aca2-6Galb1-4GlcNAcb1-2)Mana1-6(GlcNAcb1-4)(Neu5Aca2-6Galb1-4GlcNAcb1-4(Neu5Aca2-6Galb1-4GlcNAcb1-2)Mana1-3)Manb1-4GlcNAcb1-4GlcNAcb-Sp21
467	Gala1-3(Fuca1-2)Galb1-3GalNAca-Sp8
468	Gala1-3(Fuca1-2)Galb1-3GalNAcb-Sp8
469	Glca1-6Glca1-6Glca1-6Glcb-Sp10
470	Glca1-4Glca1-4Glca1-4Glcb-Sp10
471	Neu5Aca2-3Galb1-4GlcNAcb1-6(Neu5Aca2-3Galb1-4GlcNAcb1-3)GalNAca-Sp14

472	Fuca1-2Galb1-4(Fuca1-3)GlcNAcb1-2Mana1-6(Fuca1-2Galb1-4(Fuca1-3)GlcNAcb1-2Mana1-3)Manb1-4GlcNAcb1-4(Fuca1-6)GlcNAcb-Sp24
473	Fuca1-2Galb1-3(Fuca1-4)GlcNAcb1-2Mana1-6(Fuca1-2Galb1-3(Fuca1-4)GlcNAcb1-2Mana1-3)Manb1-4GlcNAcb1-4(Fuca1-6)GlcNAcb1-4(Fuca1-6)GlcNAcb-Sp19
474	Neu5Aca2-3Galb1-3GlcNAcb1-6(Neu5Aca2-3Galb1-3GlcNAcb1-2)Mana1-6(Neu5Aca2-3Galb1-3GlcNAcb1-2Mana1-3)Manb1-4GlcNAcb1-4GlcNAcb-Sp19
475	GlcNAcb1-6(GlcNAcb1-2)Mana1-6(GlcNAcb1-2Mana1-3)Manb1-4GlcNAcb1-4(Fuca1-6)GlcNAcb-Sp24
476	Galb1-3GlcNAcb1-2Mana1-6(GlcNAcb1-4)(Galb1-3GlcNAcb1-2Mana1-3)Manb1-4GlcNAcb1-4GlcNAcb-Sp21
477	Neu5Aca2-6Galb1-4GlcNAcb1-6(Galb1-3GlcNAcb1-3)Galb1-4Glcb-Sp21
478	Neu5Aca2-3Galb1-4GlcNAcb1-2Mana-Sp0
479	Neu5Aca2-3Galb1-4GlcNAcb1-6GalNAca-Sp14
480	Neu5Aca2-6Galb1-4GlcNAcb1-6GalNAca-Sp14
481	Neu5Aca2-6Galb1-4 GlcNAcb1-6(Neu5Aca2-6Galb1-4GlcNAcb1-3)GalNAca-Sp14
482	Neu5Aca2-6Galb1-4GlcNAcb1-2Mana1-6(Neu5Aca2-6Galb1-4GlcNAcb1-2Mana1-3)Manb1-4GlcNAcb1-4(Fuca1-6)GlcNAcb-Sp24
483	Neu5Aca2-3Galb1-4GlcNAcb1-2Mana1-6(Neu5Aca2-3Galb1-4GlcNAcb1-2Mana1-3)Manb1-4GlcNAcb1-4(Fuca1-6)GlcNAcb-Sp24
484	Mana1-6(Mana1-3)Manb1-4GlcNAcb1-4(Fuca1-6)GlcNAcb-Sp19
485	Galb1-4GlcNAcb1-6(Galb1-4GlcNAcb1-2)Mana1-6(Galb1-4GlcNAcb1-2Mana1-3)Manb1-4GlcNAcb1-4(Fuca1-6)GlcNAcb-Sp24
486	Neu5Aca2-3Galb1-3GlcNAcb1-2Mana1-6(GlcNAcb1-4)(Neu5Aca2-3Galb1-3GlcNAcb1-2Mana1-3)Manb1-4GlcNAcb1-4GlcNAc-Sp21
487	Neu5Aca2-6Galb1-4GlcNAcb1-6(Fuca1-2Galb1-4(Fuca1-3)GlcNAcb1-3)Galb1-4Glc-Sp21
488	Galb1-3GlcNAcb1-6GalNAca-Sp14
489	Gala1-3Galb1-3GlcNAcb1-6GalNAca-Sp14
490	Galb1-3(Fuca1-4)GlcNAcb1-6GalNAca-Sp14
491	Neu5Aca2-3Galb1-3GlcNAcb1-6GalNAca-Sp14
492	(3S)Galb1-3(Fuca1-4)GlcNAcb-Sp0
493	Galb1-4(Fuca1-3)GlcNAcb1-6(Neu5Aca2-6(Neu5Aca2-3Galb1-3)GlcNAcb1-3)Galb1-4Glc-Sp21
494	Fuca1-2Galb1-4GlcNAcb1-6GalNAca-Sp14
495	Gala1-3Galb1-4GlcNAcb1-6GalNAca-Sp14
496	Galb1-4(Fuca1-3)GlcNAcb1-2Mana-Sp0
497	Fuca1-2(6S)Galb1-3GlcNAcb-Sp0
498	Gala1-3(Fuca1-2)Galb1-4GlcNAcb1-6GalNAca-Sp14
499	Fuca1-2Galb1-4GlcNAcb1-2Mana-Sp0
500	Fuca1-2Galb1-3(6S)GlcNAcb-Sp0
501	Fuca1-2(6S)Galb1-3(6S)GlcNAcb-Sp0
502	Neu5Aca2-6GalNAcb1-4(6S)GlcNAcb-Sp8
503	GalNAcb1-4(Fuca1-3)(6S)GlcNAcb-Sp8
504	(3S)GalNAcb1-4(Fuca1-3)GlcNAcb-Sp8
505	Fuca1-2Galb1-3GlcNAcb1-6(Fuca1-2Galb1-3GlcNAcb1-3)GalNAca-Sp14
506	GalNAca1-3(Fuca1-2)Galb1-3GlcNAcb1-6GalNAca-Sp14
507	GlcNAcb1-6(GlcNAcb1-2)Mana1-6(GlcNAcb1-4)(GlcNAcb1-4(GlcNAcb1-2)Mana1-3)Manb1-4GlcNAcb1-4(Fuca1-6)GlcNAc-Sp21
508	Galb1-4GlcNAcb1-6(Galb1-4GlcNAcb1-2)Mana1-6(GlcNAcb1-4)Galb1-4GlcNAcb1-4(Galb1-4GlcNAcb1-2)Mana1-3)Manb1-4GlcNAcb1-4(Fuca1-6)GlcNAc-Sp21
509	Galb1-3GlcNAca1-3Galb1-4GlcNAcb-Sp8

510	Galb1-3(6S)GlcNAcb-Sp8
511	(6S)(4S)GalNAcb1-4GlcNAc-Sp8
512	(6S)GalNAcb1-4GlcNAc-Sp8
513	(3S)GalNAcb1-4(3S)GlcNAc-Sp8
514	GalNAcb1-4(6S)GlcNAc-Sp8
515	(3S)GalNAcb1-4GlcNAc-Sp8
516	(4S)GalNAcb-Sp10
517	Galb1-4(6P)GlcNAcb-Sp0
518	(6P)Galb1-4GlcNAcb-SP0
519	GalNAca1-3(Fuca1-2)Galb1-4GlcNAcb1-6GalNAc-Sp14
520	Neu5Aca2-6Galb1-4GlcNAcb1-2Man-Sp0
521	Gala1-3Galb1-4GlcNAcb1-2Mana-Sp0
522	Gala1-3(Fuca1-2)Galb1-4GlcNAcb1-2Mana-Sp0
523	GalNAca1-3(Fuca1-2)Galb1-4 GlcNAcb1-2Mana-Sp0
524	Galb1-3GlcNAcb1-2Mana-Sp0
525	Gala1-3(Fuca1-2)Galb1-3GlcNAcb1-6GalNAc-Sp14
526	Neu5Aca2-3Galb1-3GlcNAcb1-2Mana-Sp0
527	Gala1-3Galb1-3GlcNAcb1-2Mana-Sp0
528	GalNAcb1-4GlcNAcb1-2Mana-Sp0
529	Neu5Aca2-3Galb1-3GalNAcb1-4Galb1-4Glcb-Sp0
530	GlcNAcb1-2 Mana1-6(GlcNAcb1-4)(GlcNAcb1-2Mana1-3)Manb1-4GlcNAcb1-4(Fuca1-6)GlcNAc-Sp21
531	Galb1-4GlcNAcb1-2 Mana1-6(GlcNAcb1-4)(Galb1-4GlcNAcb1-2Mana1-3)Manb1-4GlcNAcb1-4(Fuca1-6)GlcNAc-Sp21
532	Galb1-4GlcNAcb1-2 Mana1-6(Galb1-4GlcNAcb1-4)(Galb1-4GlcNAcb1-2Mana1-3)Manb1-4GlcNAcb1-4(Fuca1-6)GlcNAc-Sp21
533	Fuca1-4(Galb1-3)GlcNAcb1-2 Mana-Sp0
534	Neu5Aca2-3Galb1-4(Fuca1-3)GlcNAcb1-2Mana-Sp0
535	GlcNAcb1-3Galb1-4GlcNAcb1-6(GlcNAcb1-3)Galb1-4GlcNAc-Sp0
536	GalNAca1-3(Fuca1-2)Galb1-3GalNAcb1-3Gala1-4Galb1-4Glc-Sp21
537	Gala1-3(Fuca1-2)Galb1-3GalNAcb1-3Gala1-4Galb1-4Glc-Sp21
538	Galb1-3GalNAcb1-3Gal-Sp21
539	GlcNAcb1-3Galb1-4GlcNAcb1-2Mana1-6(GlcNAcb1-3Galb1-4GlcNAcb1-2Mana1-3)Manb1-4GlcNAcb1-4GlcNAcb-Sp12
540	GlcNAcb1-3Galb1-4GlcNAcb1-2Mana1-6(GlcNAcb1-3Galb1-4GlcNAcb1-2Mana1-3)Manb1-4GlcNAcb1-4GlcNAcb-Sp25
541	Galb1-4GlcNAcb1-3Galb1-4GlcNAcb1-2Mana1-6(Galb1-4GlcNAcb1-3Galb1-4GlcNAcb1-2Mana1-3)Manb1-4GlcNAcb1-4GlcNAcb-Sp12
542	Galb1-4GlcNAcb1-3Galb1-4GlcNAcb1-2Mana1-6(Galb1-4GlcNAcb1-3Galb1-4GlcNAcb1-2Mana1-3)Manb1-4GlcNAcb1-4GlcNAcb-Sp24
543	Neu5Gca2-3Galb1-4GlcNAcb1-3Galb1-4GlcNAcb1-2Mana1-6(Neu5Gca2-3Galb1-4GlcNAcb1-3Galb1-4GlcNAcb1-2Mana1-3)Manb1-4GlcNAcb1-4GlcNAcb-Sp24
544	Fuca1-2Galb1-4GlcNAcb1-3Galb1-4GlcNAcb1-2Mana1-6(Fuca1-2Galb1-4GlcNAcb1-3Galb1-4GlcNAcb1-2Mana1-3)Manb1-4GlcNAcb1-4GlcNAcb-Sp24
545	GlcNAcb1-3Galb1-4GlcNAcb1-3Galb1-4GlcNAcb1-2Mana1-6(GlcNAcb1-3Galb1-4GlcNAcb1-3Galb1-4GlcNAcb1-2Mana1-3)Manb1-4GlcNAcb1-4GlcNAcb-Sp12
546	GlcNAcb1-3Galb1-4GlcNAcb1-3Galb1-4GlcNAcb1-2Mana1-6(GlcNAcb1-3Galb1-4GlcNAcb1-3Galb1-4GlcNAcb1-2Mana1-3)Manb1-4GlcNAcb1-4GlcNAcb-Sp25
547	Galb1-4GlcNAcb1-3Galb1-4GlcNAcb1-3Galb1-4GlcNAcb1-2Mana1-6(Galb1-4GlcNAcb1-3Galb1-4GlcNAcb1-3Galb1-4GlcNAcb1-2Mana1-3)Manb1-4GlcNAcb1-4GlcNAcb-Sp12

548	Galb1-4GlcNAcb1-3Galb1-4GlcNAcb1-3Galb1-4GlcNAcb1-2Mana1-6(Galb1-4GlcNAcb1-3Galb1-4GlcNAcb1-3Galb1-4GlcNAcb1-2Mana1-3)Manb1-4GlcNAcb1-4GlcNAcb-Sp24
549	GlcNAcb1-3Galb1-4GlcNAcb1-3Galb1-4GlcNAcb1-3Galb1-4GlcNAcb1-2Mana1-6(GlcNAcb1-3Galb1-4GlcNAcb1-3Galb1-4GlcNAcb1-3Galb1-4GlcNAcb1-2Mana1-3)Manb1-4GlcNAcb1-4GlcNAcb-Sp25
550	Galb1-4GlcNAcb1-3Galb1-4GlcNAcb1-3Galb1-4GlcNAcb1-3Galb1-4GlcNAcb1-2Mana1-6(Galb1-4GlcNAcb1-3Galb1-4GlcNAcb1-3Galb1-4GlcNAcb1-3Galb1-4GlcNAcb1-2Mana1-3)Manb1-4GlcNAcb1-4GlcNAcb-Sp25
551	Galb1-3GlcNAcb1-3Galb1-4GlcNAcb1-2Mana1-6(Galb1-3GlcNAcb1-3Galb1-4GlcNAcb1-2Mana1-3)Manb1-4GlcNAcb1-4GlcNAc-Sp25
552	Neu5Gca2-8Neu5Gca2-3Galb1-4GlcNAc-Sp0
553	Neu5Aca2-8Neu5Gca2-3Galb1-4GlcNAc-Sp0
554	Neu5Gca2-8Neu5Aca2-3Galb1-4GlcNAc-Sp0
555	Neu5Gca2-8Neu5Gca2-3Galb1-4GlcNAcb1-3Galb1-4GlcNAc-Sp0
556	Neu5Gca2-8Neu5Gca2-6Galb1-4GlcNAc-Sp0
557	Neu5Aca2-8Neu5Aca2-3Galb1-4GlcNAc-Sp0
558	GlcNAcb1-3Galb1-4GlcNAcb1-6(GlcNAcb1-3Galb1-4GlcNAcb1-2)Mana1-6(GlcNAcb1-3Galb1-4GlcNAcb1-2Man a1-3)Manb1-4GlcNAcb1-4GlcNAc-Sp24
559	Galb1-4GlcNAcb1-3Galb1-4GlcNAcb1-6(Galb1-4GlcNAcb1-3Galb1-4GlcNAcb1-2)Mana1-6(Galb1-4GlcNAcb1-3Galb1-4GlcNAcb1-2Mana1-3)Mana1-4GlcNAcb1-4GlcNAc-Sp24
560	Gala1-3Galb1-4GlcNAcb1-2Mana1-6(Gala1-3Galb1-4GlcNAcb1-2Mana1-3)Manb1-4GlcNAcb1-4GlcNAc-Sp24
561	GlcNAcb1-3Galb1-4GlcNAcb1-6(GlcNAcb1-3Galb1-3)GalNAca-Sp14
562	GalNAcb1-3GlcNAcb-Sp0
563	GalNAcb1-4GlcNAcb1-3GalNAcb1-4GlcNAcb-Sp0
564	GlcNAcb1-3Galb1-4GlcNAcb1-3Galb1-4GlcNAcb1-3Galb1-4GlcNAcb1-3Galb1-4GlcNAcb1-2Mana1-6(GlcNAcb1-3Galb1-4GlcNAcb1-3Galb1-4GlcNAcb1-3Galb1-4GlcNAcb1-3Galb1-4GlcNAcb1-2Mana1-3)Manb1-4GlcNAcb1-4GlcNAcb-Sp25
565	Galb1-4GlcNAcb1-3Galb1-4GlcNAcb1-3Galb1-4GlcNAcb1-3Galb1-4GlcNAcb1-3Galb1-4GlcNAcb1-2Mana1-6(Galb1-4GlcNAcb1-3Galb1-4GlcNAcb1-3Galb1-4GlcNAcb1-3Galb1-4GlcNAcb1-3Galb1-4GlcNAcb1-2Mana1-3)Manb1-4GlcNAcb1-4GlcNAcb-Sp25
566	GlcNAb1-3Galb1-3GalNAc-Sp14
567	Galb1-3GlcNAcb1-6(Galb1-3)GalNAc-Sp14
568	Galb1-4GlcNAcb1-3Galb1-4GlcNAcb1-3Galb1-4GlcNAcb1-3Galb1-4GlcNAcb1-3Galb1-4GlcNAcb1-3Galb1-4GlcNAcb1-2Mana1-6(Galb1-4GlcNAcb1-3Galb1-4GlcNAcb1-3Galb1-4GlcNAcb1-3Galb1-4GlcNAcb1-3Galb1-4GlcNAcb1-3Galb1-4GlcNAcb1-3Galb1-4GlcNAcb1-2Mana1-3)Manb1-4GlcNAcb1-4GlcNAcb-Sp25
569	(3S)GlcAb1-3Galb1-4GlcNAcb1-3Galb1-4Glc-Sp0
570	(3S)GlcAb1-3Galb1-4GlcNAcb1-2Mana-Sp0
571	Galb1-3GlcNAcb1-3Galb1-4GlcNAcb1-3Galb1-4GlcNAcb1-6(Galb1-3GlcNAcb1-3Galb1-4GlcNAcb1-3Galb1-4GlcNAb1-2)Mana1-6(Galb1-3GlcNAcb1-3Galb1-4GlcNAcb1-3Galb1-4GlcNAcb1-2Mana1-3)Manb1-4GlcNAcb1-4(Fuca1-6)GlcNAcb-Sp24
572	Galb1-3GlcNAcb1-3Galb1-4GlcNAcb1-6(Galb1-3GlcNAcb1-3Galb1-4GlcNAb1-2)Mana1-6(Galb1-3GlcNAcb1-3Galb1-4GlcNAcb1-2Mana1-3)Manb1-4GlcNAcb1-4(Fuca1-6)GlcNAcb-Sp24
573	Neu5Aca2-8Neu5Aca2-3Galb1-3GalNAcb1-4(Neu5Aca2-3)Galb1-4Glc-Sp21
574	GlcNAcb1-3Galb1-4GlcNAcb1-2Mana1-6(GlcNAcb1-3Galb1-4GlcNAcb1-2Mana1-3)Manb1-4GlcNAcb1-4(Fuca1-6)GlcNAcb-Sp24
575	Galb1-4GlcNAcb1-3Galb1-4GlcNAcb1-2Mana1-6(Galb1-4GlcNAcb1-3Galb1-4GlcNAcb1-2Mana1-3)Manb1-4GlcNAcb1-4(Fuca1-6)GlcNAcb-Sp24

576	GlcNAcb1-3Galb1-4GlcNAcb1-3Galb1-4GlcNAcb1-2Mana1-6(GlcNAcb1-3Galb1-4GlcNAcb1-3Galb1-4GlcNAcb1-2Mana1-3)Manb1-4GlcNAcb1-4(Fuca1-6)GlcNAcb-Sp24
577	Galb1-4GlcNAcb1-3Galb1-4GlcNAcb1-3Galb1-4GlcNAcb1-2Mana1-6(Galb1-4GlcNAcb1-3Galb1-4GlcNAcb1-3Galb1-4GlcNAcb1-2Mana1-3)Manb1-4GlcNAcb1-4(Fuca1-6)GlcNAcb-Sp24
578	GlcNAcb1-3Galb1-4GlcNAcb1-3Galb1-4GlcNAcb1-3Galb1-4GlcNAcb1-2Mana1-6(GlcNAcb1-3Galb1-4GlcNAcb1-3Galb1-4GlcNAcb1-3Galb1-4GlcNAcb1-2Mana1-3)Manb1-4GlcNAcb1-4(Fuca1-6)GlcNAcb-Sp24
579	Galb1-4GlcNAcb1-3Galb1-4GlcNAcb1-3Galb1-4GlcNAcb1-3Galb1-4GlcNAcb1-2Mana1-6(Galb1-4GlcNAcb1-3Galb1-4GlcNAcb1-3Galb1-4GlcNAcb1-3Galb1-4GlcNAcb1-2Mana1-3)Manb1-4GlcNAcb1-4(Fuca1-6)GlcNAcb-Sp24
580	GlcNAcb1-3Galb1-4GlcNAcb1-3Galb1-4GlcNAcb1-3Galb1-4GlcNAcb1-3Galb1-4GlcNAcb1-2Mana1-6(GlcNAcb1-3Galb1-4GlcNAcb1-3Galb1-4GlcNAcb1-3Galb1-4GlcNAcb1-3Galb1-4GlcNAcb1-2Mana1-3)Manb1-4GlcNAcb1-4(Fuca1-6)GlcNAcb-Sp19
581	Galb1-4GlcNAcb1-3Galb1-4GlcNAcb1-3Galb1-4GlcNAcb1-3Galb1-4GlcNAcb1-3Galb1-4GlcNAcb1-2Mana1-6(Galb1-4GlcNAcb1-3Galb1-4GlcNAcb1-3Galb1-4GlcNAcb1-3Galb1-4GlcNAcb1-3Galb1-4GlcNAcb1-2Mana1-3)Manb1-4GlcNAcb1-4(Fuca1-6)GlcNAcb-Sp19
582	Galb1-4GlcNAcb1-3Galb1-4GlcNAcb1-6(Galb1-4GlcNAcb1-3Galb1-4GlcNAb1-2)Mana1-6(Galb1-4GlcNAcb1-3Galb1-4GlcNAcb1-2Mana1-3)Manb1-4GlcNAcb1-4(Fuca1-6)GlcNAcb-Sp24
583	GlcNAcb1-3Galb1-4GlcNAcb1-3Galb1-4GlcNAcb1-6(GlcNAcb1-3Galb1-4GlcNAcb1-3Galb1-4GlcNAb1-2)Mana1-6(GlcNAcb1-3Galb1-4GlcNAcb1-3Galb1-4GlcNAcb1-2Mana1-3)Manb1-4GlcNAcb1-4(Fuca1-6)GlcNAcb-Sp24
584	Galb1-4GlcNAcb1-3Galb1-4GlcNAcb1-3Galb1-4GlcNAcb1-6(Galb1-4GlcNAcb1-3Galb1-4GlcNAcb1-3Galb1-4GlcNAb1-2)Mana1-6(Galb1-4GlcNAcb1-3Galb1-4GlcNAcb1-3Galb1-4GlcNAcb1-2Mana1-3)Manb1-4GlcNAcb1-4(Fuca1-6)GlcNAcb-Sp24
585	GlcNAcb1-3Galb1-4GlcNAcb1-3Galb1-4GlcNAcb1-3Galb1-4GlcNAcb1-6(GlcNAcb1-3Galb1-4GlcNAcb1-3Galb1-4GlcNAcb1-3Galb1-4GlcNAb1-2)Mana1-6(GlcNAcb1-3Galb1-4GlcNAcb1-3Galb1-4GlcNAcb1-3Galb1-4GlcNAcb1-2Mana1-3)Manb1-4GlcNAcb1-4(Fuca1-6)GlcNAcb-Sp24
586	Galb1-4GlcNAcb1-3Galb1-4GlcNAcb1-3Galb1-4GlcNAcb1-3Galb1-4GlcNAcb1-6(Galb1-4GlcNAcb1-3Galb1-4GlcNAcb1-3Galb1-4GlcNAcb1-3Galb1-4GlcNAb1-2)Mana1-6(Galb1-4GlcNAcb1-3Galb1-4GlcNAcb1-3Galb1-4GlcNAcb1-3Galb1-4GlcNAcb1-2Mana1-3)Manb1-4GlcNAcb1-4(Fuca1-6)GlcNAcb-Sp24
587	GlcNAcb1-3Galb1-4GlcNAcb1-3Galb1-4GlcNAcb1-3Galb1-4GlcNAcb1-3Galb1-4GlcNAcb1-6(GlcNAcb1-3Galb1-4GlcNAcb1-3Galb1-4GlcNAcb1-3Galb1-4GlcNAcb1-3Galb1-4GlcNAb1-2)Mana1-6(GlcNAcb1-3Galb1-4GlcNAcb1-3Galb1-4GlcNAcb1-3Galb1-4GlcNAcb1-3Galb1-4GlcNAcb1-2Mana1-3)Manb1-4GlcNAcb1-4(Fuca1-6)GlcNAcb-Sp24
588	Galb1-4GlcNAcb1-3Galb1-4GlcNAcb1-3Galb1-4GlcNAcb1-3Galb1-4GlcNAcb1-3Galb1-4GlcNAcb1-6(Galb1-4GlcNAcb1-3Galb1-4GlcNAcb1-3Galb1-4GlcNAcb1-3Galb1-4GlcNAcb1-3Galb1-4GlcNAb1-2)Mana1-6(Galb1-4GlcNAcb1-3Galb1-4GlcNAcb1-3Galb1-4GlcNAcb1-3Galb1-4GlcNAcb1-3Galb1-4GlcNAcb1-2Mana1-3)Manb1-4GlcNAcb1-4(Fuca1-6)GlcNAcb-Sp24
589	Galb1-4GlcNAcb1-3Galb1-4GlcNAcb1-3GalNAca-Sp14
590	Galb1-4GlcNAcb1-3Galb1-4GlcNAcb1-6(Galb1-3)GalNAca-Sp14
591	Galb1-4GlcNAcb1-3Galb1-4GlcNAcb1-6(Galb1-4GlcNAcb1-3Galb1-4GlcNAcb1-3)GalNAca-Sp14
592	Neu5Aca2-3Galb1-4GlcNAcb1-3Galb1-4GlcNAcb1-3GalNAca-Sp14
593	GlcNAcb1-3Galb1-4GlcNAcb1-3GalNAca-Sp14
594	GlcNAcb1-3Galb1-4GlcNAcb1-6(Galb1-3)GalNAca-Sp14
595	GlcNAcb1-3Galb1-4GlcNAcb1-6(GlcNAcb1-3Galb1-4GlcNAcb1-3)GalNAca-Sp14

596	Neu5Aca2-3Galb1-4GlcNAcb1-3Galb1-4GlcNAcb1-6(Neu5Aca2-3Galb1-4GlcNAcb1-3Galb1-4GlcNAcb1-3)GalNAca-Sp14
597	Neu5Aca2-6Galb1-4GlcNAcb1-3Galb1-4GlcNAcb1-3GalNAca-Sp14
598	GlcNAcb1-3Galb1-4GlcNAcb1-3Galb1-4GlcNAcb1-3GalNAca-Sp14
599	Galb1-4GlcNAcb1-3Galb1-3GalNAca-Sp14
600	Neu5Aca2-3Galb1-4GlcNAcb1-3Galb1-4GlcNAcb1-6(Galb1-3)GalNAca-Sp14
601	Neu5Aca2-6Galb1-4GlcNAcb1-3Galb1-4GlcNAcb1-6(Galb1-3)GalNAca-Sp14
602	Neu5Aca2-6Galb1-4GlcNAcb1-6(Galb1-3)GalNAca-Sp14
603	Neu5Aca2-3Galb1-4GlcNAcb1-3Galb1-4GlcNAcb1-2Mana1-6(Neu5Aca2-3Galb1-4GlcNAcb1-3Galb1-4GlcNAcb1-2Mana1-3)Manb1-4GlcNAcb1-4GlcNAcb-Sp12
604	GlcNAcb1-6(Neu5Aca2-3Galb1-3)GalNAca-Sp14
605	Neu5Aca2-6Galb1-4GlcNAcb1-3Galb1-4GlcNAcb1-6(Neu5Aca2-6Galb1-4GlcNAcb1-3Galb1-4GlcNAcb1-3)GalNAca-Sp14
606	Neu5Aca2-6Galb1-4GlcNAcb1-3Galb1-4GlcNAcb1-3Galb1-4GlcNAcb1-2Mana1-6(Neu5Aca2-6Galb1-4GlcNAcb1-3Galb1-4GlcNAcb1-3Galb1-4GlcNAcb1-2Mana1-3)Manb1-4GlcNAcb1-4GlcNAcb-Sp12
607	Neu5Aca2-3Galb1-4GlcNAcb1-3Galb1-4GlcNAcb1-3Galb1-4GlcNAcb1-2Mana1-6(Neu5Aca2-3Galb1-4GlcNAcb1-3Galb1-4GlcNAcb1-3Galb1-4GlcNAcb1-2Mana1-3)Manb1-4GlcNAcb1-4GlcNAcb-Sp12
608	Neu5Aca2-6Galb1-4GlcNAcb1-3Galb1-4GlcNAcb1-2Mana1-6(Neu5Aca2-6Galb1-4GlcNAcb1-3Galb1-4GlcNAcb1-2Mana1-3)Manb1-4GlcNAcb1-4GlcNAcb-Sp12
609	GlcNAcb1-3Fuca-Sp21
610	Galb1-3GalNAcb1-4(Neu5Aca2-8Neu5Aca2-8Neu5Aca2-3)Galb1-4Glcb-Sp21